

MICROSTRUCTURES AND SENSE OF SHEAR IN THE  
BREVARD ZONE, SOUTHERN APPALACHIANS

by

CAROL ANNE EVANS, B.S.

THESIS

Presented to the Faculty of the Graduate School of

The University of Texas at Austin

in Partial Fulfillment

of the Requirements

for the Degree of

MASTER OF ARTS

THE UNIVERSITY OF TEXAS AT AUSTIN

December 1986

MICROSTRUCTURES AND SENSE OF SHEAR IN THE  
BREVARD ZONE, SOUTHERN APPALACHIANS

by

CAROL ANNE EVANS, B.S.

Copyright

Presented to the Faculty of the Graduate School of  
by

The University of Texas at Austin

Carol A. Evans

in Partial Fulfillment

1986

of the Requirements

for the Degree of

MASTER OF ARTS

THE UNIVERSITY OF TEXAS AT AUSTIN

October 1986



## ACKNOWLEDGEMENTS

To Mark,  
for understanding and waiting.

First and foremost I thank Sharon, my advisor, for her encouragement and advice, and for patiently enduring the various difficulties in the field and my seemingly endless stream of questions. The following persons I thank accordingly: Bob Hatcher for the generous use of his unpublished geologic maps and deluxe housing accommodations while in the field August, 1966; Mark and Beth Hartford for their hospitality at home and in the field; Bill Carlson for the use of his petrographic microscope for thin section photography; Suzanna Rose Moses for her generous help in making thin sections and for her hospitality and special friendship; John and Madelyn La Fave for their wonderful friendship and support; and Charles and Ruby Evans, my parents, for their never-ending support and belief in me and their financial assistance with a field vehicle. Last, but forever first in my life, I thank my husband Mark Avery to whom this volume is dedicated.

Generous grants from the Geological Society of America, Sigma Xi and the University of Texas Geology Foundation made this research possible. Their receipt is gratefully acknowledged.

## ACKNOWLEDGEMENTS

First and foremost I thank Sharon, my advisor, for her encouragement and advice, and for patiently enduring the various difficulties in the field and my seemingly endless stream of questions. The following persons I thank accordingly: Bob Hatcher for the generous use of his unpublished geologic maps and deluxe housing accommodations while in the field August, 1986; Mark and Beth Hartford for their hospitality at home and in the field; Bill Carlson for the use of his petrographic microscope for thesis photography; Suzanna Ross Moses for her generous help in making thin sections and for her hospitality and special friendship; John and Madelyn La Fave for their wonderful friendship and support; and Charles and Ruby Evans, my parents, for their never-ending support and belief in me and their financial assistance with a field vehicle. Last, but forever first in my life, I thank my husband Mark Avery to whom this volume is dedicated.

Generous grants from the Geological Society of America, Sigma Xi and the University of Texas Geology Foundation made this research possible. Their receipt is gratefully acknowledged.



## ABSTRACT

### **Microstructures and Sense of Shear in the Brevard Zone, Southern Appalachians**

Carol Anne Evans, M.A.

The University of Texas at Austin, 1986

Supervising Professor: Sharon Mosher, Ph.D.

The Brevard Zone, which separates the Blue Ridge and Inner Piedmont geologic provinces in the southern Appalachians, is a major structural feature with a multiple deformation history. Microstructures in oriented thin sections from rocks in the Brevard Zone in Tugaloo, Whetstone and Tamassee quadrangles, South Carolina, Rosman quadrangle, North Carolina, and in the sheared Ben Hill Granite in Atlanta, Georgia, indicate that there were at least two early ductile deformations and a later, locally developed, brittle deformation.

The oldest recognizable microstructures are a prominent foliation ( $S_1$ ), quartz ribbons and garnets. The age of these features and the sense of shear during their formation is unknown. The remainder of the observed microstructures are categorized into groups A, B, C and D on the basis of orientation, overprinting relationships and direction of motion as indicated by sense of shear criteria present. Group A is the oldest of these microstructures and group D is the youngest.



Group A features consists of northwest-verging, tight to isoclinal  $F_2$  folds, a weakly developed, axial planar foliation ( $S_2$ ), and scattered  $F_3$  folds, coaxial with  $F_2$ . The  $F_1$  folds of Roper and Dunn (1973) are not observed due to later deformation. Group A microstructures are ductile features which formed during a west-to northwest-directed thrusting motion. Group B features include type II s-c mylonites, c-surfaces, scattered  $F_4$  folds and garnet pressure shadows. The orientation of these features indicates that they formed during a period of dextral strike-slip shearing with a possible thrust component. Group C contains an extensional crenulation cleavage (ECC) which is relatively younger than features in groups A and B. The orientation of ECC is incompatible with dextral motion, thus they suggest a change in the direction of bulk motion in the Brevard Zone, the direction of which is unknown.

Along strike a notable change in deformation conditions occurred during the ductile deformation(s) which formed features in groups A, B and C. This change is reflected in highly recrystallized quartz textures in Tugaloo, relative to partially recrystallized textures in Rosman quadrangle. Retrograde metamorphism postdates the formation of features in groups A, B and C.

Group D contains the youngest microstructures which formed during a localized brittle deformation. Brecciation is visible in thin section and outcrop, however no sense of shear direction can be determined. Drag folds and faults are present in several outcrops but their geometry is highly variable. The bulk motion during brittle deformation is unknown.

Sense of shear criteria in group A are compatible with tectonic models for both the Taconic and Alleghanian orogenies in the southern Appalachians. How-



ever, group A probably formed in the Taconic because the most intense ductile deformation has been reported for this time period. Microstructures in group B and C are found in the sheared, Permian Ben Hill Granite in Atlanta and thus are Alleghanian in age. Rocks containing group B and C in the northeastern study areas cannot be radiometrically dated with confidence, however, their orientations, deformation conditions and sense of shear is similar to group B and C in the Ben Hill Granite indicating that they are also Alleghanian in age. The dextral strike-slip motion indicated by groups B is compatible with the results of previous workers (Reed and Bryant, 1964; Bobyarchick, 1983) elsewhere along the Brevard Zone who have also demonstrated Alleghanian dextral motion. Thus the results of this study confirm an episode of ductile, dextral strike-slip motion in the Brevard Zone during the Alleghanian.

Group C and D may also be Alleghanian or they may be the result of a separate and more recent deformation, possibly related to the Triassic opening of the present-day Atlantic ocean.

Introduction	1
Geological setting	2
Geological map	3
Geological cross-sections	4
Geological summary	5
Group A	6
Geological setting	6
Geological map	7
Geological cross-sections	8
Geological summary	9
Group B	10
Geological setting	10
Geological map	11
Geological cross-sections	12
Geological summary	13
Group C	14
Geological setting	14
Geological map	15
Geological cross-sections	16
Geological summary	17
Group D	18
Geological setting	18
Geological map	19
Geological cross-sections	20
Geological summary	21
Conclusions	22
References	23
Appendix A	24
Appendix B	25
Appendix C	26
Appendix D	27
Appendix E	28
Appendix F	29
Appendix G	30
Appendix H	31
Appendix I	32
Appendix J	33
Appendix K	34
Appendix L	35
Appendix M	36
Appendix N	37
Appendix O	38
Appendix P	39
Appendix Q	40
Appendix R	41
Appendix S	42
Appendix T	43
Appendix U	44
Appendix V	45
Appendix W	46
Appendix X	47
Appendix Y	48
Appendix Z	49



## TABLE OF CONTENTS

<b>Abstract</b> .....	<b>vi</b>
<b>List of Tables</b> .....	<b>xi</b>
<b>List of Figures</b> .....	<b>xii</b>
<b>Introduction</b> .....	<b>1</b>
Nature and scope of project .....	1
Study Area .....	4
Methods .....	6
Geologic setting .....	8
Lithologies .....	12
Northeastern areas .....	12
Atlanta area .....	13
Microstructures .....	18
Oldest Microstructures .....	19
<b>Group A</b> .....	<b>24</b>
Folds .....	24
Axial planar foliation .....	27
Summary .....	28
<b>Group B</b> .....	<b>30</b>
Type II s-c mylonites .....	30
Northeastern areas .....	30
Atlanta area .....	35
Other c-surfaces .....	39
Folds .....	43
Pressure shadows .....	47
Summary .....	49
<b>Group C</b> .....	<b>51</b>
Extensional Crenulation Cleavage .....	51
Northeastern areas .....	52
Atlanta area .....	54
Summary .....	58
<b>Changes in deformation conditions</b> .....	<b>61</b>
<b>Retrograde metamorphism</b> .....	<b>63</b>
<b>Group D</b> .....	<b>64</b>
Atlanta area .....	64
Whetstone Quadrangle .....	66
Tamassee Quadrangle .....	70



Rosman Quadrangle .....	74
Sega Lake .....	74
Quarry .....	78
Summary .....	82
<b>Summary .....</b>	<b>85</b>
<b>Timing .....</b>	<b>87</b>
<b>Conclusions .....</b>	<b>93</b>
<b>Appendices .....</b>	<b>96</b>
<b>Appendix A .....</b>	<b>97</b>
Tables of microstructures .....	97
<b>Appendix B .....</b>	<b>105</b>
Structural Data .....	105
Brittle Faults .....	107
<b>Appendix C .....</b>	<b>112</b>
Minor Microstructural Features .....	112
Crenulations .....	112
Rare Pressure Shadows .....	113
Veins .....	114
Kinks and Shear Bands .....	114
<b>Appendix D .....</b>	<b>117</b>
Quartz c-axis data .....	117
<b>References .....</b>	<b>122</b>
<b>Vita .....</b>	<b>126</b>

## LIST OF TABLES

Table 1. Microstructure groupings .....	20
Table A.1: Microstructure Table for Tugaloo Quadrangle .....	98
Table A.2: Microstructure Table for Whetstone Quadrangle .....	101
Table A.3: Microstructure Table for Tamassee Quadrangle .....	102
Table A.4: Microstructure Table for Rosman Quadrangle .....	103
Table A.5: Microstructure Table for Northwest Atlanta Quadrangle .....	104



## LIST OF FIGURES

Fig. 1. Major geologic provinces in the southern Appalachians . . . . .	109
Fig. 2. Study area . . . . .	110
Fig. 3. Generalized geologic map of the greater Atlanta, Georgia area . . . .	111
Fig. 4. Late Precambrian-Early Paleozoic Tectonic Setting . . . . .	115
Fig. 5. Structure produced during the Taconic Orogeny (400-440 Ma) . . . .	116
Fig. 6. Cross-section of the present structural setting of Brevard Zone . . . .	119
Fig. 7. Geologic map of Tugaloo quadrangle, SC . . . . .	120
Fig. 8. Geologic map of Whetstone quadrangle, SC . . . . .	121
Fig. 9. Geologic map of Tamassee quadrangle, SC . . . . .	16
Fig. 10. Geologic map of Rosman quadrangle, NC . . . . .	17
Fig. 11. Foliation in the Brevard phyllite . . . . .	21
Fig. 12. Weathered garnets . . . . .	22
Fig. 13. Group A folds . . . . .	25
Fig. 14. Relic hinges of early isoclinal folds . . . . .	26
Figure 15. Group A coaxial folds . . . . .	27
Fig. 16. Axial planar foliation to Group A folds . . . . .	29
Fig. 17. S-surfaces in Type II s-c mylonite from the Henderson Mylonite . . .	32
Fig. 18. S-surfaces defined by muscovite folia . . . . .	33
Fig. 19. S-surfaces defined by dimensional preferred orientation . . . . .	34
Fig. 20. C-surfaces are defined by muscovite and biotite . . . . .	35
Fig. 21. Shear zone in Henderson Mylonite . . . . .	36
Fig. 22. Henderson Mylonite away from shear zone . . . . .	37
Fig. 23. Highly recrystallized quartz ribbons . . . . .	38



Fig. 24. High shear strain in type II mylonite . . . . .	39
Fig. 25. No microstructure development outside a small shear zone . . . . .	40
Fig. 26. Type II s-c mylonite . . . . .	41
Fig. 27. Crystallographic preferred orientation in a type II s-c mylonite . . . . .	42
Fig. 28. Highly deformed quartz ribbons . . . . .	43
Figure 29. C-surface defined by deflected muscovite . . . . .	44
Figure 30. A c-surface has sheared garnets . . . . .	45
Fig. 31. Group B fold . . . . .	46
Fig. 32. Sketch of a possible fold interference pattern . . . . .	48
Fig. 33. Poorly developed pressure shadows . . . . .	49
Fig. 34. ECC from the Brevard Phyllite . . . . .	54
Fig. 35. ECC's deform a quartz ribbon . . . . .	55
Fig. 36. ECC deforms a group B pressure shadow . . . . .	56
Fig. 37. ECC deform group B c-surfaces in the Brevard Phyllite . . . . .	57
Fig. 38. ECC deforms group B fold . . . . .	58
Figure 39. Closeup of ECC . . . . .	59
Fig. 40. Quartz ribbon necked by an ECC from the Ben Hill Granite . . . . .	60
Figure 41. Partially recrystallized quartz ribbon . . . . .	62
Fig. 42. Brittle imbricate fault zone . . . . .	66
Fig. 43. Field sketch of imbricate faults in the Ben Hill Granite . . . . .	67
Fig. 44. Late quartz-filled fractures in the Ben Hill Granite . . . . .	68
Fig. 45. Brecciation near exotic slice . . . . .	71
Fig. 46. Faults in Tamassee quadrangle . . . . .	73
Fig. 47. Prominent faults and fault slivers . . . . .	75



Fig. 48. Field sketch of Sega Lake roadcut, Rosman	76
Fig. 49. Intense deformation along the Rosman fault	79
Fig. 50. Folds in graphitic phyllite	81
Fig. 51. Incipient brecciation of folded quartz ribbons	82
Fig. 52. Intensely brecciated phyllite	83
Fig. B.1. Stereonet plots of foliation planes across faults	109
Fig. B.2. Stereonet plots of foliation planes across faults	110
Fig. B.3. Stereonet plots of foliation planes across faults	111
Fig. C.1. Rotated quartz pressure shadows on opaque grains	115
Fig. C.2. Sheared veins	116
Fig. D.1. Quartz c-axes plots for Tu3 and Ta142	119
Fig. D.2. Quartz c-axes plots for Tu137A and Ros162	120
Fig. D.3. Quartz c-axes plots for At12	121

[PLATES 1-4]

[pocket]



## INTRODUCTION

The Brevard Shear Zone is a narrow, linear, deformed belt of rocks which stretches approximately 375 miles (625 km) within the southern Appalachians. This zone separates the Blue Ridge and Inner Piedmont geologic provinces (Fig. 1) and is a major structural feature with a multiple deformation history. The zone trends northeast from eastern Alabama where it disappears under coastal plain deposits, to northwest North Carolina near the James River synclinorium (Roper and Justus, 1973).

## NATURE AND SCOPE OF PROJECT

The Brevard Zone has been intensively studied over the past 20 years by numerous researchers. A wide range of theories on its origin have been proposed because of the complex deformation history of the zone. For example, the initial research of Keith (1905) suggests that the Brevard Zone is a simple fold belt. More recent workers postulate that the zone is a normal fault (White, 1950) or an alpine-type root zone (Livingston, 1966). Roper and Justus (1973) believe it has a polytectonic origin. The latter theory is probably the most accurate one given the long and complex history of the zone. Several reasons for this diversity of theories are the quality and nature of exposures, the somewhat variable structure along the length of the zone and the lack of offset geologic markers. An extensive list of theories which further illustrates the past controversy over the origin of the Brevard Zone appears in Roper and Justus (1973, p.119).

At present this controversy is focused on the two most widely accepted theories. These theories are that the Brevard Zone is: 1) a thrust fault (Jonas, 1932;



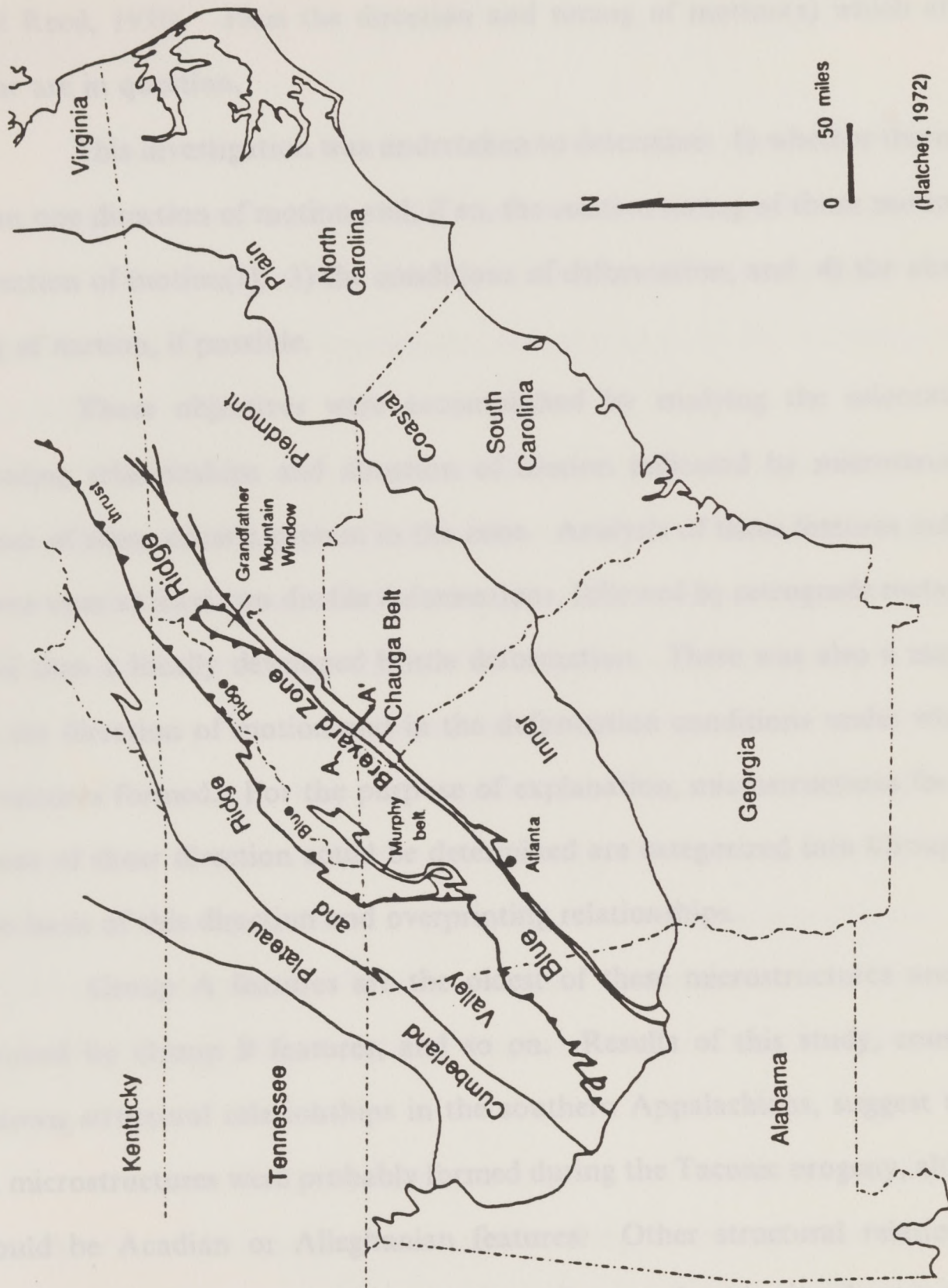


Fig. 1. Major geologic provinces in the southern Appalachians: A-A' is position of all following cross-sections (Figs. 3-5).



Hatcher, 1969, 1971) and/or 2) a dextral (Reed and Bryant, 1964; Bobyarchick, 1983, 1984) or a sinistral strike-slip fault (Reed, Bryant and Myers, 1970; Bryant and Reed, 1970). Thus the direction and timing of motion(s) which affected the zone are in question.

This investigation was undertaken to determine: 1) whether there was more than one direction of motion and, if so, the relative timing of those motions; 2) the direction of motion(s); 3) the conditions of deformation; and 4) the absolute timing of motion, if possible.

These objectives were accomplished by studying the orientation, overprinting relationships and direction of motion indicated by microstructures and sense of shear criteria present in the zone. Analysis of these features indicates that there were at least two ductile deformations, followed by retrograde metamorphism, and then a locally developed brittle deformation. There was also a major change in the direction of motion and in the deformation conditions under which microstructures formed. For the purpose of explanation, microstructures for which the sense of shear direction could be determined are categorized into Groups A-D, on the basis of this direction and overprinting relationships.

Group A features are the oldest of these microstructures and are overprinted by Group B features, and so on. Results of this study, combined with known structural relationships in the southern Appalachians, suggest that Group A microstructures were probably formed during the Taconic orogeny, although they could be Acadian or Alleghanian features. Other structural relationships and comparison of microstructures with those that are datable elsewhere in the Brevard Zone, strongly suggest that Groups B, C and D are Alleghanian in age. The



geologic implications of these results help to better constrain tectonic models of the Brevard Zone in the study area.

## STUDY AREA

The study area consists of outcrops in the Northwest Atlanta, Georgia quadrangle and the Tugaloo, Whetstone, and Tamassee quadrangles in northwestern South Carolina, and the Rosman quadrangle in southwestern North Carolina (Fig. 2). The latter four quadrangles are referred to as the "northeastern areas" in this paper.

The Atlanta study area was chosen because at that locality the Hercynian Ben Hill granite (Sinha and Zietz, 1982) dated at 280-290 Ma (Sinha, pers. comm.) is truncated by Brevard motion (Fig. 3). One particularly well-exposed outcrop (McConnell and Costello, 1980, p.253) was the focus of sampling in this area. The other four study areas were sampled because good kinematic indicators are present. Unpublished geologic maps of Tugaloo and Whetstone quadrangles at 1:24,000 (compiled by Hatcher in 1968-1976) and the published maps, at the same scale, of Tamassee (Roper and Dunn, 1970) and Rosman quadrangles (Horton, 1982) were used to locate exposures. Other detailed field studies pertinent to the present study include those by Livingston, 1966; Higgins, 1968; Hatcher, 1969; Horton, 1974; and Roper, 1971, 1972.

Outcrop in the northeastern areas is not abundant, consisting predominantly of heavily vegetated, northeast-trending, creek exposures and a few useful road cut exposures. Outcrop quality is generally poor, ranging from poorly indurated to saprolitic, bank and road-cut outcrop, to well-indurated but water or lichen-covered creek exposure. In the southwest, the Ben Hill Granite outcrop is



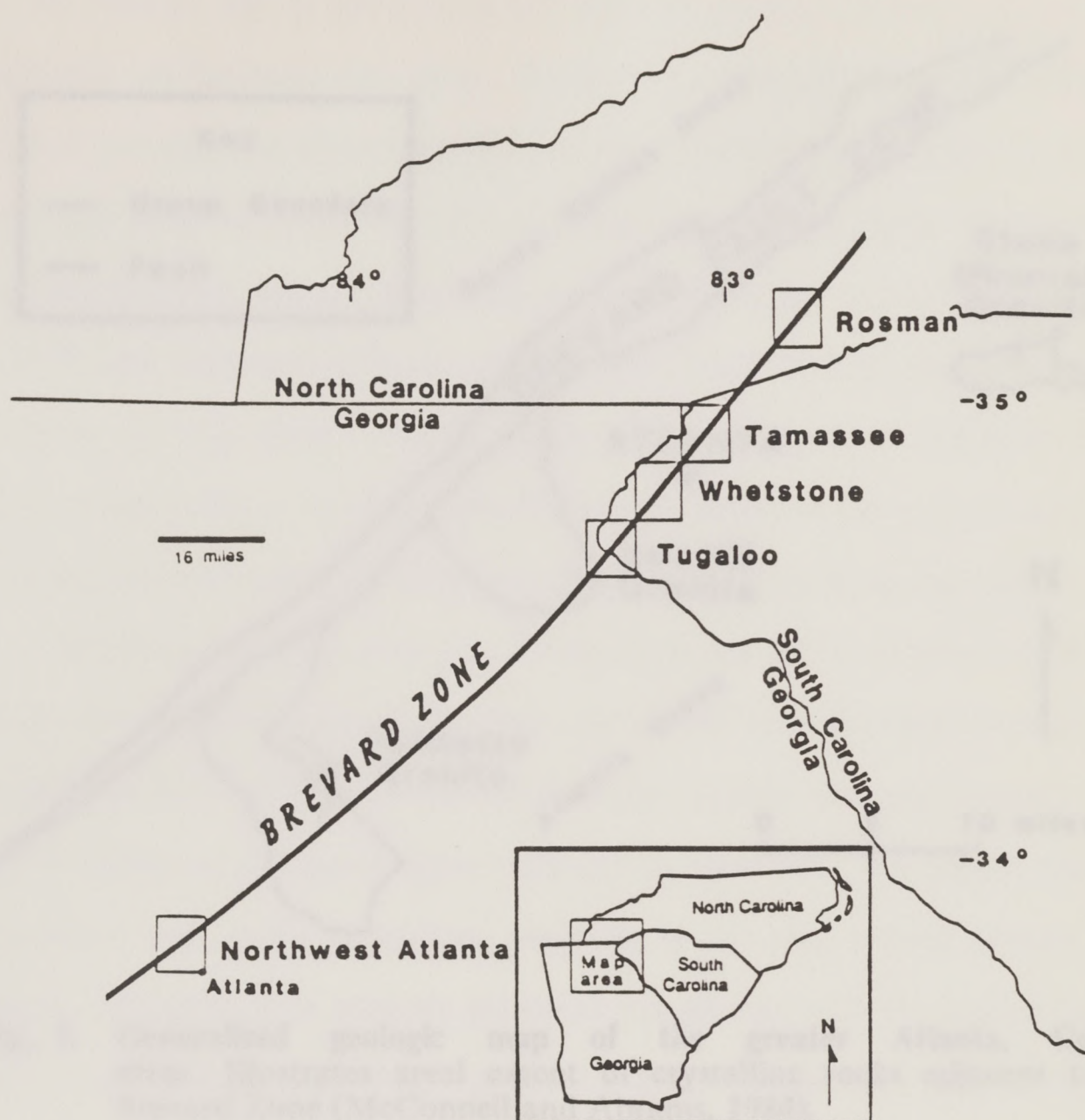


**Fig. 2. Study area:** The study area consists of five quadrangles in the southern Appalachians.

easily accessible, unvegetated, and contains fresh exposure, unlike that in the northeastern study areas. This granitic outcrop is located on I-285 2.9 miles (4.8 km) north of the I-285 and I-20 junction and 0.5 miles (0.8 km) south of the Chattahoochee River. Road cut exposures of both the granite and the adjacent Long Island Gneiss are about 900 ft (2700 m) long, up to 30 ft (10 m) high, and



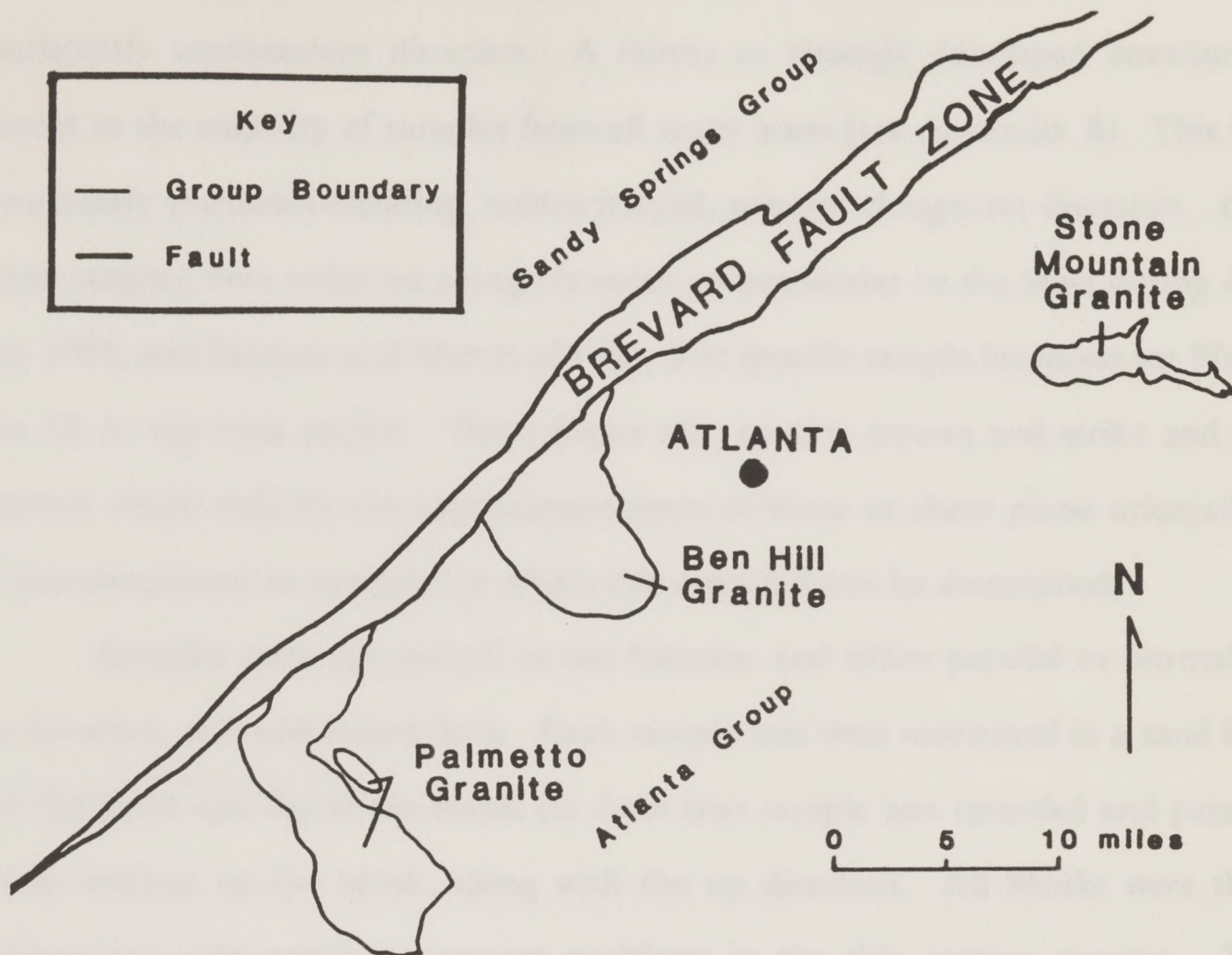


Fig. 3. Generalized geologic map of the greater Atlanta, Georgia area: Illustrates areal extent of crystalline rocks adjacent to the Brevard Zone (McConnell and Abrams, 1984).

present on both sides of the interstate highway, although sampling is confined to the west side of I-285. This outcrop is the only one sampled in this quadrangle.

## METHODS

In the northeastern study areas, surface exposure of the Brevard Zone ranges from 2500 to 6000 ft in width (830 m to 2 km), reaching a maximum width of 10,000 to 15,000 ft (3.3 km to 5 km) in the Tamasssee quadrangle. Foliation in the zone has a consistent southeast dip ranging from  $10^{\circ}$  to  $70^{\circ}$  the average is



45°. In Atlanta, dip of foliation in the outcrop sampled averages 25°, also in a consistently southeastern direction. A faintly to strongly developed lineation is present in the majority of samples from all study areas (see Appendix B). This is a consistently northeast-trending, subhorizontal, mineral elongation lineation. Oriented samples were collected along traverses perpendicular to the zone during August 1985, and January and March of 1986. For specific sample locations see Plates I to IV in the back pocket. These plates also contain arrows and strike and dip symbols which indicate the approximate sense of shear or shear plane orientation of microstructures in samples for which this direction can be determined.

Samples were cut normal to the foliation and either parallel or normal to the lineation, and sometimes both. Each sample was then reoriented in a sand box and the strike and dip of the blank cut from that sample was recorded and permanently marked on the blank, along with the up direction. All blanks were then impregnated with epoxy to prevent problems in the thin section process. The standard, 30 micron thin sections produced are marked with the sample number, up arrow, and two notches which represent a strike line for that section. By referring to the appropriate strike and dip recording, it is possible to accurately reorient each thin section in space and thus determine the true orientation, at least in two dimensions, of any kinematic indicators present. Using the hand sample and thin section together, it was possible to determine the orientation of kinematic indicators in three dimensions.

Quartz c-axis fabrics are also used as a tool to help determine the sense of shear. Plots of c-axis orientations and their interpretations are included in Appendix D.



All figure captions for photomicrographs give the thin section label in parentheses. This label consists of the quadrangle abbreviation and the thin section number which corresponds to the sample number. This number can be used to refer to the sample location and lithology on the enclosed overlays and referenced geologic maps. Sense of shear direction, where appropriate, is given in captions as "ss = ". **This direction is for features as viewed in the photomicrographs and not, in all cases, for the zone as a whole.** The long dimension, "ld = ", of each photomicrograph is also given in each caption. A total of 133 thin sections from Brevard zone rocks were analyzed, 73 from Tugaloo, 18 from Whetstone, 11 from Tamassee, 24 from Rosman, and 7 from Atlanta.

## GEOLOGIC SETTING

The Brevard Zone in the study area forms the northwestern edge of the Chauga belt synclinorium in the northeastern study areas (Fig. 1). The Chauga belt (also known as the Low Rank belt) is a narrow syncline of sheared low grade metamorphic rocks, abruptly bounded by the high grade Blue Ridge geologic province to the northwest. The southeastern boundary of the Chauga belt with the migmatitic Inner Piedmont is believed to be the result of a metamorphic gradient (Hatcher, 1972, 1978).

Rocks of the Chauga belt are apparently Precambrian in age and were deposited in a backarc basin (Fig. 4) (Roper and Justus, 1973). The first deformation occurred during the Mid-Ordovician to Earliest-Silurian Taconic orogeny (Glover et al., 1983) when the Inner Piedmont island arc collided with the North American continent. Intense shearing and the formation of the Chauga belt syncline occurred at this time (Fig. 5) (Hatcher, 1972).



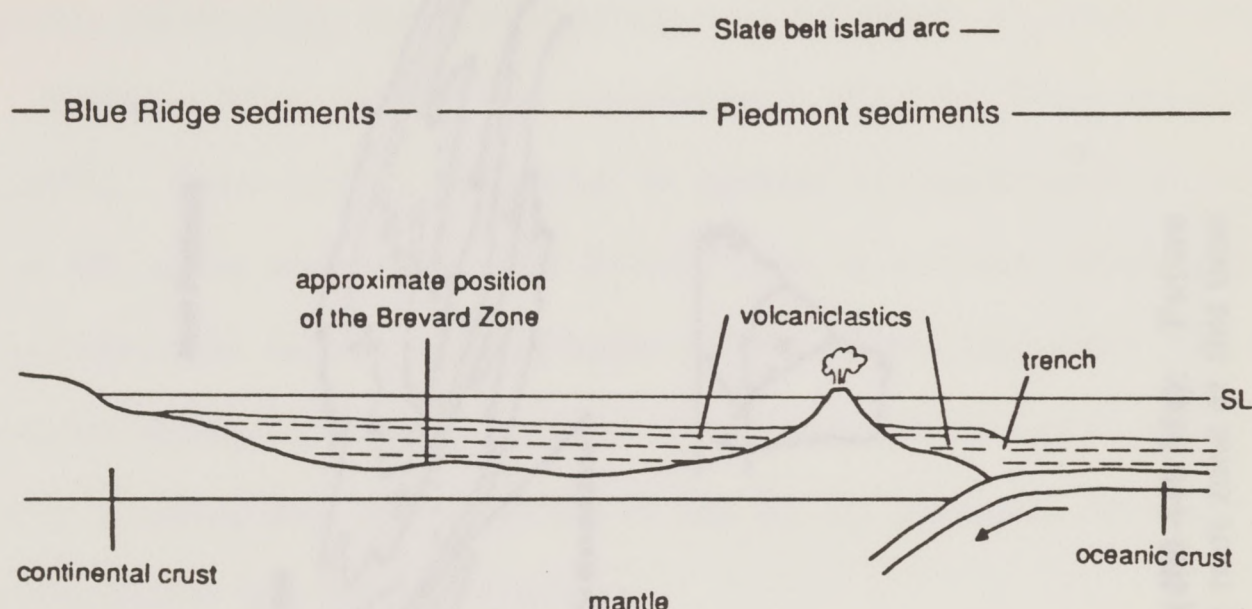
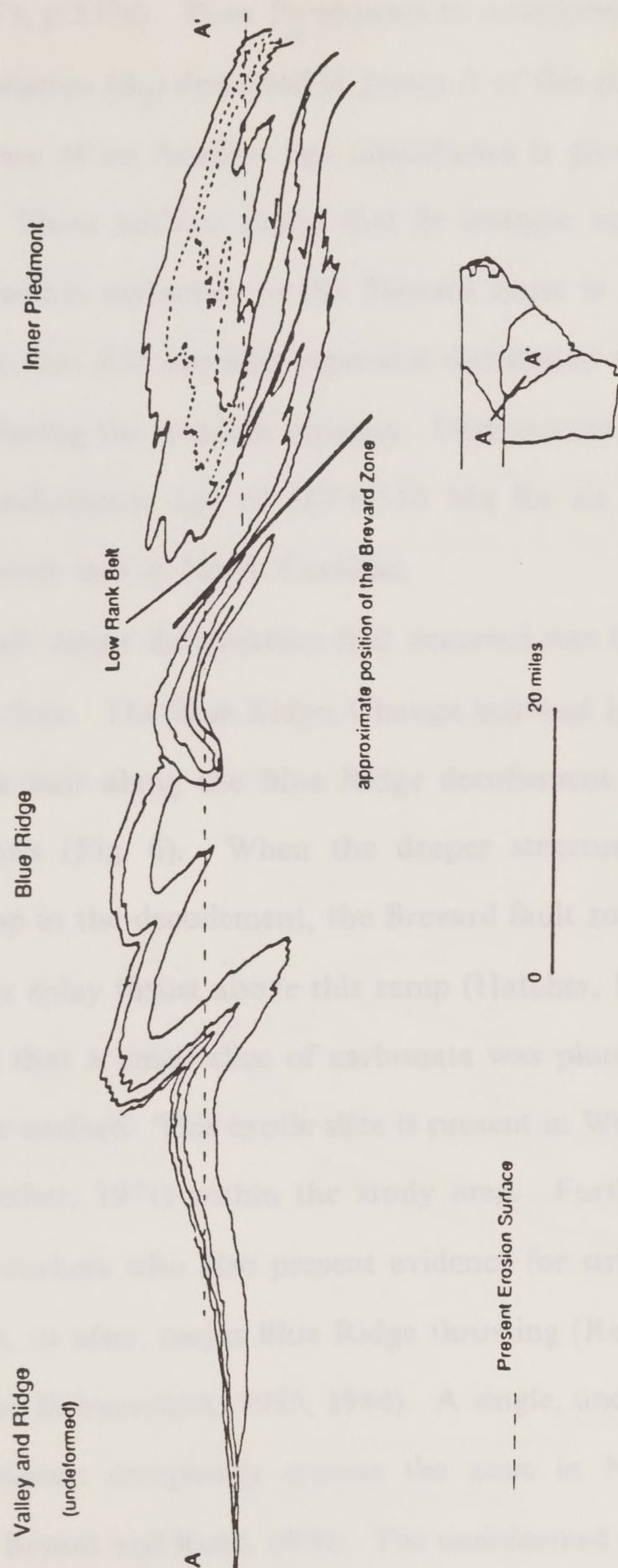


Fig. 4. Late Precambrian-Early Paleozoic Tectonic Setting: Schematic cross-section in the southern Appalachians (Roper and Justus, 1973).

Roper and Dunn (1973) have identified  $F_1$  and  $S_1$  microstructures which they correlate with the Taconic deformation. Their  $S_1$  is the prominent schistosity in the Brevard Zone, the  $S_1$  foliation of this paper, and it is parallel to  $S_0$ , strongly transposed sedimentary bedding, except in the hinges of  $F_1$  isoclinal folds where  $S_1$  is an axial planar foliation. Their  $F_1$  folds deform  $S_0$ . The  $F_1$  of these authors was not observed in the present study.

Further deformation presumably occurred during the Middle to Late-Devonian Acadian orogeny. Roper and Dunn (1973) correlate  $F_2$  and  $M_2$  features with the Acadian orogeny.  $F_2$  folds of Roper and Dunn (1973) are open to isoclinal, and also coplanar and coaxial with  $F_1$ . Many are sheared out and rootless at the microscopic scale. These  $F_2$  folds in places have an associated axial planar





**Fig. 5. Structure produced during the Taconic Orogeny (400-440 Ma): Future Brevard Zone (position indicated) acts a thrust root zone at this time (Hatcher, 1972).**



cleavage,  $S_2$ , expressed as either a schistosity,  $S_{2a}$ , or a slip cleavage,  $S_{2b}$  (Roper and Dunn, 1973, p.3374). Their  $F_2$  appears to correspond to the  $F_2$  microfolds and axial planar foliation ( $S_2$ ) described in group A of this paper.  $F_2$  folds deform  $S_1$ .

Evidence of an Acadian age disturbance is given by Odom and Fullagar (1970, 1973). These authors found that Sr isotopic homogenization occurred at  $356 \pm 8$  Ma within mylonites in the Brevard Zone in Rosman, North Carolina. They postulate that this age may represent distributed shearing rather than major displacement during the Acadian orogeny. Furthermore, Bond and Fullagar (1974) calculated a radiometric age of  $387 \pm 14$  Ma for six mylonites from the same Henderson Gneiss unit in North Carolina.

The last major deformation that occurred was the Alleghanian orogeny in late Paleozoic time. The Blue Ridge, Chauga belt and Inner Piedmont were thrust westward as a unit along the Blue Ridge decollement over flat-lying Valley and Ridge sediments (Fig. 6). When the deeper structure of the Inner Piedmont reached a ramp in the decollement, the Brevard fault zone, proper, then formed as a subsidiary or splay thrust above this ramp (Hatcher, 1972, 1978). It was during this thrusting that a small slice of carbonate was plucked from the footwall and brought to the surface. This exotic slice is present in Whetstone quadrangle, South Carolina (Hatcher, 1971) within the study area. Further Alleghanian motion is proposed by workers who also present evidence for strike-slip faulting either synchronous with, or after, major Blue Ridge thrusting (Reed and Bryant, 1964; Reed et al, 1970; and Bobyarchick, 1983, 1984). A single, undeformed diabase dike from the Upper Triassic completely crosses the zone in North Carolina (Reed and Bryant, 1964; Bryant and Reed, 1970). The undeformed nature of this dike indicates that all motion along the Brevard Zone had ceased by the Triassic.



## LITHOLOGIES

### Northeastern areas

Lithologies exposed within the Brevard Zone are part of the Precambrian Chauga River Formation which is correlative with other rocks of the Chauga belt further to the southeast (Hatcher, 1969, p.131). The Chauga River Formation dips southeast parallel to the zone and consists of a basal graphitic phyllite, and an upper and lower chlorite-muscovite phyllite which includes a thin but continuous carbonate unit. This phyllite is also known as the Brevard phyllite (Hatcher and

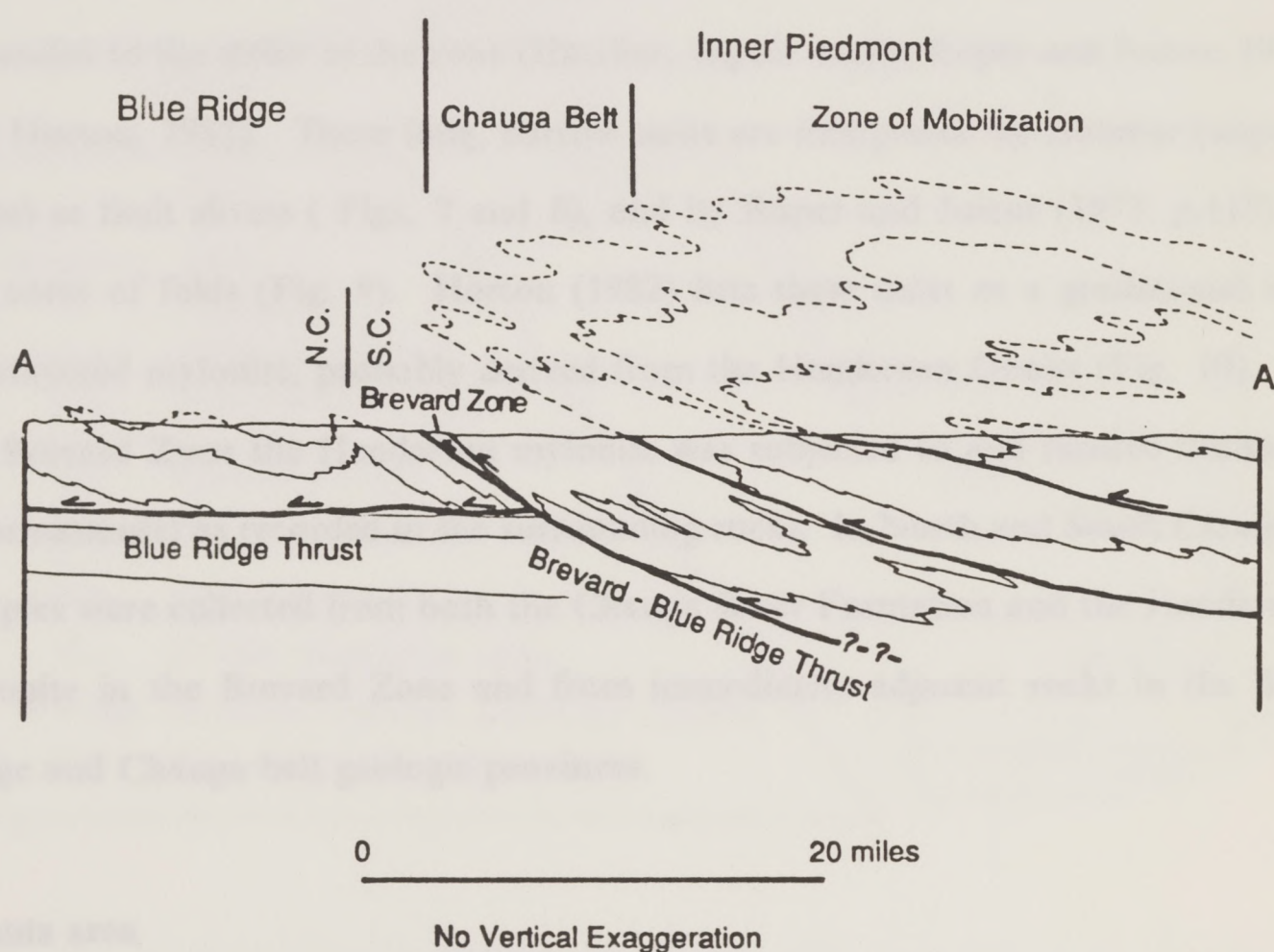


**Fig. 6.** Cross-section of the present structural setting of Brevard Zone: Exotic footwall slice not shown due to scale (Hatcher, 1978).



Griffin, 1969) and the button-schist or fish-scale schist of Roper (1972). Phyllitic units are garnetiferous and quartz-rich in some areas.

Within the Chauga River Formation there are narrow, discontinuous quartzofeldspathic units known as the Henderson Gneiss. This gneiss is also present as a large body to the southeast of the Brevard Zone in all study areas except Atlanta, Georgia. In many areas the Henderson Gneiss is more appropriately termed a mylonite and this is the terminology used here.

The Henderson mylonite is believed to be derived from a Cambrian pluton (Sinha and Glover, 1978) which intruded lithologies in the Chauga belt and Inner Piedmont prior to the Taconic orogeny. The pluton was subsequently deformed resulting in the present outcrop pattern of the mylonite in the Brevard Zone, which is parallel to the strike of the zone (Hatcher, unpub. maps; Roper and Justus, 1973; and Horton, 1982). These long, narrow units are interpreted by Hatcher (unpub. maps) as fault slivers ( Figs. 7 and 8), and by Roper and Justus (1973, p.113) as the cores of folds (Fig. 9). Horton (1982) lists these units as a gradational and interlayered mylonite, probably derived from the Henderson Gneiss (Fig. 10). In the Brevard Zone the Henderson mylonite was subjected to and records the same deformation(s) as recorded in the surrounding rocks. In North and South Carolina, samples were collected from both the Chauga River Formation and the Henderson mylonite in the Brevard Zone and from immediately adjacent rocks in the Blue Ridge and Chauga belt geologic provinces.

#### **Atlanta area**

Lithologies in the Brevard Zone in Atlanta are not stratigraphically con-



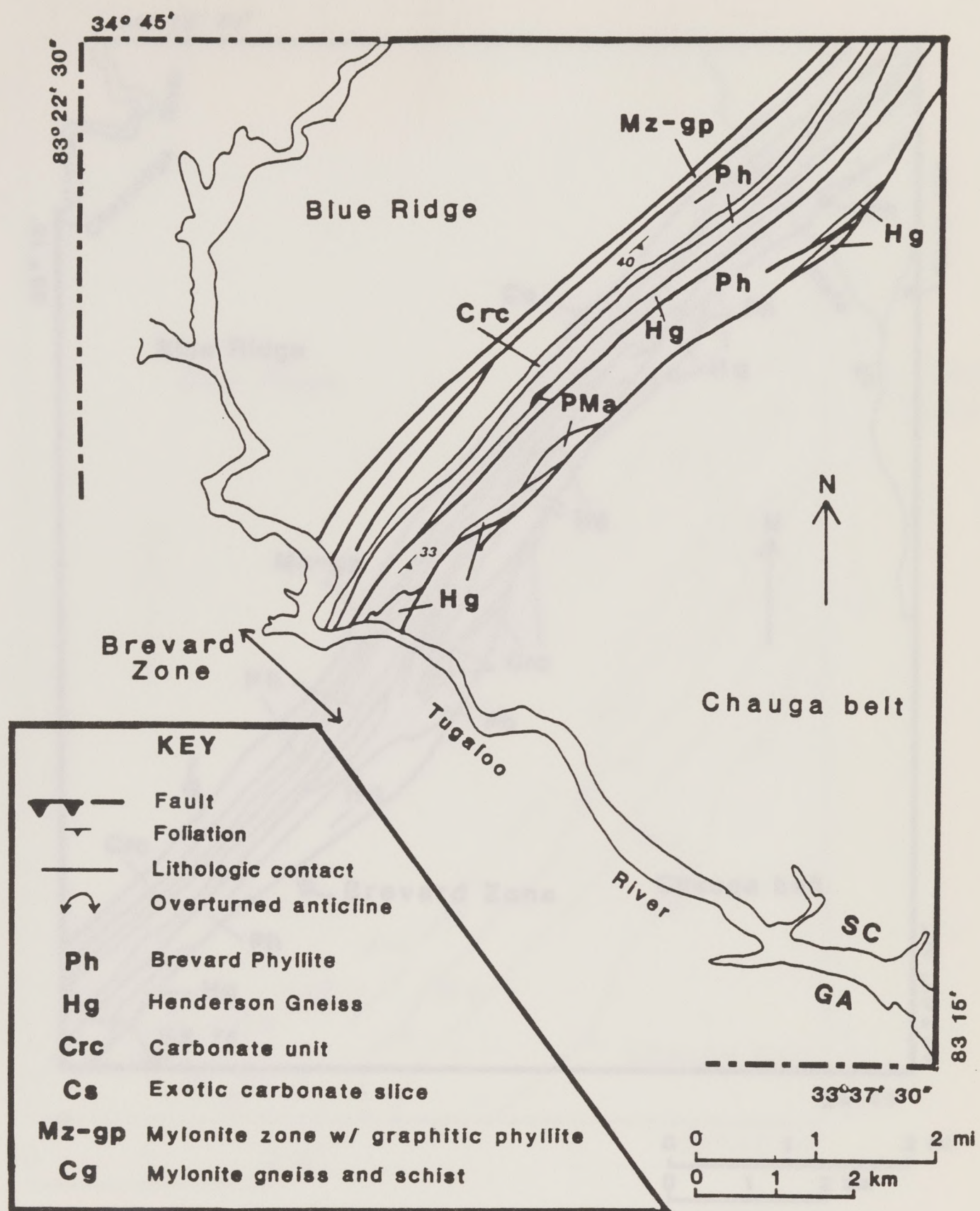


Fig. 7. Geologic map of Tugaloo quadrangle, SC: See Fig. 2 for location (simplified from Hatcher, 1969). Heavy line weight represents faults.



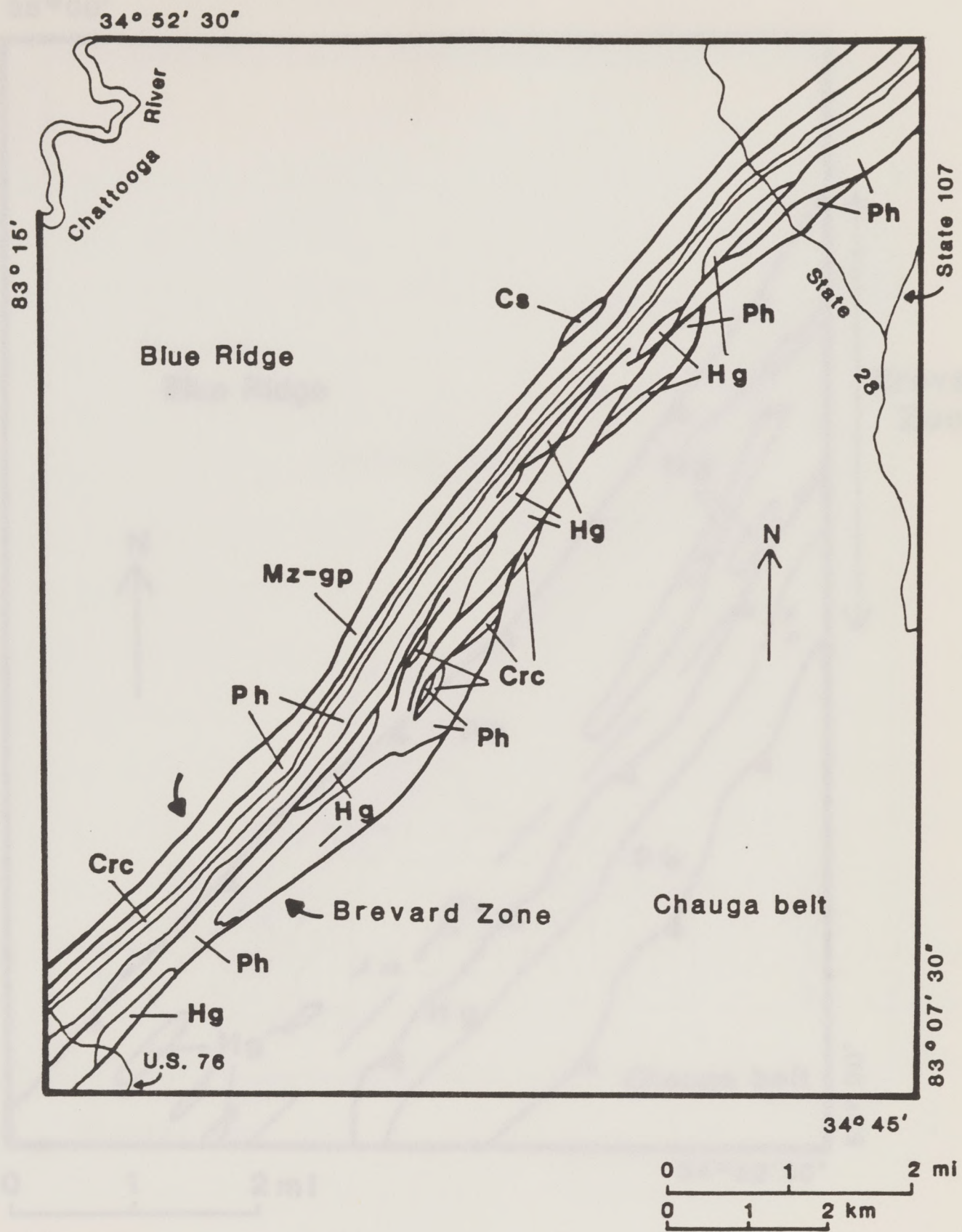


Fig. 8. Geologic map of Whetstone quadrangle, SC: See Fig. 2 for location and Fig. 7 for explanation of symbols (simplified from Hatcher, 1969).



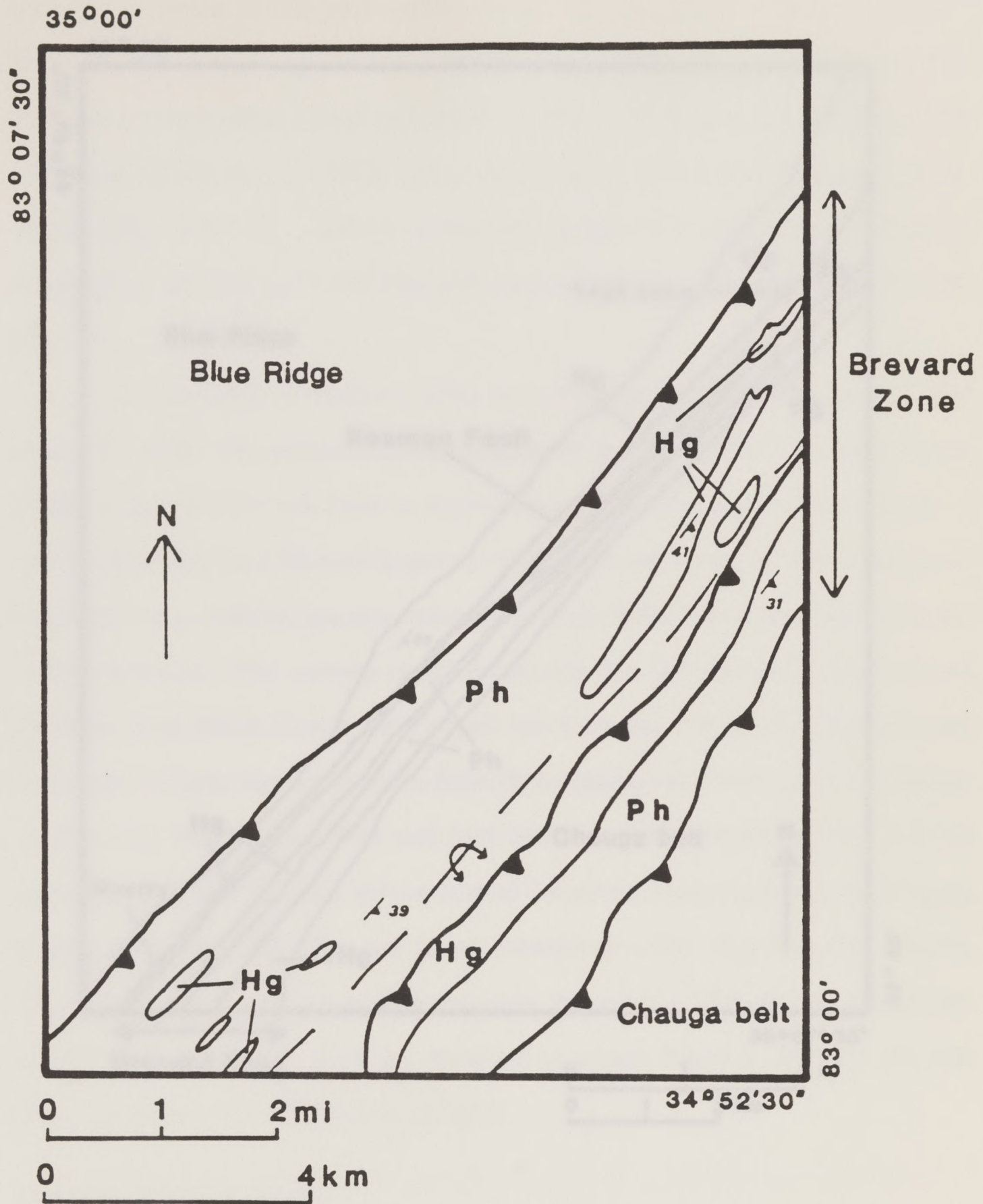


Fig. 9. Geologic map of Tamasee quadrangle, SC: See Fig. 2 for location and Fig. 7 for explanation of symbols (Roper and Justus, 1973).



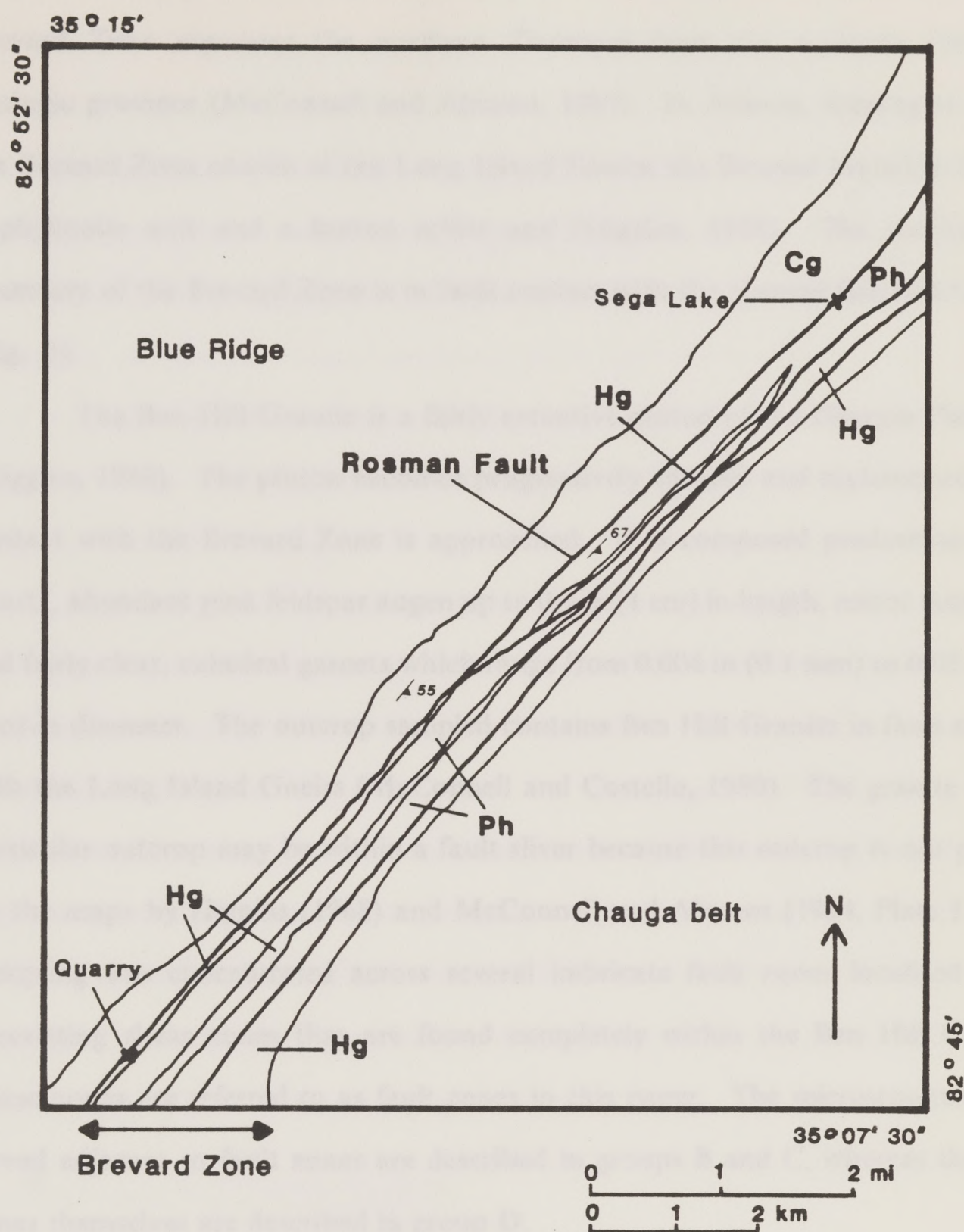


Fig. 10. Geologic map of Rosman quadrangle, NC: See Fig. 2 for location and Fig. 7 for explanation of symbols (simplified from Horton, 1982).



sistent with those in the northeastern areas. In the greater Atlanta region the Brevard Zone separates the northern Piedmont from the southern Piedmont geologic province (McConnell and Abrams, 1984). In Atlanta, lithologies within the Brevard Zone consist of the Long Island Gneiss, the Brevard Mylonite Gneiss, a phyllonite unit and a button schist unit (Higgins, 1968). The southeastern boundary of the Brevard Zone is in fault contact with the sheared Ben Hill Granite (Fig. 3).

The Ben Hill Granite is a fairly extensive pluton of the Georgia Piedmont (Higgins, 1968). The pluton becomes progressively sheared and mylonitized as its contact with the Brevard Zone is approached. It is composed predominantly of quartz, abundant pink feldspar augen up to 0.4 in (1 cm) in length, minor muscovite and fairly clear, euhedral garnets which range from 0.004 in (0.1 mm) to 0.03 in (0.8 mm) in diameter. The outcrop sampled contains Ben Hill Granite in fault contact with the Long Island Gneiss (McConnell and Costello, 1980). The granite at this particular outcrop may be within a fault sliver because this outcrop is not present on the maps by Higgins (1968) and McConnell and Abrams (1984, Plate I East). Sampling was concentrated across several imbricate fault zones localized along preexisting shear zones that are found completely within the Ben Hill Granite. These zones are referred to as fault zones in this paper. The microstructures observed adjacent to fault zones are described in groups B and C, whereas the fault zones themselves are described in group D.

## MICROSTRUCTURES

The remainder of this paper describes the microstructures, associated direction(s) of motion, and deformation conditions for each of the four groups of



features recognized. Groups are discussed in their order of overprinting relationships. Not all features and their relationships are found in each thin section. Several reasons for this absence are 1) mesoscopic/microscopic changes in lithology which may affect the development of a particular feature; 2) strain partitioning on a mesoscopic or greater scale; 3) local perturbations in the stress field; 4) obliteration of preexisting features due to later overprinting; and 5) features are not pervasively developed. Thus, microstructures have been correlated by similar morphologies, orientations, senses of shear and deformation conditions. Table 1 lists the observed microstructures in the order in which they are discussed and the group to which each is assigned.

Appendix A contains tables for each quadrangle which list thin sections, their orientation with respect to lineation and foliation in the rock, and the microstructures found in each section. Appendix B contains stereonet plots of lineations, slickensides and fold axes by quadrangle. Features such as compressional(?) crenulations, pressure shadows on opaque minerals, sheared veins, kinks and shear bands are several kinematic indicators that were also observed, but are not discussed because of their localized occurrence, varying geometry, unclear timing and inconsistent sense of shear. Descriptions of these microstructures are included in Appendix C.

## OLDEST MICROSTRUCTURES

The oldest recognizable microstructure is a pervasive foliation ( $S_1$ ) (Fig. 11). This prominent, southeast-dipping foliation is defined by quartz ribbons, muscovite and minor chlorite in quartzofeldspathic rocks, and by sheaves (buttons) or folia of muscovite, chlorite and some graphite in phyllitic rocks.  $S_1$  cannot be



<u>Relative Age</u>	<u>Group</u>	<u>Microstructure</u>
Oldest	Ungrouped	F <sub>1</sub> folds, not observed S <sub>1</sub> foliation Garnets
	Group A	F <sub>2</sub> folds S <sub>2</sub> axial planar foliation F <sub>3</sub> folds coaxial with F <sub>2</sub>
	Group B	Type II s-c microstructures C-surfaces F <sub>4</sub> folds Garnet pressure shadows
	Group C	Extensional crenulation cleavage
	Retrograde metamorphism	
Youngest	Group D	Mesoscopic and microscopic faulting and brecciation

**Table 1. Microstructure groupings:** Categorized on the basis of orientation and sense of shear.

included in the other groupings because the timing and direction of motion during formation cannot be determined except that it predates all microstructures in groups A-D. Recall that the isoclinal F<sub>1</sub> folds of Roper and Dunn (1973) which deform S<sub>0</sub> were not observed in the areas studied for this project.

Scattered garnets are present in the northeastern areas, predominantly in the upper and lower Brevard phyllite. These once euhedral garnets are fractured, cloudy and extremely altered (Fig. 12). Many garnets are so weathered that they





**Fig. 11. Foliation in the Brevard phyllite:** Note the presence of a recrystallized quartz ribbon (QR) which, in part, define  $S_1$  (Tu4, ss = unknown, xnicols, ld = 4.75 mm).

have lost their high relief and isotropic character. Garnet size ranges from 0.006 in (0.15 mm) to 0.23 in (5.9 mm).

The majority of garnets have quartz and/or opaque mineral inclusions which are either randomly oriented or overgrowing a relic foliation. "Snowball" garnets, although they record the rotation direction during growth, are not considered reliable kinematic indicators in this study because of their extreme rarity and



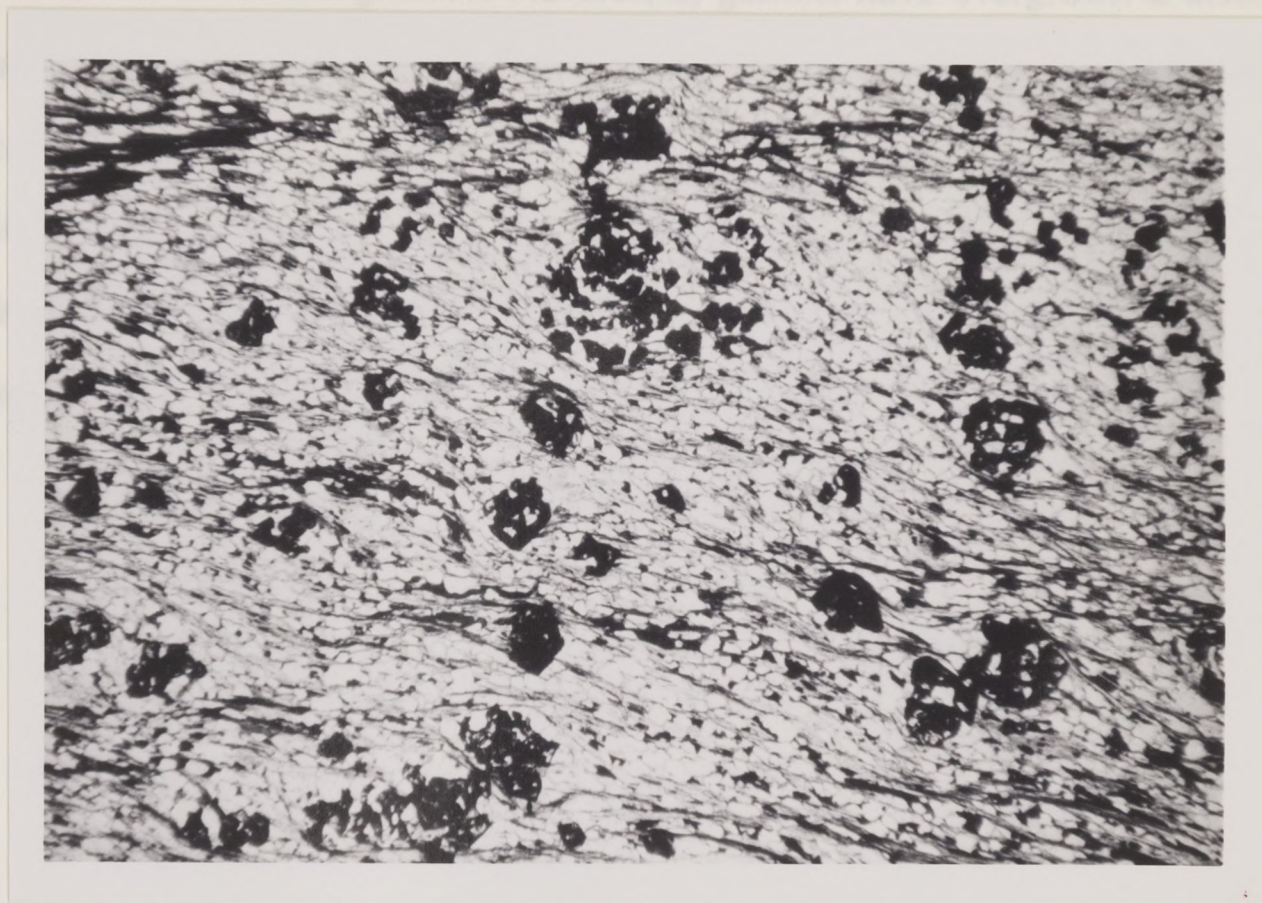


**Fig. 12. Weathered garnets:** from the Brevard Phyllite (Wh127D, plane light,  $ld = 4.75$  mm).

their possible reorientation during later deformation(s). "Snowball" structures are usually poorly defined and are observed only in samples Wh127D and Ta150A.

Garnet compositions were not determined in this study, however, on the basis of their similar appearance and textural relationships, all garnets in the Brevard Zone in the northeastern areas are believed to be associated with the same early metamorphic event. Metamorphic grade at this time was at least as high as the staurolite zone of epidote-amphibolite facies metamorphism because staurolite



was observed in two samples of Brevard Phyllite (Ta143 and Ta143A). Structural or petrologic evidence linking garnets to the prominent foliation ( $S_1$ ) is that: 1) they are both the oldest recognizable features; 2) garnets have overgrown a discernible foliation; and 3) all later events apparently occurred at lower temperature because muscovite defines an axial planar foliation in later folds. Therefore, the relative timing of metamorphism represented by these garnets is prior to formation of group A features, and probably syn- or postkinematic with respect to formation of the foliation,  $S_1$ .

Roman quadrangles

## FOLDS

Numerous asymmetric, open to closed,  $F_1$  folds which plunge west to northwest (Fig. 13) are best seen in sections normal to the foliation and foliation. These folds fold the preexisting  $S_1$  foliation. In this plane folds have the lower limb sheared out (note particularly where  $S_1$  foliation is sheared out). Although asymmetric folds are often not the most reliable kinematic indicators, these  $F_1$  folds are reliable because they have a consistent sense of asymmetry, i.e. to the northwest, and no larger folds are observed in the area. However, this evidence does not rule out the possibility that  $F_1$  folds are primary in a large undeformed fold in the Chocoma belt to the northeast.

In places where hinges of isoclinal  $F_2$  folds are found in sections and sections of muscovite. These hinges are marked by coarse muscovite blades that have re-crystallized at an angle to the sheared out limbs of the original isoclinal fold (Fig. 14). These relict hinges could be  $F_2$  fold hinges, rather than  $F_1$  hinges.



## GROUP A

Microstructures in Group A are  $F_2$  folds, a secondary foliation ( $S_2$ ), and  $F_3$  folds. The folds and  $S_2$  are grouped together because: 1)  $S_2$  is axial planar to  $F_2$  folds, and 2) they all appear to have formed under a west to northwest-directed thrust motion.

Atlanta samples do not contain group A features. Hence the following discussion pertains only to features present in Tugaloo, Whetstone, Tamassee and Rosman quadrangles.

## FOLDS

Numerous asymmetric, open to isoclinal, intrafolial  $F_2$  folds which verge west to northwest (Fig. 13) are best seen in sections normal to the lineation and foliation. These folds fold the preexisting foliation. In rare places folds have the lower limb sheared out (not pictured) which clearly shows the direction of shear. Although asymmetric folds are often not the most reliable kinematic indicators, these  $F_2$  folds are reliable because they have a consistent sense of asymmetry, i.e. to the northwest, and no larger folds are observed in the zone. However, this evidence does not rule out the possibility that  $F_2$  folds are parasitic to a larger unobserved fold in the Chauga belt to the southeast.

In places relict hinges of isoclinal  $F_2$  folds are found in sheaves and buttons of muscovite. These hinges are marked by coarse muscovite blades that have recrystallized at an angle to the sheared out limbs of the original isoclinal fold (Fig. 14). These relict hinges could be  $F_1$  fold hinges, rather than  $F_2$  hinges.





**Fig. 13. Group A folds:** Asymmetric and isoclinal  $F_2$  folds deform  $S_1$  (quartz ribbons and muscovite), (Tu40, plane light,  $l_d = 6.35$  mm).

$F_3$  folds are coaxial with  $F_2$  folds (Fig. 15) indicating that they may have formed because of continued shearing in the same deformation as  $F_2$ .  $F_3$  folds are only observed in Tu89.

There are also scattered  $F_2$  folds which can be traced in cuts that are parallel, or approximately parallel to the lineation. These cuts are slightly oblique to  $F_2$  and  $F_3$  fold axes. The slight difference in orientation of these folds may be a result of the lithology, local changes in the direction of motion during deformation, or later shearing.

Quartz-feldspar layers and quartz ribbons in  $F_2$  and  $F_3$  folds have been highly, but not completely, recrystallized by subgrain enhancement (Figure 11). The surrounding matrix, which has also recrystallized, is finer-grained due to dis-



seminated muscovite which inhibited grain growth. Most grains exhibit smooth grain boundaries and uniform to undulatory extinction, although discontinuous undulatory extinction and subgrains are present. Some features in group B are also highly recrystallized suggesting that if group A features were partially recrystallized during their formation, then conditions during formation of group B may have increased their degree of recrystallization. None of the samples in this study contain evidence of annealing such as triple grain boundaries or pervasive uniform extinction in quartz grains. This absence and the presence of subgrains indicates that annealing did not occur.

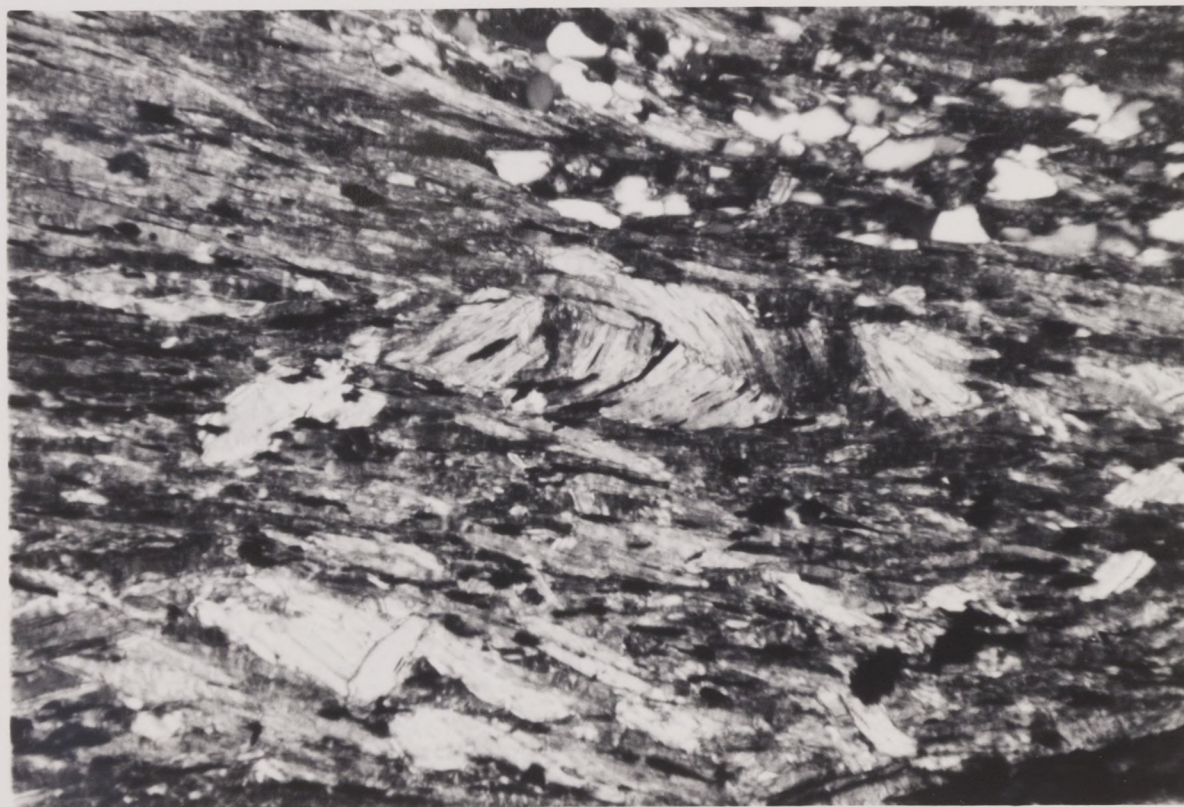


**Fig. 14.** Relic hinges of early isoclinal folds: Hinges found in muscovite sheaves in the Brevard Phyllite. These are either  $F_1$  or  $F_2$  hinges. (Tu32, xnicols,  $ld = 1.5$  mm).



## AXIAL PLANAR FOLIATION

In some places tight  $F_2$  folds, discussed above, exhibit a weakly developed, southeast-dipping, axial-planar foliation,  $S_2$ , of needle-like blades of muscovite (Fig. 16). In thin section this axial planar foliation is oriented from  $0^\circ$  to  $37^\circ$  clockwise from  $S_1$ . In some isoclinal folds  $S_2$  is parallel to and indistinguishable from  $S_1$  except in fold hinges. A secondary foliation is present in many sections at  $20^\circ$ - $30^\circ$  in the same clockwise orientation from  $S_1$  as  $S_2$  but no  $F_2$  folds are visible. This foliation is also defined by scattered muscovite grains and in sections

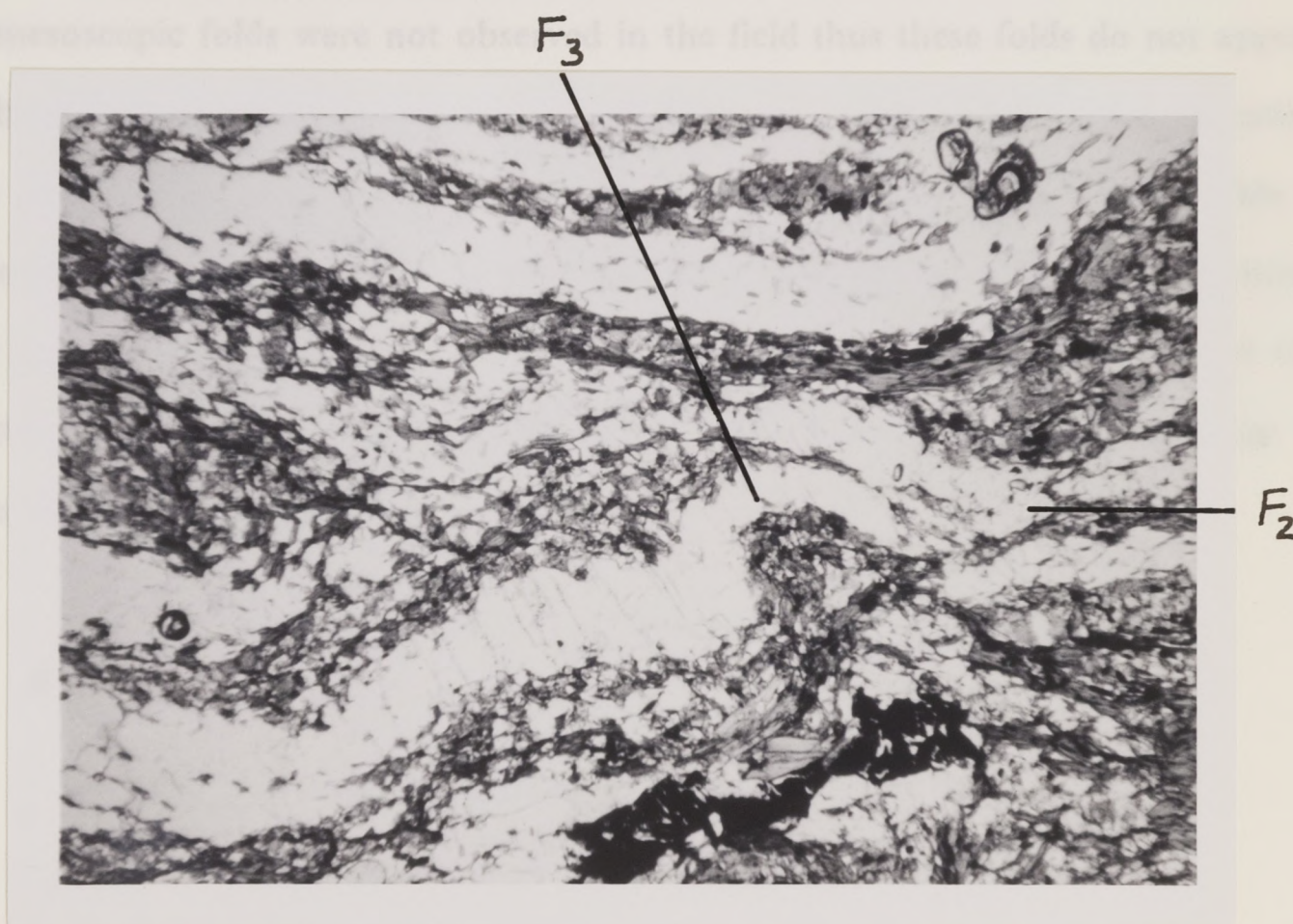


**Figure 15.** Group A coaxial folds: These  $F_3$  folds deform a preexisting  $F_2$  fold in a quartz ribbon (Tu89, plane light,  $ld = 3.95$  mm).



without  $F_2$  folds, it is equated with the axial-planar foliation ( $S_2$ ) because they have the same character and general orientation with respect to  $S_1$ .

## SUMMARY

Group A features consist of asymmetric  $F_2$  folds,  $F_3$  folds that appear coaxial with  $F_2$ , and a poorly-developed secondary foliation,  $S_2$ , which is axial-planar to  $F_2$  folds.  $F_2$  deforms the preexisting foliation ( $S_1$ ) which is the oldest recognizable feature and is of unknown age and origin. Asymmetric  $F_2$  and  $F_3$  microfolds indicate a bulk motion of west- to northwest-directed thrusting that occurred under ductile conditions. These asymmetric folds are reliable kinematic indicators because: 1) all folds have a consistent asymmetry and direction of motion; 2) mesoscopic folds were not observed in the field thus these folds do not appear to be parasitic folds; 3) in rare places folds have a sheared out lower limb indicating the direction of motion; and 4) the thrusting motion indicated by these folds is compatible with both a Taconic and Alleghanian history whereas normal faulting, the alternative, is not compatible. This shear sense is consistent throughout the northeastern study areas. The Ben Hill Granite does not contain any group A microstructures.



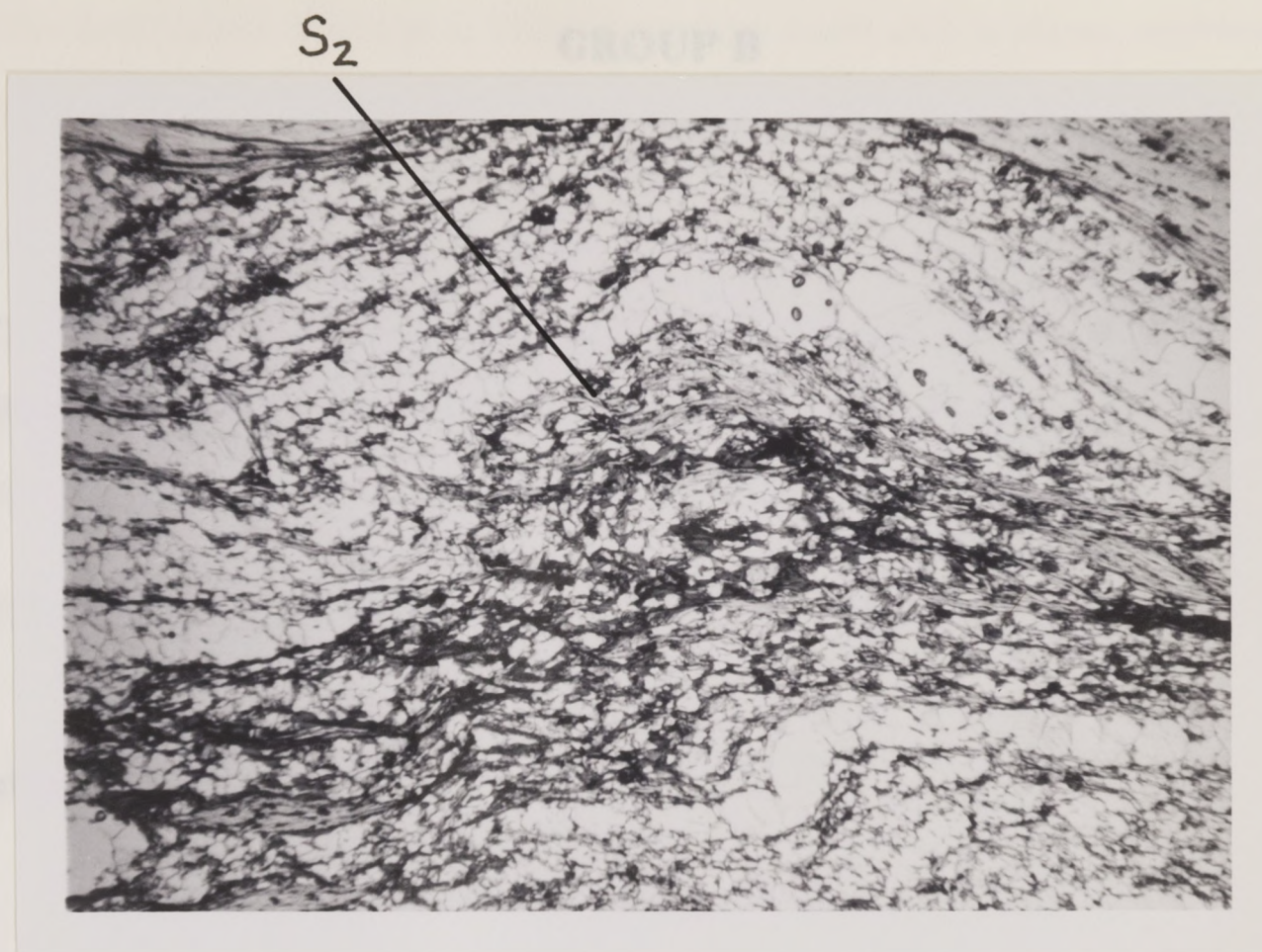


**Fig. 16. Axial planar foliation to Group A folds: Muscovite defines  $S_2$  in  $F_2$  folds (Tu32, plane light,  $1d = 4.95$  mm).**



## GROUP B

Group B microstructures include type II s-c mylonites, c-surfaces, minor  $F_4$  folds and garnet pressure shadows. These features are grouped together because they were formed under ductile deformation conditions and, more importantly, they indicate a dextral strike-slip period of shearing in the Brevard Zone with a possible thrust component. For sample locations see plates in back pocket.

### TYPE II S-C MYLONITES

#### Northeastern areas

In the Tugaloo, Whetstone, Tamasssee and Rosman quadrangles, type II s-c mylonites (Lister and Snoke, 1984) are present only within the Henderson Mylonite, as this lithology is the only one appropriate for the formation of such a feature (Mosher et al., 1985). These structures are seen in thin sections cut perpendicular to foliation and parallel to the northeast-trending, subhorizontal mineral lineation in the zone. This lineation, although usually faint, is present in virtually all samples and is always in the same general orientation (see Appendix B). In the Henderson Mylonite, lineation is defined by a streaking of quartz ribbons, augen tails and minor muscovite, and is undoubtedly a kinematic **a** lineation. In the Brevard Phyllite, the lineation is defined by an elongation of muscovite and chlorite which appears parallel to  $F_2$  and  $F_3$  (group  $\Lambda$ ) fold axes, suggesting that this lineation is a kinematic **b** lineation.

Type II s-c mylonites contain s and c surfaces using the terminology of Berthe et al. (1979). In the Henderson Mylonite, s-surfaces are defined by: 1) rare



to abundant, round to elongate feldspar porphyroclasts and, in places, recrystallized tails of feldspar and some quartz (Fig. 17); 2) scattered muscovite folia; 3) folia which wrap porphyroclasts (Fig. 18); 4) elongate grains in the matrix; and in places by 5) a dimensional preferred orientation of obliquely recrystallized quartz that shows a strong crystallographic preferred orientation (Fig. 19). C-surfaces (zones of high shear strain) are defined by fairly continuous, planar zones of muscovite and rare biotite and by tails on porphyroclasts which wrap smoothly into c-surfaces, giving some indication of the direction of motion ( Figs. 17 and 20). Zones are usually 0.3 mm or less in width and are regularly spaced in thin sections at up to 1.5 mm increments. Spacing between c-surfaces varies among sections.

Recrystallized tails of feldspar which, in part, define s and c surfaces, reflect high temperatures and/or slow strain rates during deformation. These structures are true s-c mylonites because s and c-surfaces formed simultaneously as indicated by recrystallized augen tails (s-surfaces) that wrap into c-surfaces.

Areas of more intense strain or smaller shear zones occur within the Henderson Mylonite. In Rosman, NC, just east of the US64 and Rt178 junction, several small shear zones, which strike and dip parallel to the Brevard Zone, were observed within the Henderson Mylonite. These zones were also noted by Bond (1974) and Sinha and Glover (1978). An example, shown in Fig. 21, is 11 in (27.5 cm) wide, well-exposed and well-indurated. Thin sections taken across the zone indicate a decrease toward the center of the zone in augen size and abundance and in muscovite content, but an increase in very thin zones of muscovite rather than disseminated grains. Progressing inward from SzA and SzE, which have a very similar appearance in thin section, to SzD in the center of the zone, there is: 1) an increase in extremely fine-grained recrystallized layers in the matrix; 2) an increase



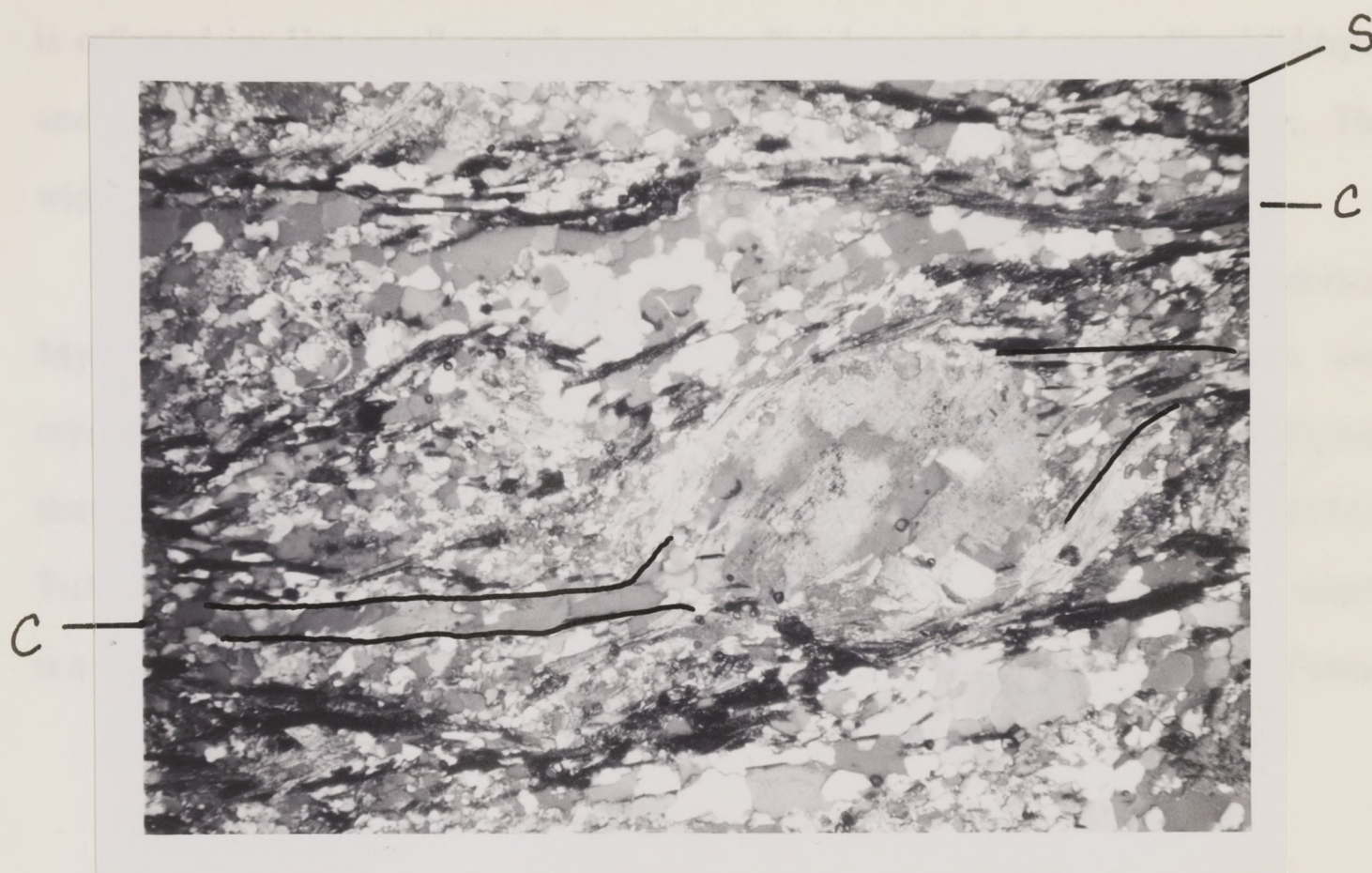


**Fig. 17. S-surfaces in Type II s-c mylonite from the Henderson Mylonite:** are defined by feldspar augen with long, recrystallized tails (outlined). Tails wrap into c-surfaces (Tu31, gypsum plate, ss = dextral, ld = 5.55 mm).

in the grain size in recrystallized quartz ribbons; and 3) an increase in the completeness of recrystallization in ribbons, i.e. grain boundaries are more distinct and grains somewhat more equidimensional (compare Fig. 22 to Fig. 23).

There is also a faint type II s-c microstructure developed in SzD (not pictured) where s-surfaces are defined by elongate grain and subgrain shapes and scattered muscovite grains, and c-surfaces are defined by very thin zones of finely recrystallized muscovite.

Ros126A was collected from the Henderson Mylonite in an adjacent shear zone near the fault contact of the mylonite with the Brevard Phyllite (Plate IV



overlay for Horton, 1982). In this shear zone high shear strain during deformation is reflected in: 1) a small c-surface spacing; 2) a long tail of recrystallized feldspar and quartz (Fig. 24); and 3) a lack of many augen in outcrop and thin section. The width of this particular shear zone is unknown due to lack of exposure.

An example from Tugaloo quadrangle of a shear zone in the Henderson Mylonite shows poorly-developed to undeveloped type II structures and crystallographic preferred orientations of quartz (Tu92 and Tu137B) (Fig. 25), less than 30 ft (10 m) from a well-developed type II s-c microstructure (Tu137A). Tu137A also exhibits a crystallographic preferred orientation of quartz grains which is a result of partial oblique recrystallization (Fig. 19). The close proximity of these

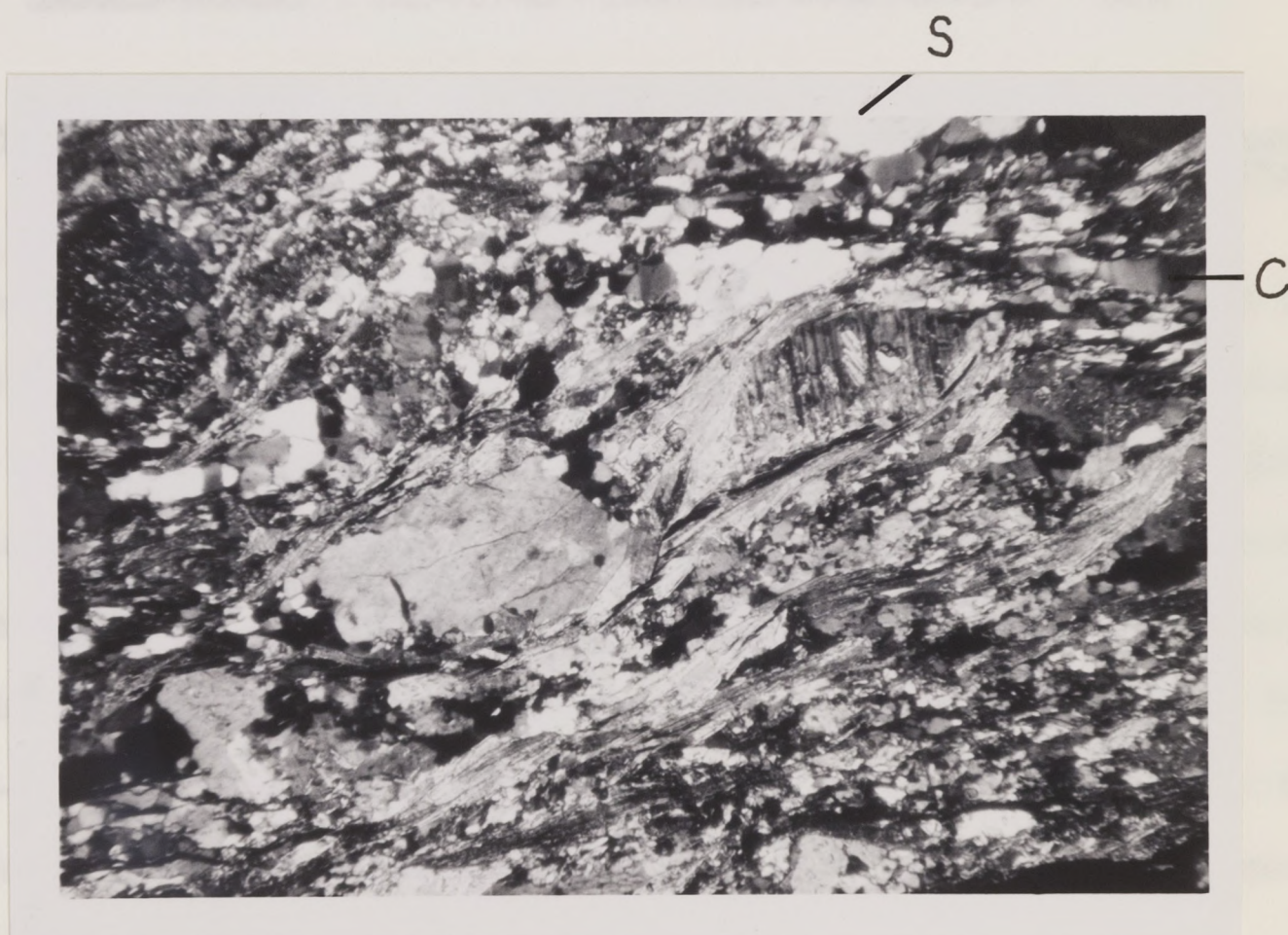


**Fig. 18.** S-surfaces defined by muscovite folia: Folia wrapping elongate porphyroclasts also define S in the Henderson Mylonite (Wh138, xnicols, ss = dextral, ld = 4.35 mm).





**Fig. 19. S-surfaces defined by dimensional preferred orientation:** of elongate subgrains in quartz ribbons, from the Henderson Mylonite (Tu137A, gypsum plate, ss = dextral, ld = 4.35 mm).

three samples and their differences in microstructure development, suggest that Tu137A is from a small shear zone although this zone was not observed in outcrop.

In summary, well-developed type II s-c mylonites are present in Tugaloo, Whetstone, Tamasssee and Rosman. The orientation of these microstructures indicates that they formed during dextral strike-slip motion. The presence of recrystallized quartz indicates that deformation occurred under ductile conditions. Type II s-c microstructures may be concentrated in discrete, small-scale shear zones. One zone indicates a component of oblique-slip (thrust) motion (Fig. 21) when microstructures in SzD are reoriented.



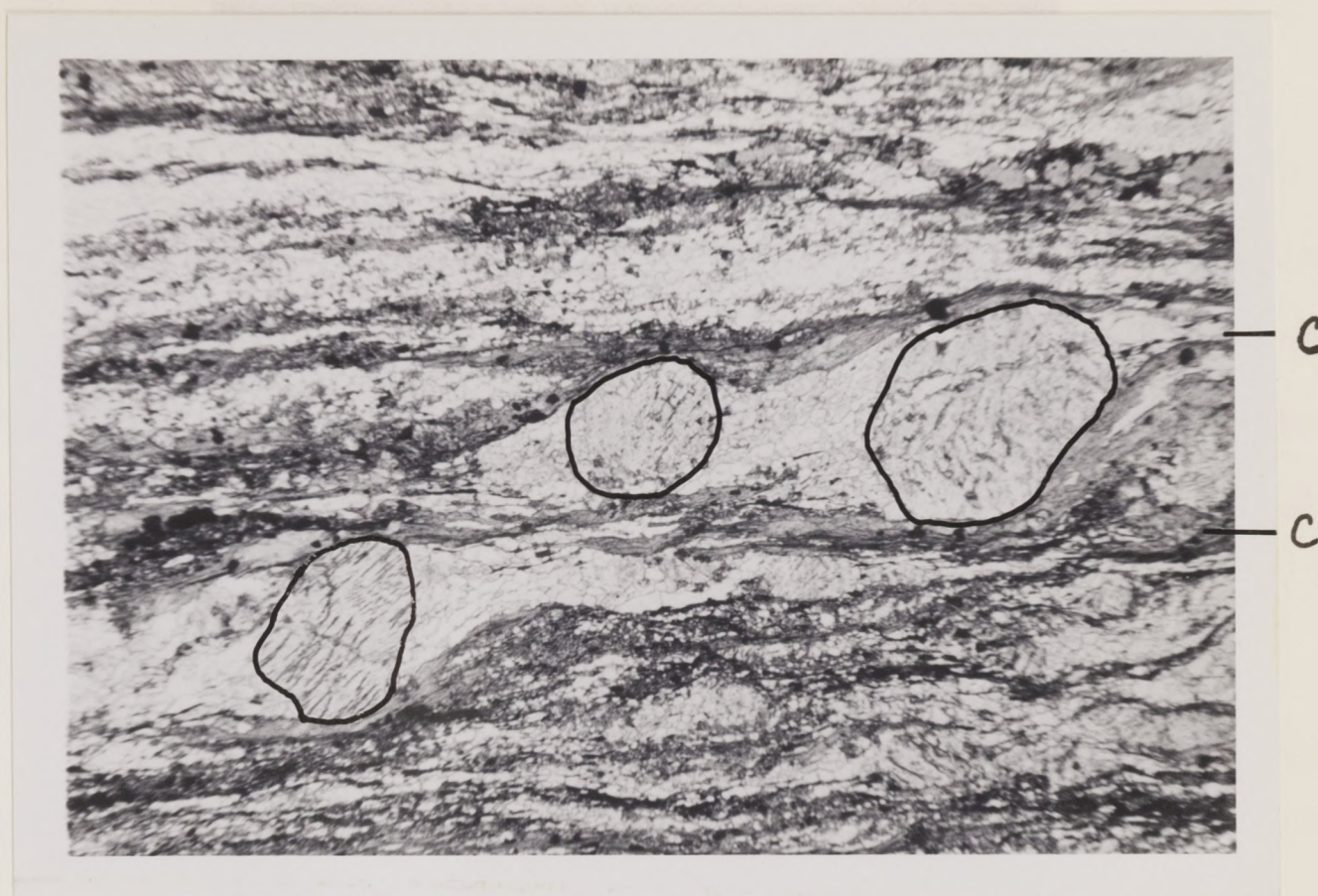


**Fig. 20. C-surfaces are defined by muscovite and biotite:** Large tails wrap into C's, from the Henderson Mylonite (Wh127C, plane light, ss = dextral, ld = 12.7 mm).

#### Atlanta area

Type II s-c mylonites are also present in Atlanta samples adjacent to relatively narrow fault zones in the sheared Ben Hill Granite (see for reference Fig. 43). These structures are found in sections cut perpendicular to the foliation and parallel to the lineation. Recall that foliation and lineation in the Ben Hill Granite have the same general orientation as that in the northeastern study areas. Abundant quartz ribbons and minor muscovite define the foliation. Lineation is defined by recrystallized feldspar tails on feldspar augen and ribbons of quartz (Appendix B).

Type II microstructures in Atlanta samples differ only slightly from those previously discussed. Here, s-surfaces are defined by very small, elongate feldspar



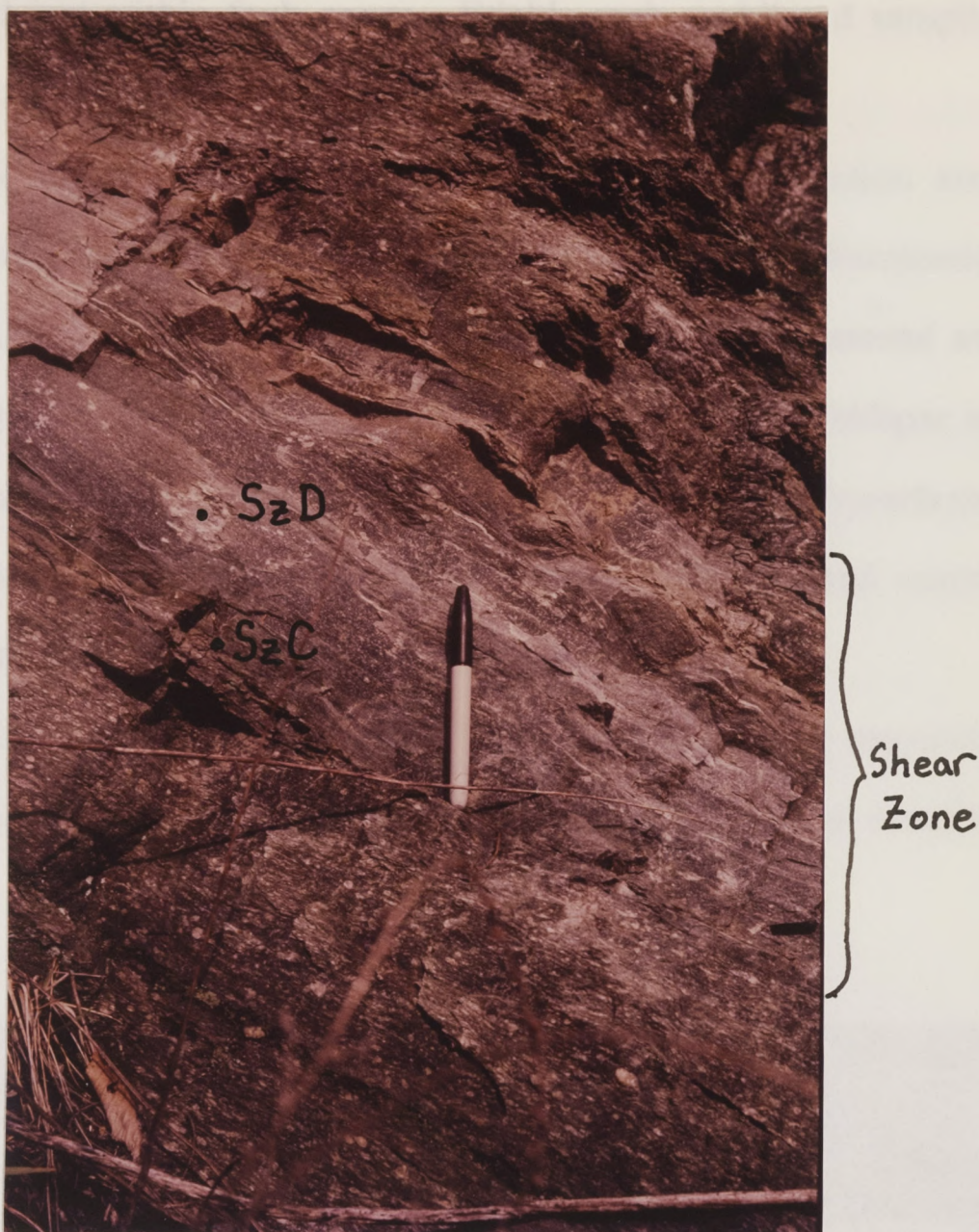


**Fig. 21. Shear zone in Henderson Mylonite:** Note abrupt absence of augen in center of zone. Sample locations, where pictured, are labeled. (Rosman quadrangle).

augen and oblique subgrains in quartz ribbons. C-surfaces are marked by extremely fine-grained muscovite (Fig. 26). Partial oblique recrystallization, by both subgrain enhancement and bulge nucleation, is responsible for the development of a dimensional preferred orientation of quartz and feldspar (Fig. 27). Thin layers in the quartzofeldspathic matrix are extremely fine-grained, a result of dynamic recrystallization during mylonitization. Type II microstructures are only developed



adjacent to and just within fault zones. Friable rock prohibited sampling in the center of these zones.

Away from fault zones mylonitization and recrystallization are less advanced, grain size is coarser, and augen are more abundant. Extremely sheared quartz ribbons, yet unrecrystallized quartz ribbons are well-preserved away from fault zones (Fig. 28). Quartz-feldspar tails are present on some feldspar augen and recrystallization has developed around the edges of some porphyroclasts. Alteration to sericite is extensive in some feldspar porphyroclasts and matrix grains. Annealed textures are not present in any of the samples studied.

In all five study areas, type II microstructures and their associated augen tails and quartz ribbons were formed under ductile deformation conditions at a



**Fig. 22.** Henderson Mylonite away from shear zone: (SzA, plane light,  $1d = 13.7$  mm).



relatively high temperature and slow strain rate. When these microstructures are reoriented, they indicate a dextral strike-slip sense of shear possibly with a thrust component.

## OTHER C-SURFACES

The Brevard Phyllite in the northeastern areas does not exhibit type II structures because its lithology is inappropriate, i.e., a lack of feldspar porphyroclasts and quartz, and a predominance of muscovite. C-surfaces are recognized in lineation-parallel thin sections as this orientation appears to be parallel to their kinematic direction. Thus, dextral shearing is expressed in phyllite units as

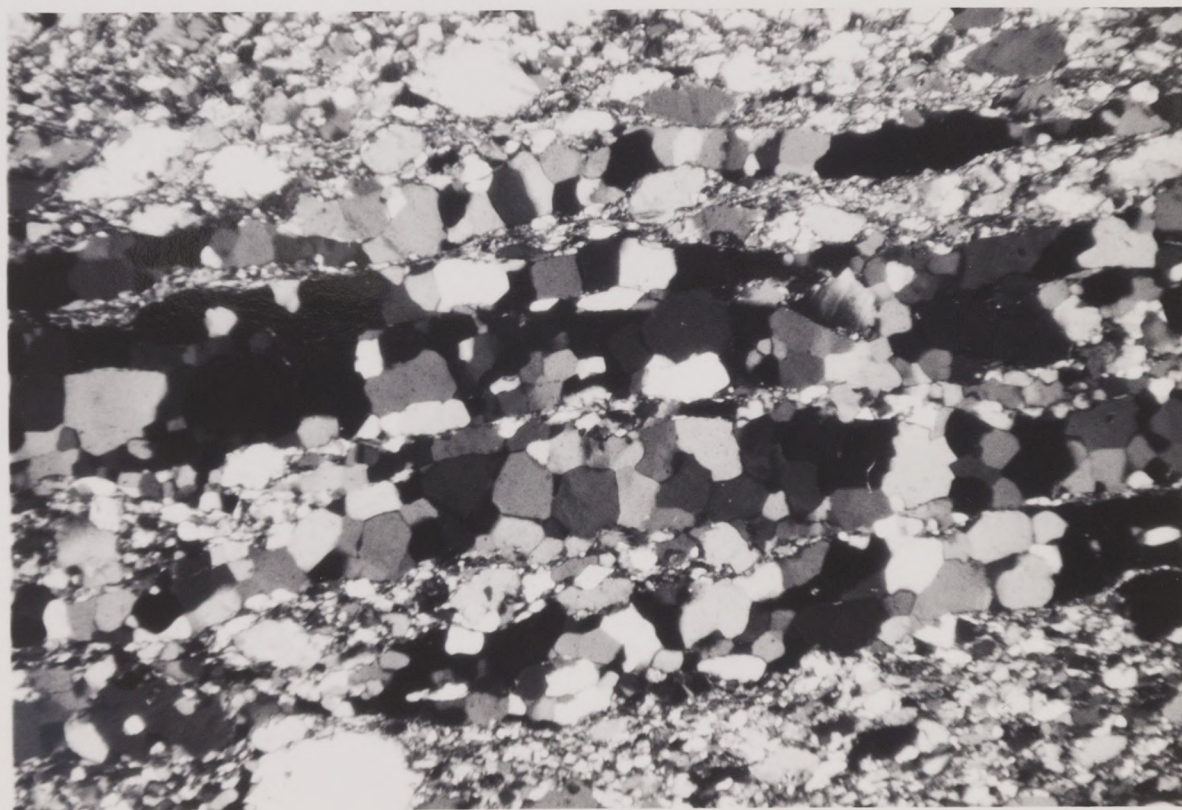


**Fig. 23. Highly recrystallized quartz ribbons:** From ultramylonite in center of shear zone in the Henderson Mylonite (SzD, xnicols,  $ld = 4.75$  mm).



c-surfaces which crosscut the preexisting foliation ( $S_1$ ) rather than as type II s-c microstructures.

These c-surfaces are defined by muscovite ( $S_1$ ) which bends smoothly but abruptly into c-surfaces. C-surfaces (Fig. 29) are thin, planar zones of muscovite and rarely biotite, 0.25-1.0 mm wide but slightly wider where poorly developed. C-surfaces are often iron-stained and fairly discontinuous in thin section. Figure 30 shows the sheared edge of a garnet indicating offset and high shear strain along this c-surface. An extensional crenulation cleavage (ECC from group D) which deforms this c-surface is also pictured in Figure 30. Note that garnet pressure shadows are wrapping into the c-surface. Muscovite has not recrystallized

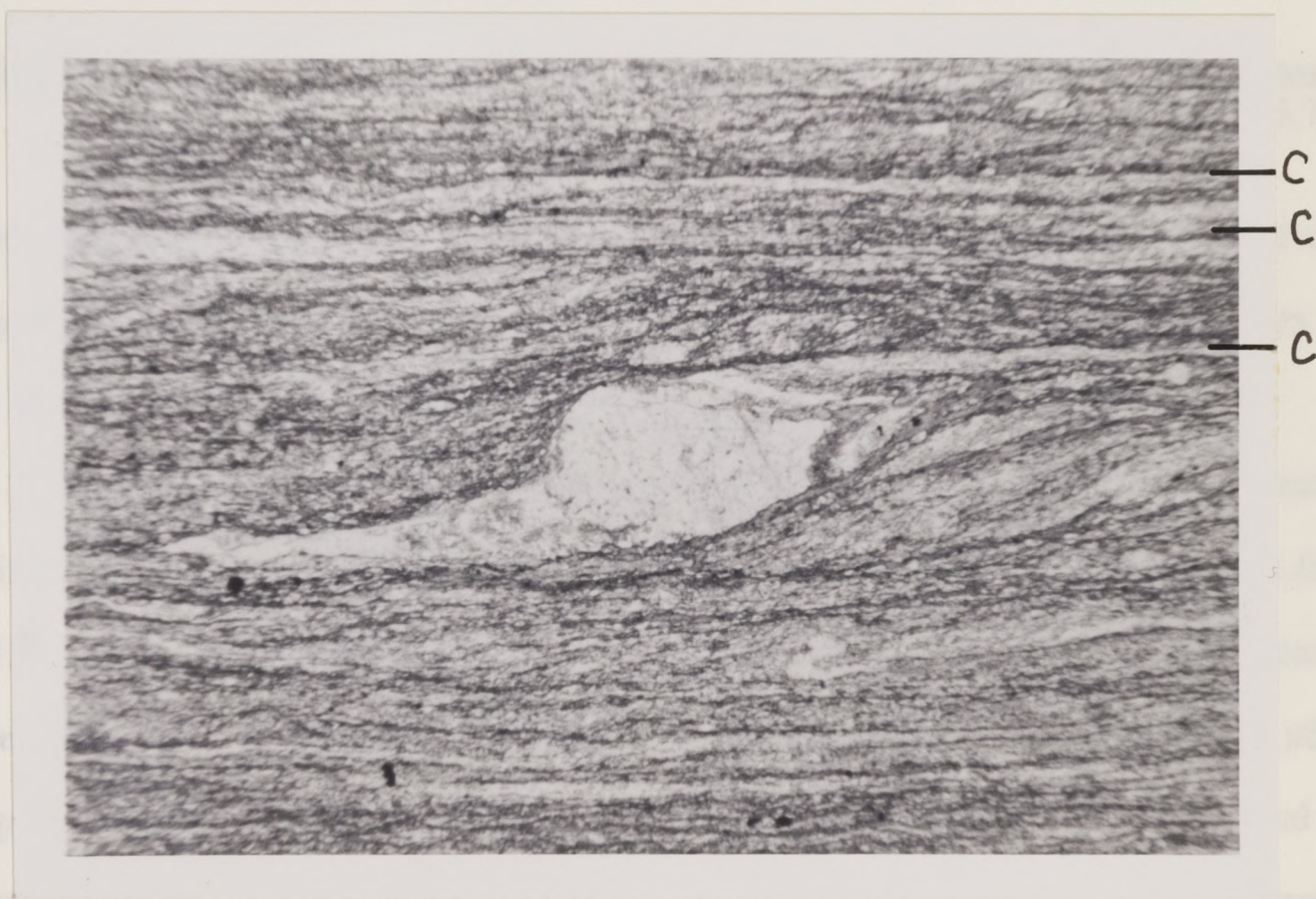


**Fig. 24.** High shear strain in type II mylonite: resulted in a long quartz-feldspar tail and small c-spacing (Ros126A, plane light, ss = dextral, ld = 11.76 mm).



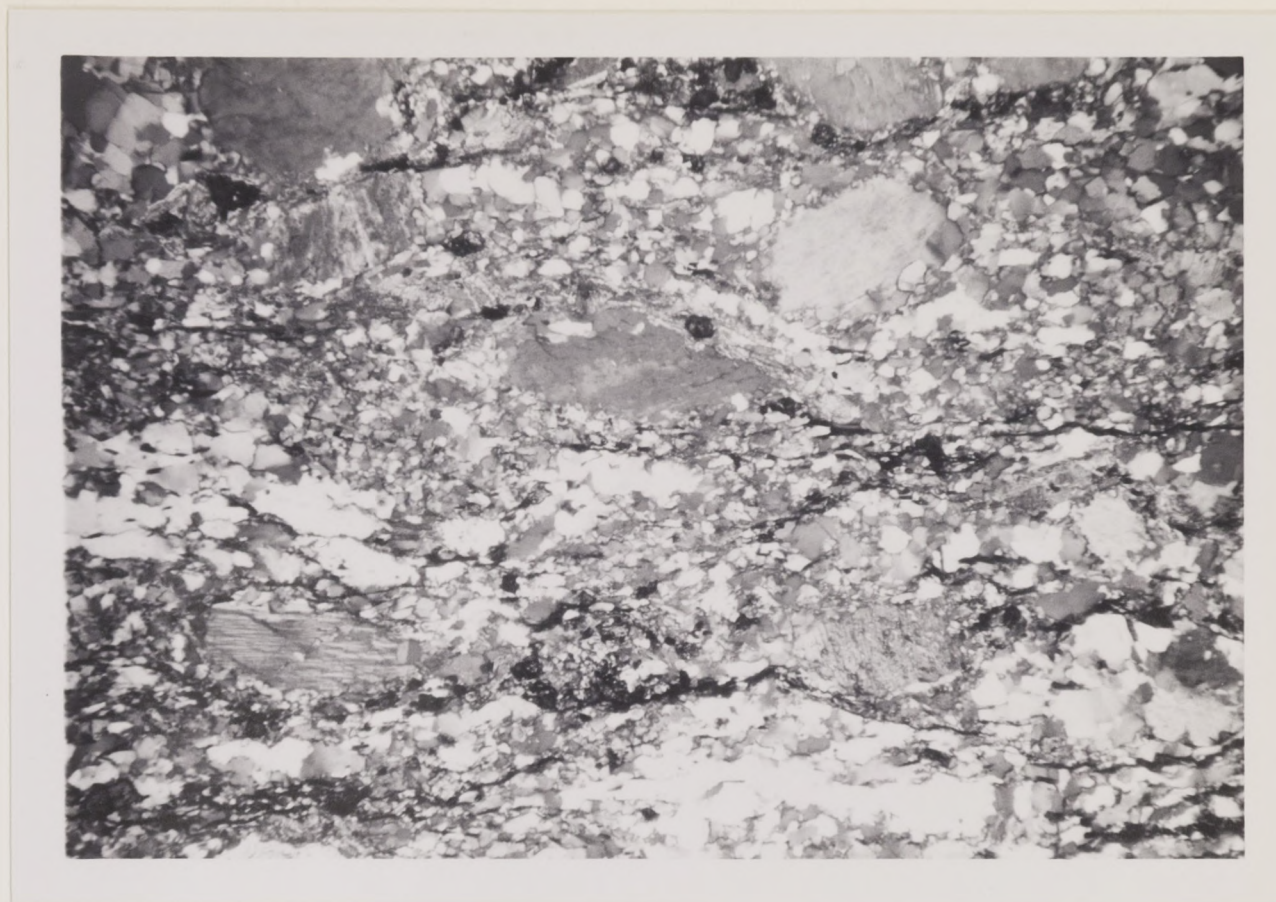


**Fig. 25. No microstructure development outside a small shear zone:** Compare to Fig. 19 collected inside the zone. (Tu92, gypsum plate,  $ld = 5.75$  mm).

along c-surfaces. Figure 29 illustrates the crosscutting nature of a c-surface with earlier, preexisting  $F_2$  folds, indicating that s-surfaces (i.e.  $S_1$ ) and c-surfaces did not form synchronously and thus are not true s-c microstructures.

The c-surfaces strike northeast and dip southeast, with an approximately horizontal trace in most thin sections.  $S_1$  ranges from  $28^\circ$  to  $50^\circ$  clockwise from this trace, but  $30^\circ$  to  $40^\circ$  is the most common orientation. C-surfaces appear to have the same angular relationship with  $S_1$  and the same apparent sense of offset as group D extensional crenulations. However, the two features are separated because extensional crenulations are at an angle to c-surfaces and they deform c-surfaces (see for example Figs. 30 and 37). When crosscutting relationships are



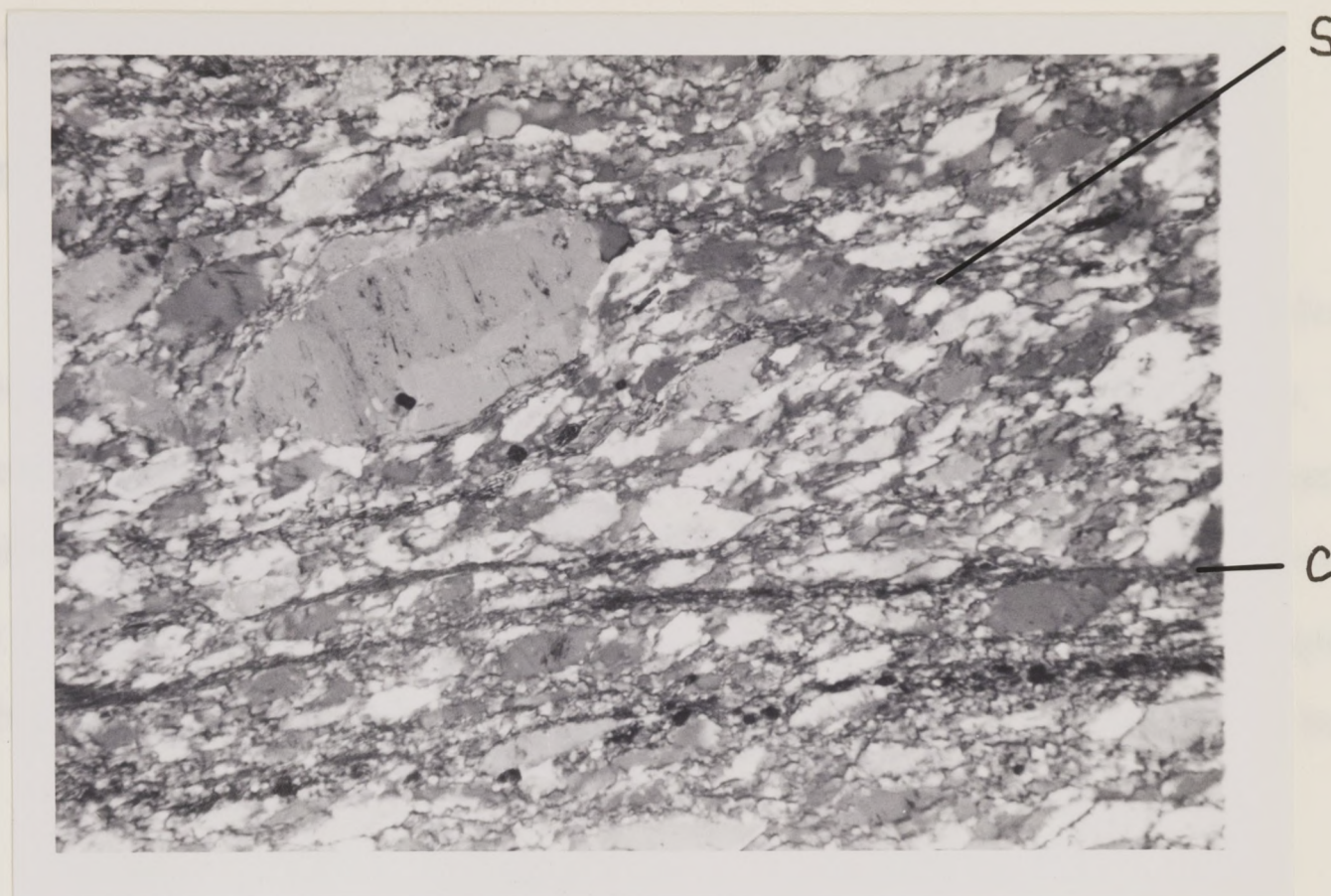


**Fig. 26. Type II s-c mylonite:** S's defined by elongate grains. C's marked by extremely fine-grained muscovite in the Ben Hill Granite (At5, ss = dextral, gypsum plate, ld = 2.26 mm)

absent, these two fabrics are difficult to distinguish, even in thin section, because of the lithology or their lack of development (see Fig. 38).

Deformation conditions cannot be well constrained, although muscovite has not recrystallized along c-surfaces but bends into parallelism with c-surfaces.

C-surfaces have been found only within the Tamassee study area adjacent to the Brevard/Blue Ridge contact (see Appendix A). They are not present in the majority of phyllite samples collected possibly because of strain partitioning, that is, movement occurred along discrete small-scale shear zones as was the case with type II s-c microstructures in the Henderson Mylonite. Alternatively, this absence could be a function of exposure and sampling. C-surfaces are included in group B



because they reflect the same dextral strike-slip movement history and ductile conditions as other group B microstructures.

## FOLDS

A number of microfolds ( $F_4$  folds) which support an episode of dextral shearing in the Brevard zone are present, but only in the northeastern areas. The Ben Hill Granite where sampled does not contain either mesoscopic or microscopic folds. In the northeast  $F_4$  folds are present in northeast-trending sections, parallel to the lineation. These are ductile folds, most of which deform recrystallized quartz ribbons or quartz-feldspar layers. All folds discussed below are believed to be  $F_4$



**Fig. 27. Crystallographic preferred orientation in a type II s-c mylonite:** Augen tail (outlined) wraps into a c-surface from the Ben Hill Granite (At5, gypsum plate, ss = dextral, ld = 4.75 mm).



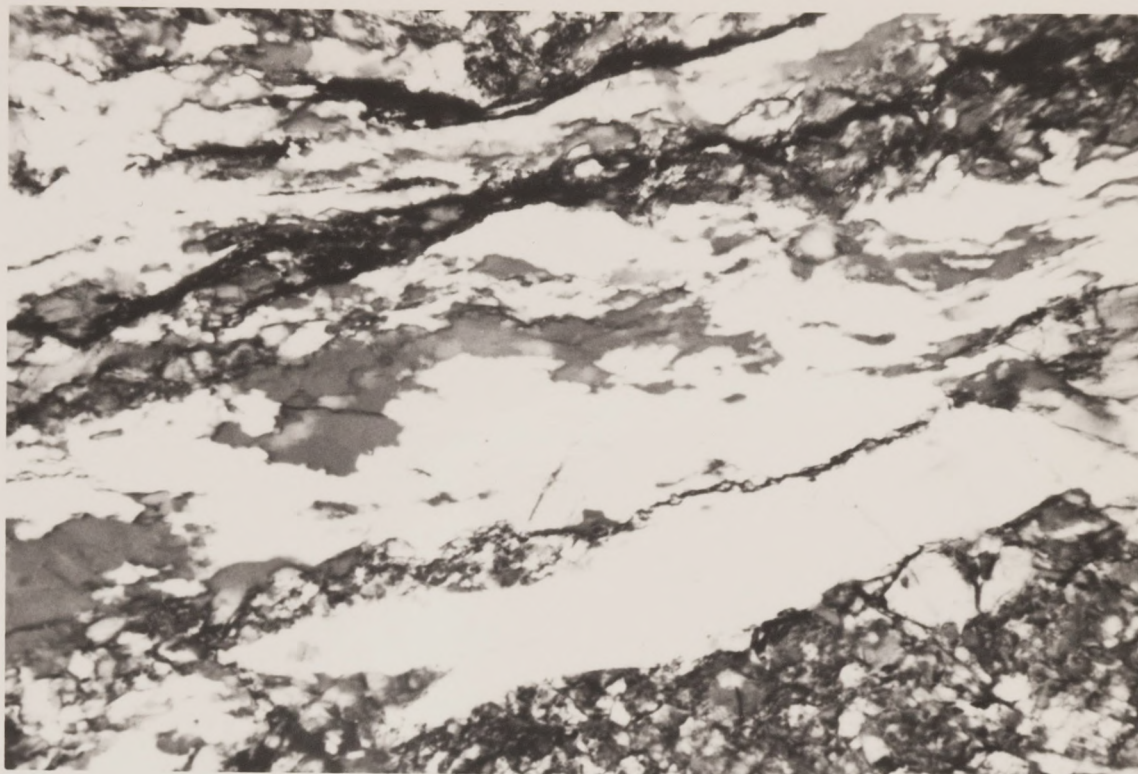


**Fig. 28. Highly deformed quartz ribbons:** Ribbons are not extensively recrystallized, from the Ben Hill Granite (At12, gypsum plate, ss = dextral, ld = 1.86 mm).

folds and to have formed as a result of dextral shearing under ductile conditions. Thus these  $F_4$  folds are group B features on the basis of their orientation and overprinting relationships.

Several examples of  $F_4$  folds which appear only in lineation-parallel sections are Ta153 from the Brevard Phyllite (Fig. 31) and Ros126A and Tu78A (not illustrated) from the Henderson Mylonite. All three contain southwest-verging folds (southeast plunging axes). No fold interference patterns are present in these samples even though  $F_4$  fold axes are approximately perpendicular to  $F_2$  and  $F_3$  fold axes discussed previously. The Brevard Phyllite (Ta153) contains tightly folded quartz-feldspar layers ( $F_4$  folds) which verge southwest and contain an axial planar





**Figure 29. C-surface defined by deflected muscovite:** This c-surface truncates a probable group A fold (outlined) (Ta143, xnicols, ss = dextral, ld = 5.55 mm).

muscovite foliation (Fig. 31). This foliation is present throughout the slide. Ros126A contains a similar southwest-verging fold in hand sample and Tu78A contains a southwest-verging microfold that deforms a type II s-c microstructure. The latter crosscutting relationship suggests that  $F_4$  folding occurred just after the formation of type II microstructures during continued dextral shearing.

It is significant that these  $F_4$  folds do not appear in lineation-normal (northwest-trending) cuts and sections because this suggests that the kinematic **a** direction of these folds lies in a lineation-parallel (southwest-trending) orientation, i.e. parallel to the thin section.

Figure 30. A c-surface has defined group A and deflected group A folds in the Brevard Phyllite (Ta143, plane light, ss = dextral, ld = 4.75 mm).



Evidence for interference between  $F_2$  and  $F_4$  folds is present in mutually perpendicular sections Tu23 and Tu23A. Tu23, oriented normal to the lineation, contains northwest-verging asymmetric  $F_2$  folds. Tu23A, oriented parallel to the lineation and normal to Tu23, contains a possible interference pattern which resulted from shearing of the preexisting  $F_2$  folds in Tu23 (Figs. 32). Interference patterns are not unusual or unlikely because dextral shearing in a northeast-trending shear zone, of preexisting, northwest-verging  $F_2$  and  $F_3$  folds, will not reorient fold axes, but rather shear out fold limbs in the new shear direction. In some instances (e.g. Wh52A) folds can be traced from lineation-parallel to lineation-normal cuts. This observation suggests that locally some  $F_2$  and  $F_3$  fold axes are



**Figure 30.** A c-surface has sheared garnets: and deflected pressure shadows in the Brevard Phyllite (Ta150A, plane light, ss = normal for ECC, ld = 4.75 mm).



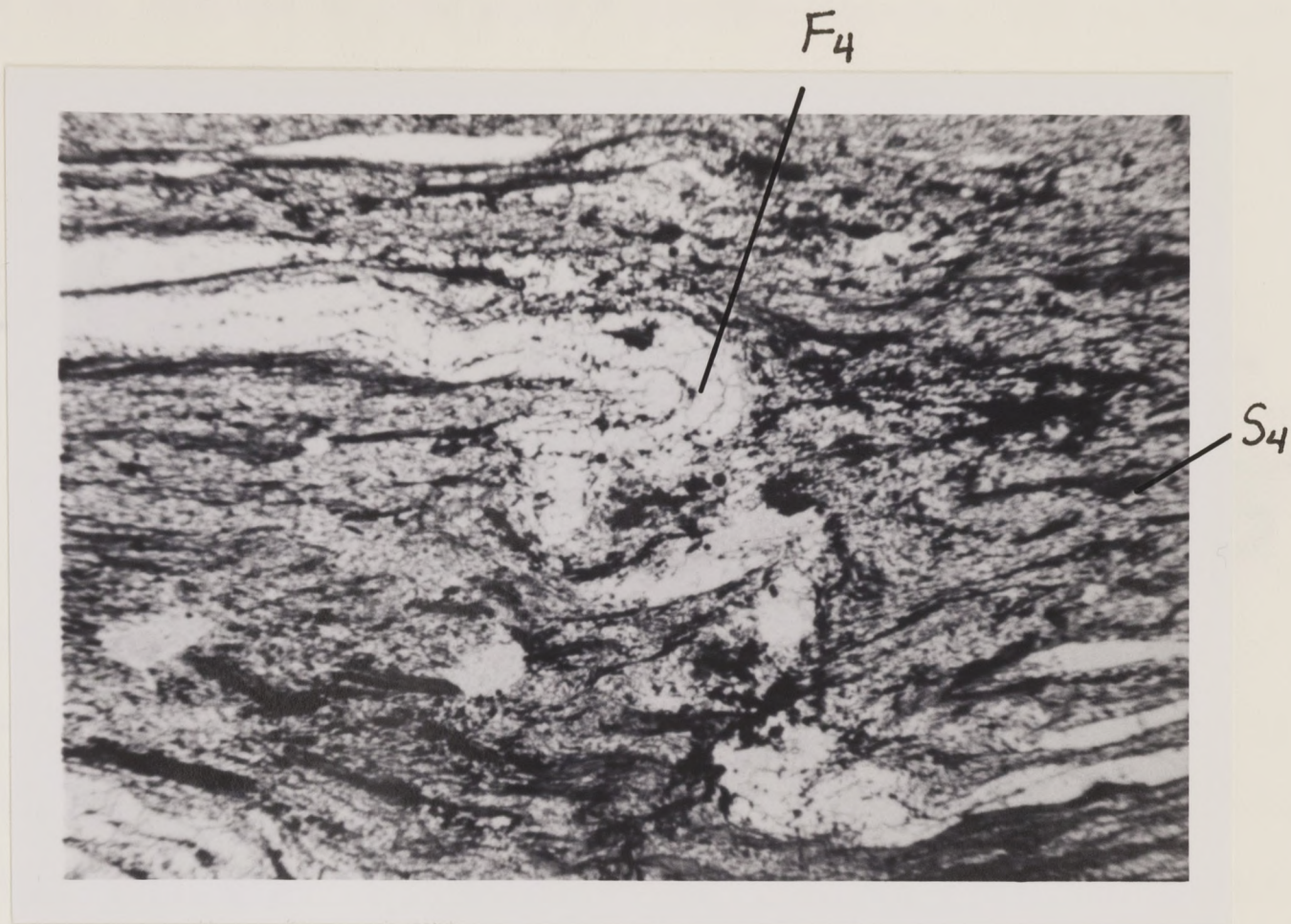


**Fig. 31. Group B fold:**  $F_4$  fold with an axial planar foliation of muscovite, from the Brevard Phyllite (Ta153, plane light, ss = dextral, ld = 11.76 mm).

oblique to the dominant northeast trend and/or that locally  $F_4$  fold axes are oblique to the dominant southeast trend of other  $F_4$  axes. Alternatively, dextral shearing with an oblique-slip component could be responsible for  $F_4$  folds with oblique fold axes. Thus dextral shearing of preexisting  $F_2$  and  $F_3$  microfolds probably resulted in: 1) the observed interference pattern; and 2) the scattered lineation-parallel folds which can be traced in lineation-normal cuts.

One problem with the above explanation for lineation-parallel folds ( $F_4$  folds) is the presence of isoclinal folds ( $F_2$  folds) in muscovite sheaves also found in lineation-parallel sections (Fig. 29). The latter folds are group A features because they have the same morphology as  $F_2$  and  $F_3$  folds and they are truncated



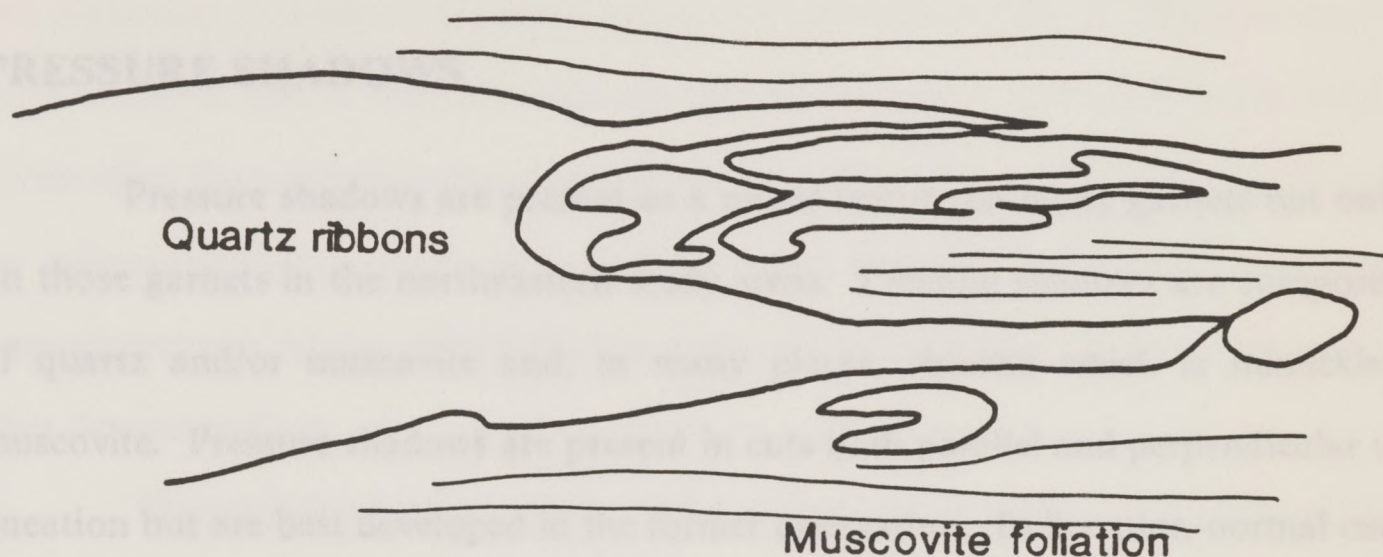


**Fig. 32. Sketch of a possible fold interference pattern:  $F_2$  and  $F_4$  fold interference resulted from dextral shearing in quartz-rich Brevard Phyllite (Tu23A).**

by c-surfaces (Fig. 29). A possible explanation for group A folds within sections cut normal or at a high angle to the original vergence direction of these folds is that strike-slip motion rotated preexisting muscovite buttons, some of which contained  $F_2$  folds. Rotation of buttons is feasible because of their high muscovite content. However, reorientation of folded quartz layers and ribbons ( $F_2$ ) due to later shearing (discussed earlier) is less likely because of the competent nature of  $F_2$  folds. Thus, some  $F_2$  folds are now present in cuts approximately perpendicular to their original vergence direction.

In summary, the presence of southwest-verging, open to tight  $F_4$  micro-folds, with southeast-dipping axes, indicates that some folding occurred during, or



just after, formation of other group B microstructures as a result of continued dextral shearing. Possible interference patterns of  $F_4$  with  $F_2$  folds are evidence of dextral shearing of preexisting, northwest-verging  $F_2$  folds from group A.

## PRESSURE SHADOWS

Pressure shadows are present as a minor feature on many garnets but only on those garnets in the northeastern study areas. Pressure shadows are composed of quartz and/or muscovite and, in many places, chlorite which is mimicking muscovite. Pressure shadows are present in cuts both parallel and perpendicular to lineation but are best developed in the former orientation. In lineation-normal cuts pressure shadows are shorter and usually present on only one side of garnets indicating that they are not as well-developed as in lineation-parallel cuts (Compare Fig. 30 and Fig. 36 with Fig. 33). These differences in development suggest that some pressure shadows are group A features that were largely obliterated by a more recent deformation (i.e. dextral shearing) and/or that the kinematic  $a$  direction for pressure shadows is lineation-parallel.

Pressure shadow formation occurred after garnet growth. Thus garnets are group A features or older and pressure shadows are group B features. Pressure shadows formed just prior to, or synchronous with, c-surfaces because shadows bend smoothly into c's (Fig. 30), and are in the proper orientation to have been formed by the same sense of shear. Furthermore, crosscutting relationships with extensional crenulations indicate pressure shadows formed prior to group C features.

Fig. 33. Poorly developed pressure shadows (muscovite or quartz) present on only one side of garnets in lineation-parallel cuts (Tal50A1, plane light,  $\lambda d = 4.95 \text{ mm}$ )



## SUMMARY

Group B microstructures useful for determining sense of shear are type II s-c mylonites, c-surfaces,  $F_4$  folds and garnet pressure shadows. These ductile features indicate that a dextral strike-slip period of motion occurred in the Brevard Zone after the northwest-directed thrusting responsible for the formation of group A microstructures. Some thin sections from group B (SzD and Ta143) have microstructures whose orientation suggests an oblique-slip, thrust component to this dextral motion.

Group B features post-date group A features because: 1) c-surfaces truncate possible group A folds in muscovite sheaves; and 2) microstructures from the

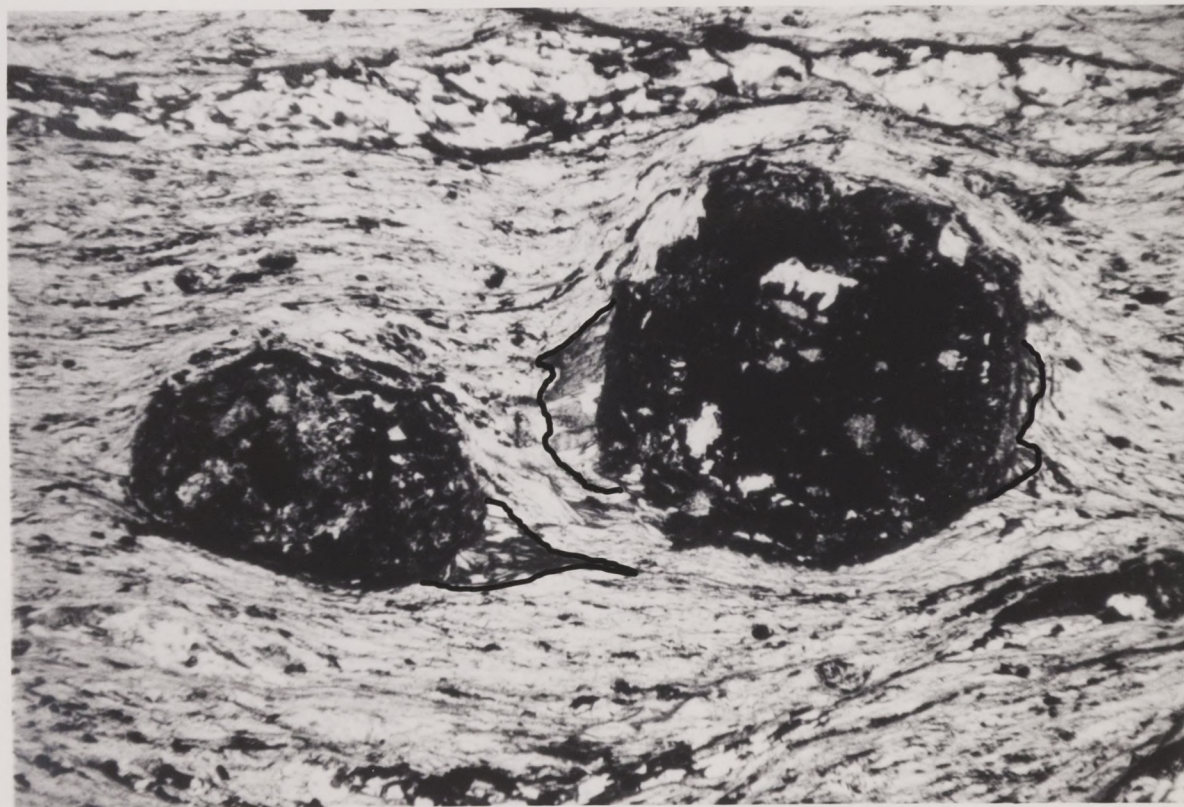


**Fig. 33. Poorly developed pressure shadows:** Shadows (outlined) are usually present on only one side of garnets in lineation-normal sections (Ta150A1, plane light,  $ld = 4.95$  mm).



two groups reflect different directions of bulk motion in the Brevard Zone. Dextral oblique-slip motion can account for west-verging folds in group A, but not for those folds that verge northwest, further suggesting separate episodes of motion, but not necessarily distinct deformation events.

### EXTENSIONAL CREULATION CLEAVAGE

The extensional cleavage in the section is a result of extension of the preexisting  $S_1$  foliation and is related to extensional unroofing of the BCC using the terminology of Platt (1986). The term "extensional unroofing" is used to describe these features because the process of unroofing involves a definite component of extension along  $S_1$ . The BCC has the following characteristics: 1) creulations are very open; 2) cleavage lies at a low angle ( $< 10^\circ$ ) to the enveloping surface of the older foliation; 3) cleavage is related to the unroofing of intense deformation; 4) it occurs in rocks with a very strong preexisting foliation and 5) the sense of displacement along cleavage most often is a component of extension parallel to the preexisting foliation (Platt, 1986). Platt (1986) also notes that ECC are responsible for the burial shift of major-sense thrust faults in many shear zones. Refer to Platt and Vissler (1980, p. 402-403, Figs. 5 and 7) for other field and thin section examples of extensional unroofing.

ECC's are fairly common in the section studied which is possibly a function of sampling. ECC's, however, are significant microstructures for two reasons: 1) they are geographically pervasive as they are found in all sample zones



## GROUP C

Three sets of crenulations are considered group C microstructures. One set of crenulations is definitely a result of extension of the preexisting foliation. The other two sets are either compressional or extensional crenulations which cannot be used as kinematic indicators because of their questionable origin. These two crenulations and an associated foliation are described in Appendix C.

### EXTENSIONAL CRENULATION CLEAVAGE

The crenulation discussed in this section is a result of extension of the preexisting  $S_1$  foliation and is called an extensional crenulation cleavage or ECC using the terminology of Platt (1979). The term ECC rather than shear band is used to describe these features because the presence of necked quartz ribbons indicate a definite component of extension along  $S_1$ . An ECC has the following characteristics: 1) crenulations are very open; 2) cleavage lies at a low angle ( $< 45^\circ$ ) to the enveloping surface of the older foliation; 3) cleavage is defined by narrow zones of intense deformation; 4) it occurs in rocks with a very strong preexisting foliation; and 5) the sense of displacement along cleavage zones results in a component of extension parallel to the preexisting foliation (Platt, 1979). Platt (1979) also states that ECC are responsible for the button-schist or augen-schist texture found in many shear zones. Refer to Platt and Visser (1980, p. 402-403, Figs. 6 and 7) for other field and thin section examples of extensional crenulations.

ECC's are fairly uncommon in the sections studied which is possibly a function of sampling. ECC's, however, are significant microstructures for two reasons: 1) they are geographically persistent as they are found in all sample areas



except in the Whetstone quadrangle; and 2) they all generally have the same orientation and local sense of shear. The local motion on ECC's is normal with top down to the southwest. These microstructures crosscut those in groups A and B. The orientation and sense of shear of ECC's is not compatible with either primary or secondary shears due to thrusting and/or strike-slip motion, that is, if ECC's are related to bulk motion on the Brevard Zone. Thus ECC's appear to reflect a change in the direction of motion.

### Northeastern areas

Extensional crenulation cleavages appear mainly in lineation-parallel sections. ECC's are localized in phyllites along the northwestern edge of the Brevard Zone in Tamassee and Rosman quadrangles and are found in both the Brevard Phyllite and Henderson Mylonite in the northwestern half of the zone in Tugaloo quadrangle. Localization may be apparent and a result of sample distribution in the first two areas, or it may be real and related to late, brittle faulting (group D). However, sample distribution in Tugaloo quadrangle suggests that ECC's are, in fact, localized at the Brevard Zone/Blue Ridge contact (see plate I) as are features in group 4. ECC's are not observed in Whetstone quadrangle possibly because of outcrop and sample distribution or their lack of development.

Most ECC's are poorly-developed in three dimensions. However, on the basis of those that are well-developed in hand sample, combined with lineation-normal thin sections from the same samples, the general orientation of ECC's was determined. The ECC plane varies in strike from north to west-northwest and dips west to south-southwest, with a mean northwest strike and southwest dip. Dips are



approximately  $25^{\circ}$ - $45^{\circ}$ , but may be slightly steeper at the Brevard/Blue Ridge contact (e.g. Ros118A) because  $S_1$  also steepens. The trace of ECC's in thin section lies between  $20^{\circ}$  to  $47^{\circ}$  counterclockwise from  $S_1$ . This angle varies along the length of individual traces. The local sense of shear on individual ECC's is always normal with top down towards the west to south-southwest. The orientation of ECC's cannot be more precisely determined because of their poor development in three dimensions. All of the photomicrographs in this section are from lineation-parallel thin sections.

Several examples of the ECC developed in the study area are Ta150B and Ros118A. Ta150B (Fig. 34) illustrates a quartz-feldspar layer that is extremely extended by a crosscutting ECC. Ros118A (Fig. 35) contains 3 parallel ECC's that have begun to extend and neck a quartz ribbon.

ECC's are demonstrably younger than the microstructures in groups A and B. ECC's deform group A folds (not pictured), group B pressure shadows (Figs. 36), preexisting c-surfaces (Figs. 37) and group B folds (Figs. 38). In thin section, ECC's can be differentiated from c-surfaces on the basis of the extensional nature, southwest dip direction of ECC and, in places, cross-cutting relationships. The strike of the ECC plane is approximately  $90^{\circ}$  to the strike of c-surfaces.

The ductile conditions under which ECC formed are reflected in necked muscovite sheaves, quartz ribbons (Fig. 39) and quartz-feldspar layers. Figure 39 contains a quartz ribbon which has undergone more recrystallization in the necked area of the ECC than elsewhere along the length of the ribbon. Recrystallization is more advanced in these necks because of the high strain associated with extension. Thus these areas had a higher dislocation density than the remainder of the ribbon and a greater potential for recrystallization with appropriate temperature.



### Atlanta area

Scattered ECC's are also present in lineation-parallel sections from the Ben Hill Granite. These extensional crenulations are fairly rare and are found only in samples away from fault zones where shearing was somewhat less intense. Quartz ribbons have been necked by extensional crenulations (Fig. 40) and in places are almost completely offset. A finer subgrain size in necks (high strain areas) is a result of dynamic recrystallization, indicating that conditions were still ductile.

ECC's in Atlanta are not well-developed or traceable in hand samples. It is reasonable to assume that thin sections containing ECC's are parallel to the kinematic *a* direction (northeast) of the ECC because they are not recognized in



Fig. 34. ECC from the Brevard Phyllite: Note the thinness of the extended layer, marked by arrow. Trace of ECC and preexisting c-surface are labeled. (Ta150B, plane light, ss = normal for ECC, ld = 13.7 mm).



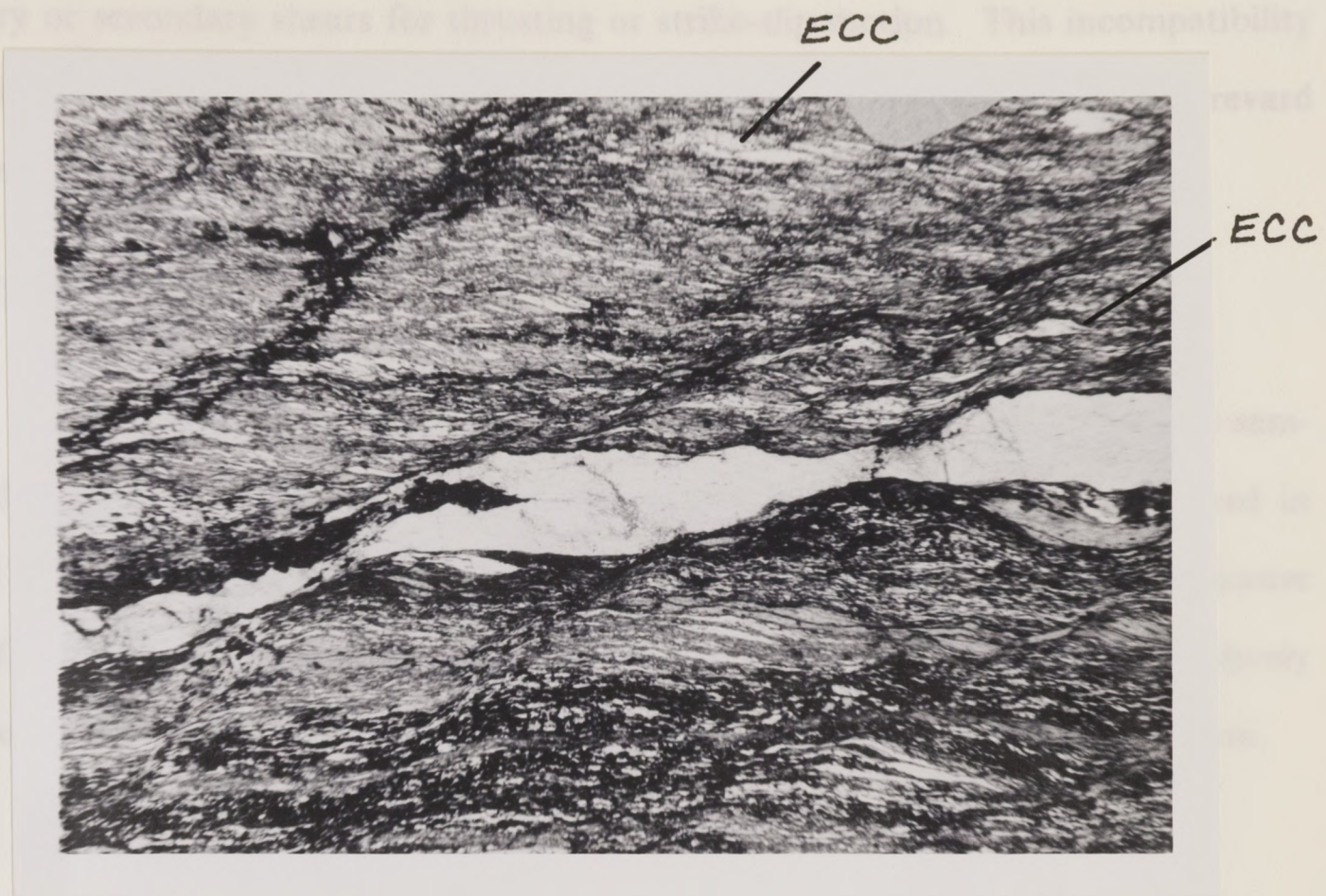


**Fig. 35. ECC's deform a quartz ribbon:** From the Brevard Phyllite next to Brevard Zone/Blue Ridge contact. Trace of ECC is labeled. (Ros118A, plane light, ss = normal, ld = 13.7 mm).

other cuts. Therefore, in Atlanta, the apparent strike of the ECC plane is northwest, perpendicular to the kinematic **a** direction. Thus from thin section observation only, the apparent local sense of shear on ECC's in the Ben Hill Granite is normal, with top down to the southwest, the same orientation and direction as ECC's in the northeastern areas. Because the strike is unconstrained, This orientation may vary from down to the west to down to the south.

The rarity and poor development of ECC's in the study areas makes it difficult to determine if they are related to bulk motion in the zone. However, if we assume that local motion on ECC's does reflect bulk motion in the Brevard Zone, then the orientation and sense of shear of ECC's is not compatible with either pri-



mary or secondary shears for thrusting or strike-slip motion. This incompatibility indicates that ECC's reflect a change in the direction of bulk motion in the Brevard Zone or are unrelated to bulk motion.

## SUMMARY

Although relatively uncommon, ECC's are present in all quadrangles sampled except the Whetstone quadrangle. Conjugate ECC's are only observed in At12. These microstructures are described separately from previous groups because ECC's crosscut microstructures in groups A and B and are therefore relatively younger. ECC's also predate retrograde metamorphism and brittle deformation.



**Fig. 36.** ECC deforms a group B pressure shadow: Muscovite in shadow (outlined) has been replaced by chlorite, from the Brevard Phyllite (Ta150A, plane light, ss = normal, ld = 5.55 mm).



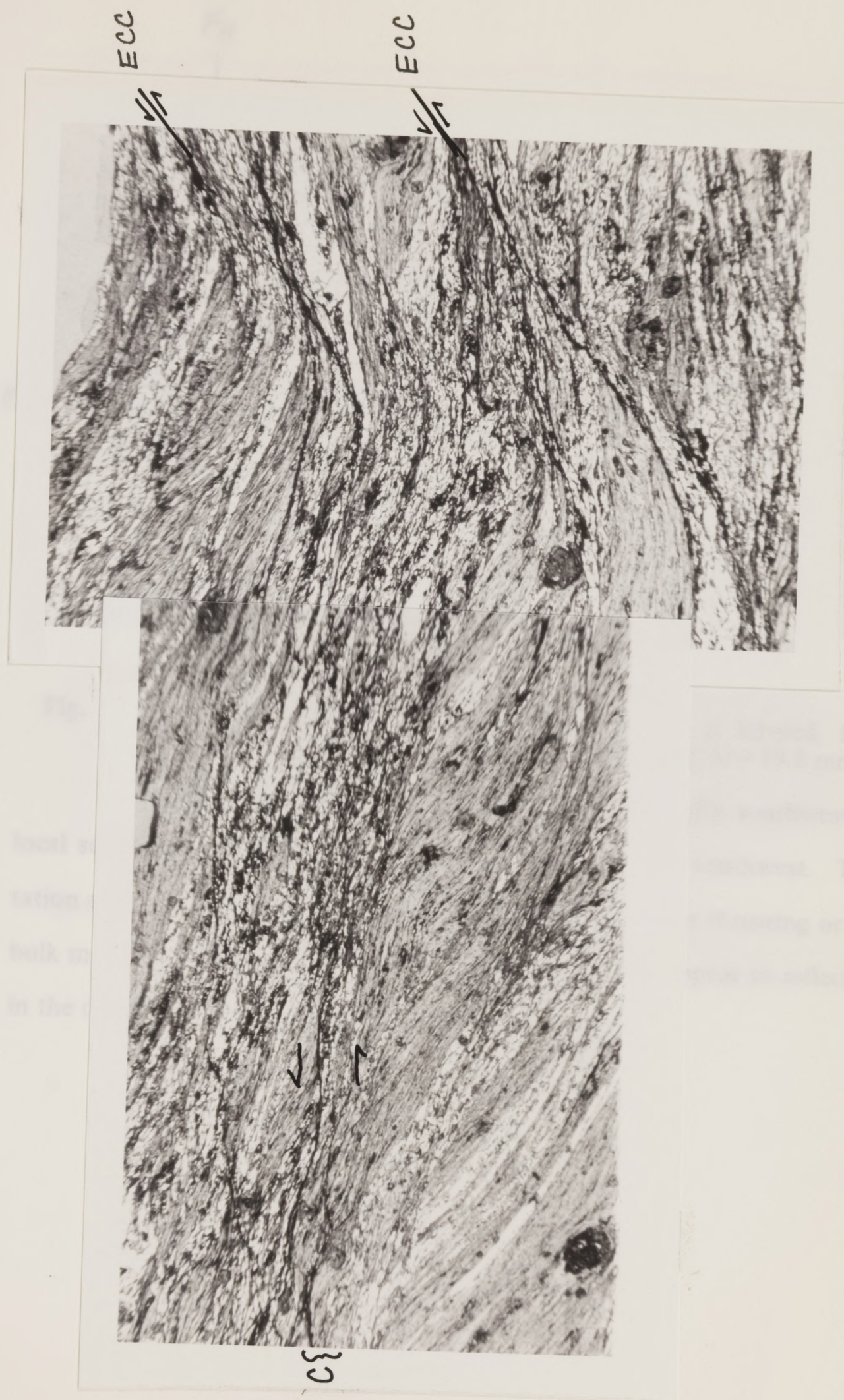
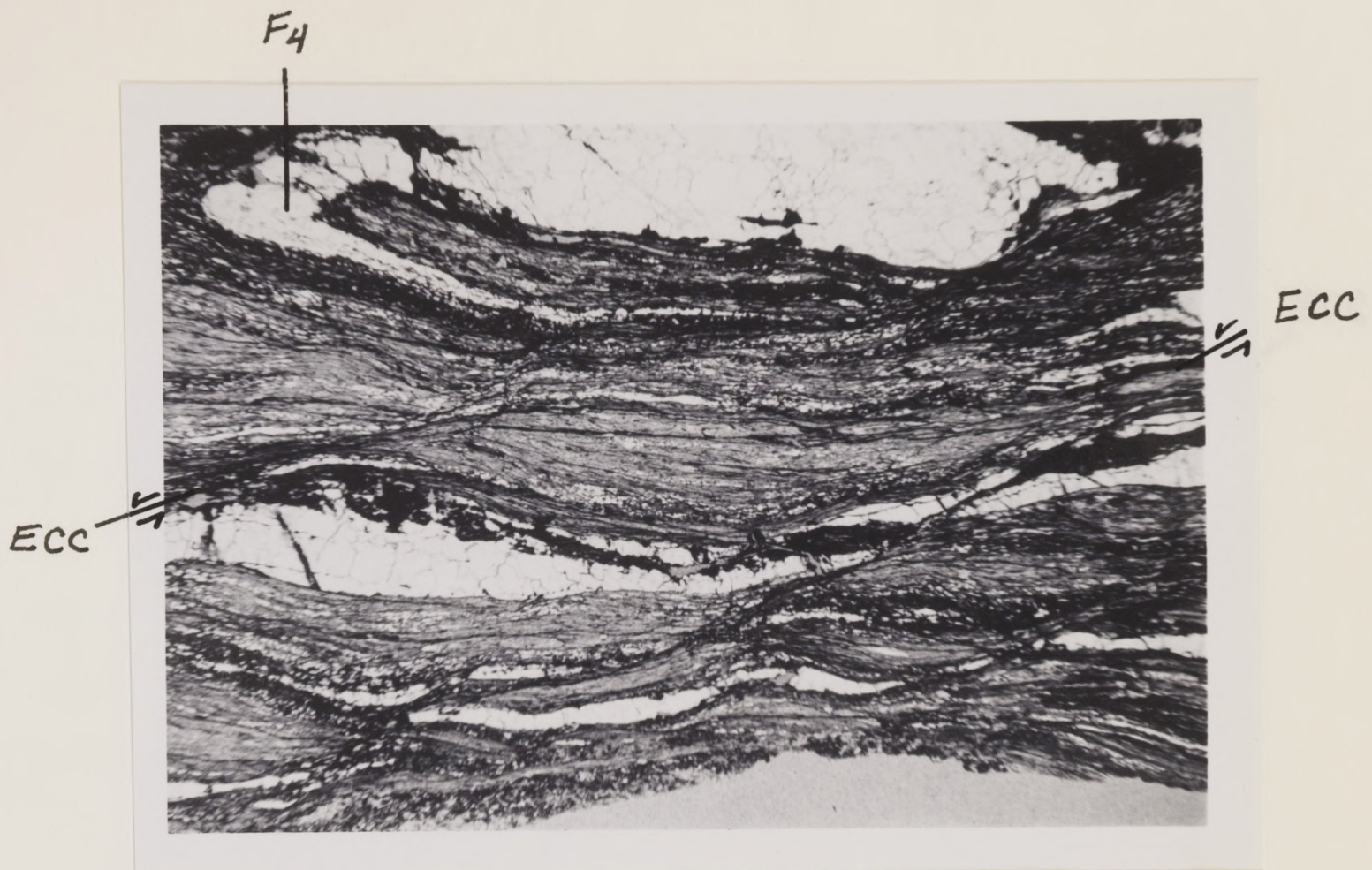


Fig. 37. ECC deform group B c-surfaces in the Brevard Phyllite: C's are often iron-stained as illustrated here. (Ta150B, plane light, ss = normal for ECC, ld = 20 mm).





**Fig. 38. ECC deforms group B fold:** Trace of ECC is labeled, from the Brevard Phyllite (Tu38, plane light, ss = normal, ld = 19.8 mm).

These microstructures generally trend northwest, dip southwest and their local sense of shear is normal with top down toward the southwest. This orientation and direction is not compatible with shears for either thrusting or strike-slip bulk motion in the Brevard Zone. In conclusion, ECC's appear to reflect a change in the direction of bulk motion in the Brevard Zone.





Figure 39. Closeup of ECC: From Figure 35. Higher strain and more recrystallization is present in necked area of quartz ribbon, from the Brevard Phyllite (Ros118A, xnicols, ss = normal, ld = 5.15 mm).



## CHANGES IN DEFORMATION CONDITIONS

Quartz deformation textures in microstructures from groups A, B and C indicate that in the northeastern study areas there was a possible change in deformation conditions along strike in the Brevard Zone. For example, the



**Fig. 40. Quartz ribbon necked by an ECC from the Ben Hill Granite:** (At12, plane light, ss = normal, ld = 4.35 mm).



## CHANGES IN DEFORMATION CONDITIONS

Quartz deformation textures in microstructures from groups A, B and C indicate that in the northeastern study areas there was a notable change in deformation conditions along strike in the Brevard Zone. For example, the quartz ribbon in Fig. 39 probably formed during earliest shearing (i.e. during formation of  $S_1$ ), prior to formation of group 1 features because ribbons are involved in  $F_2$  and  $F_3$  folds. This ribbon and others like it in the Rosman quadrangle contain partial recrystallization textures resulting from subgrain enhancement and/or bulge nucleation processes (Fig. 41). These textures are enhanced in high strain areas where ECC's have necked ribbons. However, further south in Tugaloo and Tamassee quadrangles the same-generation ECC's are deforming quartz-feldspar layers that have been highly, but not completely recrystallized by subgrain enhancement (Fig. 11). Note that recrystallization is not complete because some subgrains and discontinuous extinction are present.

This change along strike indicates that in the Rosman quadrangle relative to areas further southwest, either temperatures were not high enough and/or strain rate was not slow enough to allow for advanced recrystallization. This change did not necessarily occur during formation of group C ECC's (refer to Figure 39), but could have occurred at any point during the ductile deformation(s) which resulted in the microstructures described in this study. Because features in groups A, B and C formed under ductile conditions, it is not possible to determine whether group A features recrystallized during the deformation which formed them or later during either group B or C formation or both.



This change in conditions along strike may reflect the exposure of deeper structural levels in Tugaloo and Tamassee quadrangles relative to Rosman quadrangle, because Rosman outcrops are topographically higher than those in Tugaloo and Tamassee.



**Figure 41.** Partially recrystallized quartz ribbon: Note bulge nucleation along deformation bands in quartz-rich BP (Ros113B, xnicols,  $1d = 1.7$  mm).



## RETROGRADE METAMORPHISM

The presence of chlorite in most of the sections studied attests to a period of retrograde metamorphism in Tugaloo, Whetstone, Tamassee and Rosman quadrangles. No evidence of retrogression was observed in the Ben Hill Granite. Chlorite is most often observed in microstructures from groups A, B, and C. Because its later growth mimics preexisting muscovite, chlorite at first glance appears deformed but its formation actually postdates that of groups A-C. Figure 36 also illustrates this relationship. Chlorite is often found replacing garnet in the northeast or forming rims on garnet and mimicking muscovite in pressure shadows (Fig. 30). Chlorite is concentrated in areas of greatest muscovite strain, that is, along c-surfaces, ECC's and in fold hinges.

Chlorite appears to predate brittle faulting (group D) because it is not found in association with group D microstructures. It is possible that chlorite formation and brittle faulting were synchronous but that the latter feature obliterated any chlorite or enhanced its alteration such that chlorite is no longer present in sections containing brittle deformation. Thus, the relative timing of chlorite growth as a result of retrograde greenschist metamorphism appears to be after the formation of groups A, B and C but prior to formation of group D features.



## GROUP D

Field and thin section observations indicate that a period of brittle deformation occurred in the Brevard Zone resulting in mesoscopic and microscopic faults, breccia and drag folds ( $F_5$ ). These features are categorized as group D features because they reflect the most recent (youngest) deformation in the study area, and they overprint all previous groups of microstructures. Brittle deformation is concentrated in the Brevard Zone adjacent to the Blue Ridge contact.

Mesoscopic faulting and imbrication are present in the Ben Hill Granite in Atlanta, while faulting and brecciation are present in Whetstone, Tamassee and Rosman quadrangles but not in Tugaloo quadrangle. Brittle features appear to increase in abundance and intensity northeastward, where their expression reaches a maximum just west of Rosman, NC near U.S. 64 at an abandoned quarry. This outcrop contains the best exposures of brittle deformation in the study area. I believe the increase in intensity and distribution is real, and is not a function of exposure due to the lack of brittle microstructures observed in Tugaloo quadrangle, relative to Rosman quadrangle. The absence of faulting in Tugaloo is probably due to a lack of exposure because faulting is present in all other quadrangles in the northeast at the same stratigraphic and structural level. First field, then thin section evidence of brittle deformation is described beginning in the southwest with Atlanta and moving northeast to Rosman (Fig. 2).

## ATLANTA AREA

Faults in the Ben Hill Granite are continuous, low angle to subhorizontal zones, 2-8in in width. Faults are marked by zones of weathered, shaley-appearing



material which is foliated parallel to fault zones (Fig. 42). Because of the friable nature of fault material, samples could not be collected in the center of fault zones, see Fig. 43 for sample locations. In places gouge has developed along these zones. Neither breccia nor cataclasites are present in the Ben Hill but one set of dip-parallel slickensides was found (see Appendix B).

Faults are also delineated by the presence of two mesoscopic foliations which decrease in spacing and become more parallel as faults are approached. Augen size and abundance also decrease. The above observations coupled with the presence of ductile microstructures from groups B and C strongly suggest that imbricate fault zones are localized along preexisting ductile shear zones.

Thin section evidence for brittle deformation is almost nonexistent indicating that motion was localized in fault zones. Scattered quartz-filled fractures such as that in Fig. 44 postdate formation of all previously described ductile microstructures in Atlanta. These fractures support field evidence of ductile followed by brittle deformation.

Fault slivers of Brevard mylonite, imbricates within the Ben Hill Granite, and rare dip-parallel slickensides suggest a thrusting motion, however, the first two features can be accounted for by either dextral or sinistral, oblique-slip motion. It is possible that this brittle deformation is the result of an increase in strain rate later in the same deformation that formed the preexisting shear zones and the group B and group C microstructures associated with these shear zones. This explanation would account for localization of fault zones along shear zones, but requires that motion changed from the strike-slip motion which formed group B structures, to the oblique-slip or thrusting motion which formed the observed imbricates and fault slivers. It is impossible to determine how much thrust or strike-slip displacement



occurred along these various faults given the lack of exposure and offset markers. One vertical fault which postdates thrusting is present at this outcrop (Fig. 43). This fault has an apparent normal motion of 6 feet. This is the only such fault observed and due to its limited exposure and weathered nature, it is not known whether this fault is related to thrusting or to a more recent event.

## WHETSTONE QUADRANGLE

In Whetstone, an exotic carbonate slice is present in the Brevard zone at the northwestern edge of the zone where it is bounded by the Blue Ridge geologic province (Fig. 8). This slice was mapped by Hatcher (unpub. maps; 1971) who



Fig. 42. Brittle imbricate fault zone: in Atlanta, GA. Light unit is the Ben Hill Granite and the dark unit is Long Island Gneiss.



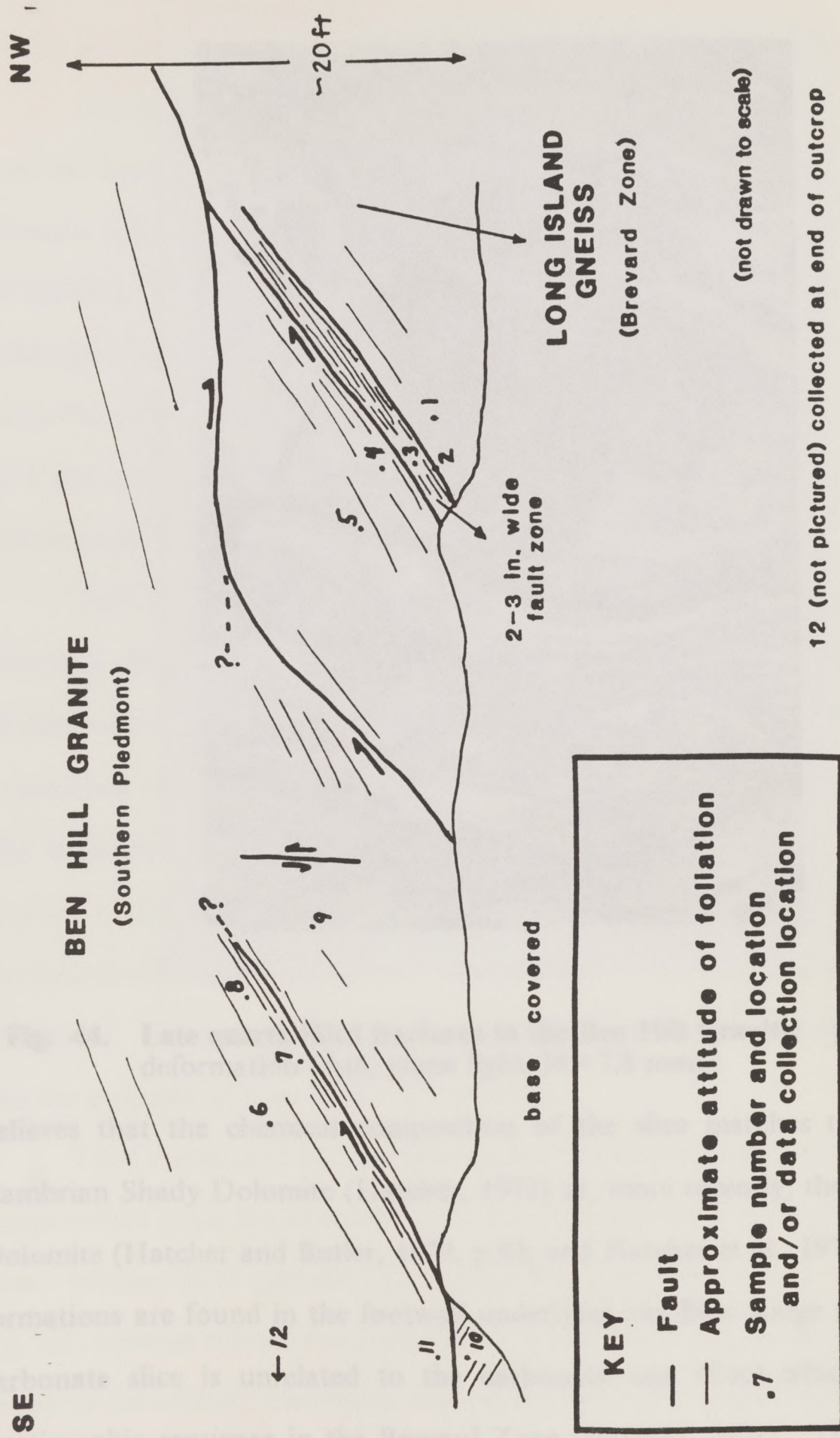
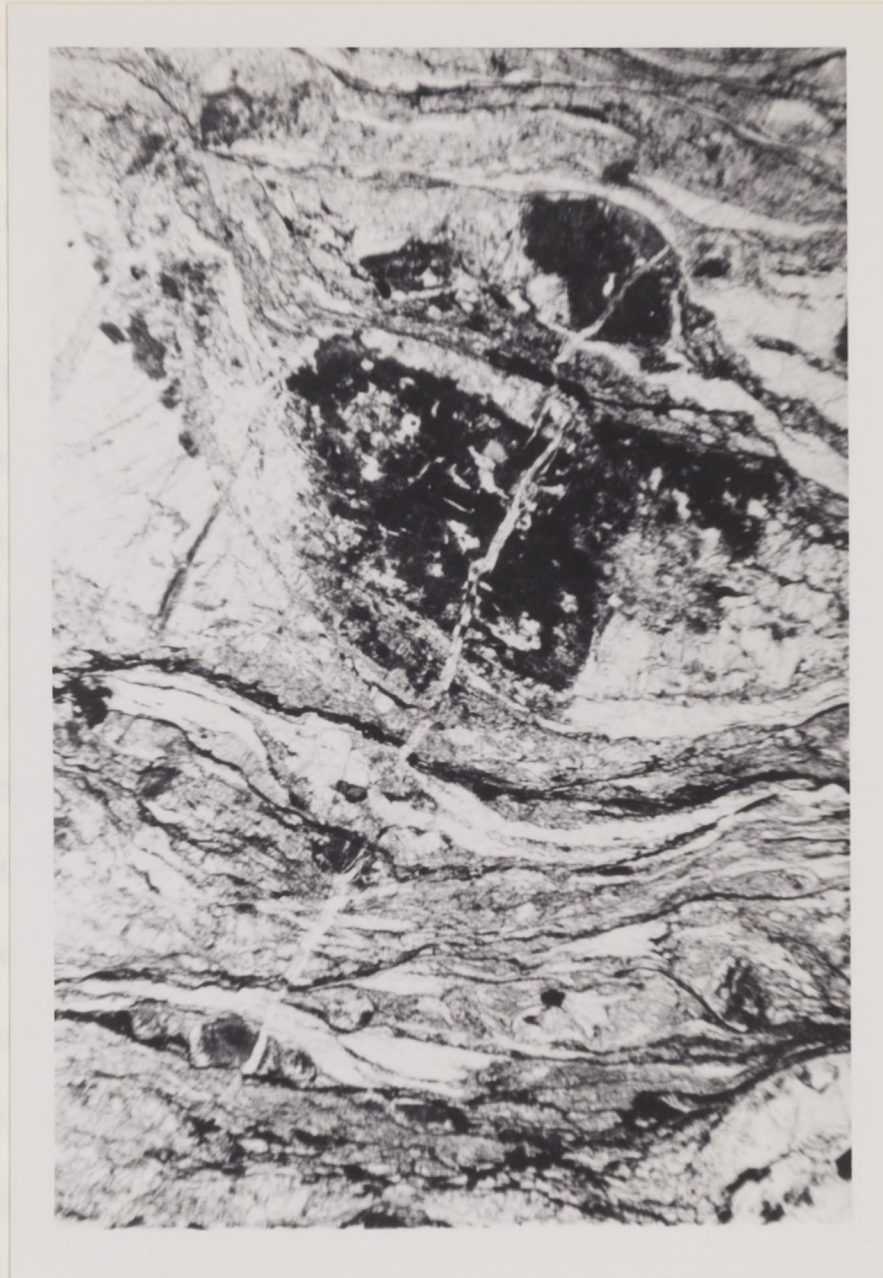


Fig. 43. Field sketch of imbricate faults in the Ben Hill Granite: This section of the roadcut exposure contains 3 brittle faults that have nucleated along preexisting ductile shear zones.





**Fig. 44. Late quartz-filled fractures in the Ben Hill Granite:** postdate ductile deformation (At6, plane light,  $ld = 7.8$  mm).

believes that the chemical composition of the slice matches that of either the Cambrian Shady Dolomite (Hatcher, 1971) or, more recently, the Cambrian Knox Dolomite (Hatcher and Butler, 1979, p.93; and Hatcher et al., 1973). Both of these formations are found in the footwall underlying the Blue Ridge decollement. The carbonate slice is unrelated to the carbonate unit (Crc) which is part of the stratigraphic sequence in the Brevard Zone (Hatcher, 1971). The creek exposure



of the exotic slice was the focus of sampling in the Whetstone quadrangle, see Hatcher and Butler (1979, p.93-94) and Plate II for specific field location.

The exposed carbonate slice is the only sampling location where field evidence for brittle deformation was observed in Whetstone. The contact of the carbonate with the graphitic phyllite to the southeast is a brecciated zone about 3 ft (1 m) wide. The exact width of this zone is unknown due to dense vegetation and limited creek exposure. The contact of the slice with Blue Ridge lithologies which bound the slice approximately 100 ft (33 m) to the northwest (Hatcher, unpub. maps) was not found. Mesoscopic sense of shear features such as asymmetric folds or slickensides were not observed.

Thin sections from the slice (CS2 and CS3) indicate that it has been disrupted in a ductile manner on the basis of deformation textures in the calcite matrix and scattered, interstitial Mg-rich chlorite (R. Folk, pers. comm.) Bent lamelli in recrystallized calcite indicate plastic deformation. Some chlorite has undergone bulge nucleation resulting in its extremely fine grain size, serrate and indistinct subgrain boundaries. Other interstitial chlorite exists as highly deformed, unrecrystallized ribbon structures. These textures could not have formed due to brecciation. Broken and disrupted calcite-filled veins which postdate chlorite textures are evidence of later brittle deformation.

Field evidence of brittle deformation is absent in creek exposure as the slice is approached from the southeast. In thin section, however, highly recrystallized quartz textures are abruptly overprinted by minor fracturing and brecciation (Fig. 45) between sample locations Wh131B and Wh133A. Sense of shear direction cannot be determined from these microstructures. This minor overprinting further



indicates that brittle deformation associated with emplacement of the slice postdates an earlier period of ductile deformation.

Samples Tg and Wh135 were collected at the first outcrop beyond the slice in the Late Precambrian Graywacke Schist unit of the Blue Ridge province (see Plate II, Fig. 8 and Hatcher, unpub. maps). This outcrop is the first creek exposure northwest of the slice. In thin section, Wh135 and Tg contain highly recrystallized quartz ribbons which record an earlier ductile deformation, however, there is no evidence of brittle deformation. This observation suggests that late, brittle deformation associated with emplacement of the exotic slice did not affect nearby rocks of the Blue Ridge because motion was localized along the slice contact with surrounding rocks. The incompetent graphitic phyllite which bounds the slice to the southeast, appears to have undergone more deformation during slice emplacement than the more rigid and competent schist to the northeast.

In summary, it appears that brecciation is mainly localized along the slice contact with the surrounding graphitic phyllite. Calcite and chlorite deformation in the slice indicate that preexisting ductile textures were overprinted in localized areas by veining and brecciation. Sense of motion during brittle deformation cannot be determined from the brecciation observed in Whetstone quadrangle.

## TAMASSEE QUADRANGLE

Brittle (group D) features are found at only two locations within the Tamassee field area: 1) at an outcrop in a curve in the road between station Ta147 and Ta148; and 2) at outcrop Ta150 (Plate III). The former outcrop lies within the Blue Ridge geologic province about 1300 ft (430 m) northwest from the Brevard Zone contact. Here, changes in foliation orientation across two faults indicate ap-





**Fig. 45. Brecciation near exotic slice:** overprints preexisting ductile fabrics in the Brevard Phyllite (Wh133A, plane light, ss = indeterminate, ld = 11.7 mm).

parent reverse motion, although poor exposure prohibited collecting any structural data, samples or the observation of any folding. These faults are 3-4 ft (1 m) in length and they probably experienced minor movement.

The second location in Tamassee quadrangle where faulting is observed is Ta150 (Plate III). These faults all appear to represent one deformation as indicated by their similar outcrop appearance and extent. The best-exposed faults are shown in Fig. 46 and are labeled  $f_a$  and  $f_b$  for reference. Samples Ta150B and C were collected where shown in the same sketch and closely-spaced foliation measurements were taken across  $f_a$ . Exposure is better at this outcrop than the one described above, revealing fairly planar, discrete faults with apparent reverse motion on  $f_a$ ,  $f_b$  and  $f_c$ .  $F_d$  and other minor faults are poorly exposed and/or the sense of



motion is indeterminant. Stereonet plots for fault planes, minor structural features (i.e. fold axes, slickensides) and foliation measurements (for sense of shear determinations) are included in Appendix B.

Particularly well developed along  $f_a$  is a pronounced foliation, probably formed during fault movement. Almost everywhere, except at the base of  $f_a$ , foliation is truncated abruptly by faults and does not curve into them. Small fault blocks have been rotated along  $f_a$  and  $f_b$ , and drag folds ( $F_5$  folds) have developed in places along several faults. Thin sections could not be made of fault material because of its friable or weathered nature. Brecciation was not observed, but gouge is present in places along several faults. Northeast-trending, horizontal slickensides were measured on  $f_b$ , but there is no evidence to suggest whether these are a result of dextral or sinistral slip.

These features indicate that late faulting occurred under brittle conditions with a fairly high confining pressure and fast strain rate because of the presence of throughgoing faults. Where measurable, faults trend east-northeast, dip to the north and have a variable direction of reverse and dextral or sinistral strike-slip motion as indicated by drag folds and slickensides, respectively. Displacement cannot be determined, but given their limited extent, it is likely that these faults also experienced minor movement. There is no evidence of this late brittle deformation in thin sections from immediately adjacent samples or from samples elsewhere in the Tamassee quadrangle.

In summary, field data from Tamassee supports an episode of localized brittle deformation in the Brevard Zone. Faults probably experienced minor displacement given their limited size and extent. Sense of shear data is lacking but foliation changes and slickensides on faults indicate a local reverse motion with a



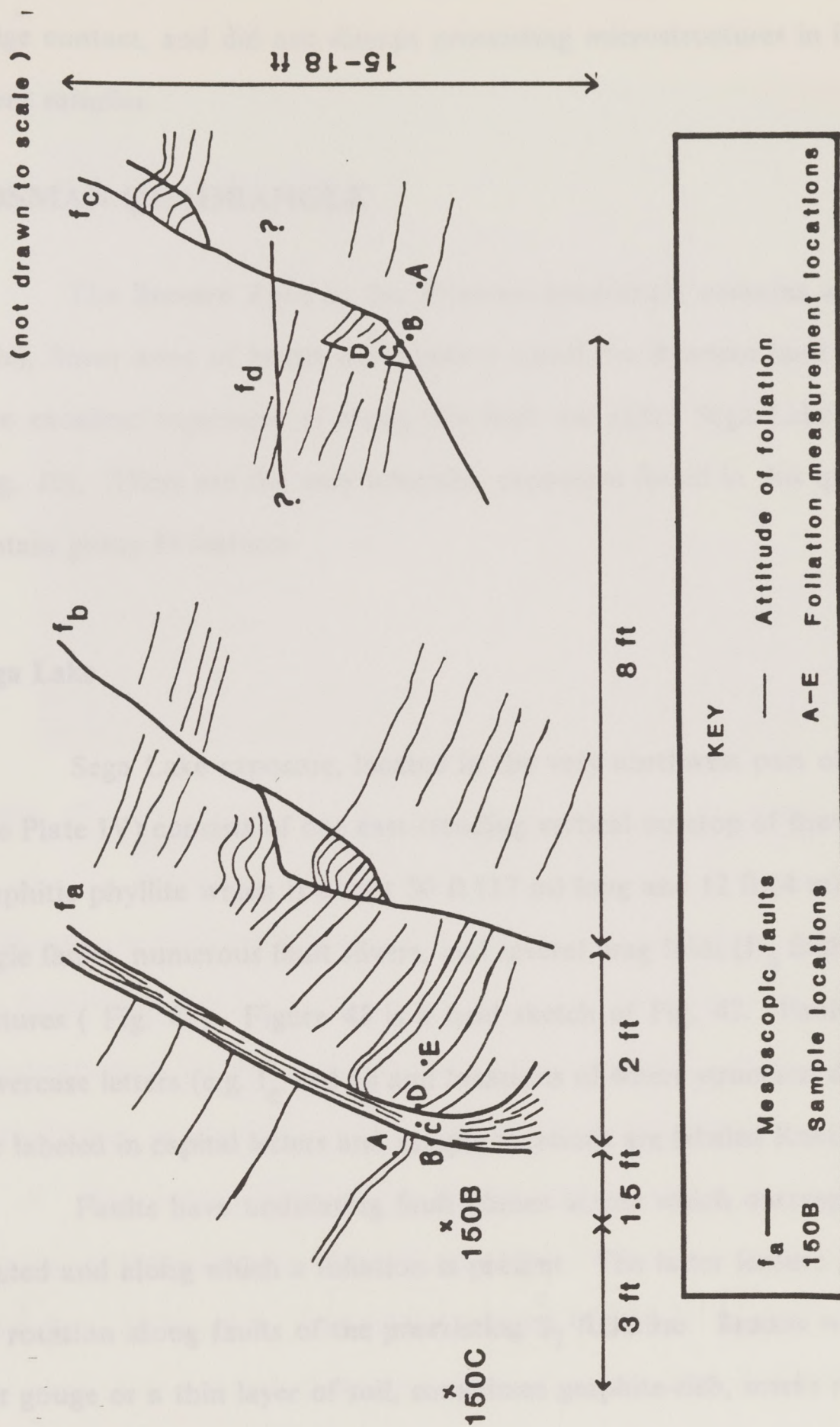


Fig. 46. Faults in Tamasee quadrangle: Field sketch of foliation changes at four faults exposed in roadcut at Tal50.



strike-slip component. This deformation was localized at the Brevard Zone/Blue Ridge contact, and did not disrupt preexisting microstructures in immediately adjacent samples.

## ROSMAN QUADRANGLE

The Brevard Zone in the Rosman quadrangle contains a narrow (200 ft wide), linear zone of brittle deformation called the Rosman fault (Horton, 1982). Two excellent exposures of along this fault are called Sega Lake and the quarry (Fig. 10). These are the only adequate exposures found in this quadrangle which contain group D features.

### Sega Lake

Sega Lake exposure, located in the very northwest part of the quadrangle (see Plate IV) consists of one east-trending vertical outcrop of Brevard Phyllite and graphitic phyllite which is about 50 ft (17 m) long and 12 ft (4 m) high. Two low angle faults, numerous fault slivers, and several drag folds ( $F_5$  folds) are prominent features ( Fig. 47). Figure 48 is a field sketch of Fig. 47. Faults are labeled in lowercase letters (e.g.  $f_e$  and  $f_p$ ) and locations of where structural data was collected are labeled in capital letters and sample locations are labeled Ros118A-C.

Faults have undulating fault planes across which outcrop foliation is disrupted and along which a foliation is present. The latter feature probably formed by rotation along faults of the preexisting  $S_1$  foliation. Breccia was not observed, but gouge or a thin layer of soil, sometimes graphite-rich, marks most faults. The strike of  $f_e$  varies from northwest to northeast. The presence of fault slivers, the





**Fig. 47. Prominent faults and fault slivers:** in Brevard Phyllite at Brevard/Blue Ridge contact, Rosman quadrangle. Dark unit (outlined) is offset in a normal sense.

differences in slickenside orientations within slivers, and the presence of slickensides on foliation planes away from faults indicates that motion in the Brevard Phyllite occurred along jostling fault slivers, not along discrete, planar faults, as is the case with faulting in the Tamassee quadrangle to the southwest (see Appendix B).

The overall direction of motion along of  $f_e$  appears to be oblique-slip, normal motion with top down towards the southeast, as seen in the offset of the dark layer in Fig. 47. This direction is substantiated by northeast-trending, sub-horizontal fold axes which are definitely related to drag on faults because they are only observed adjacent to faults. Drag folds do not disrupt preexisting lineations



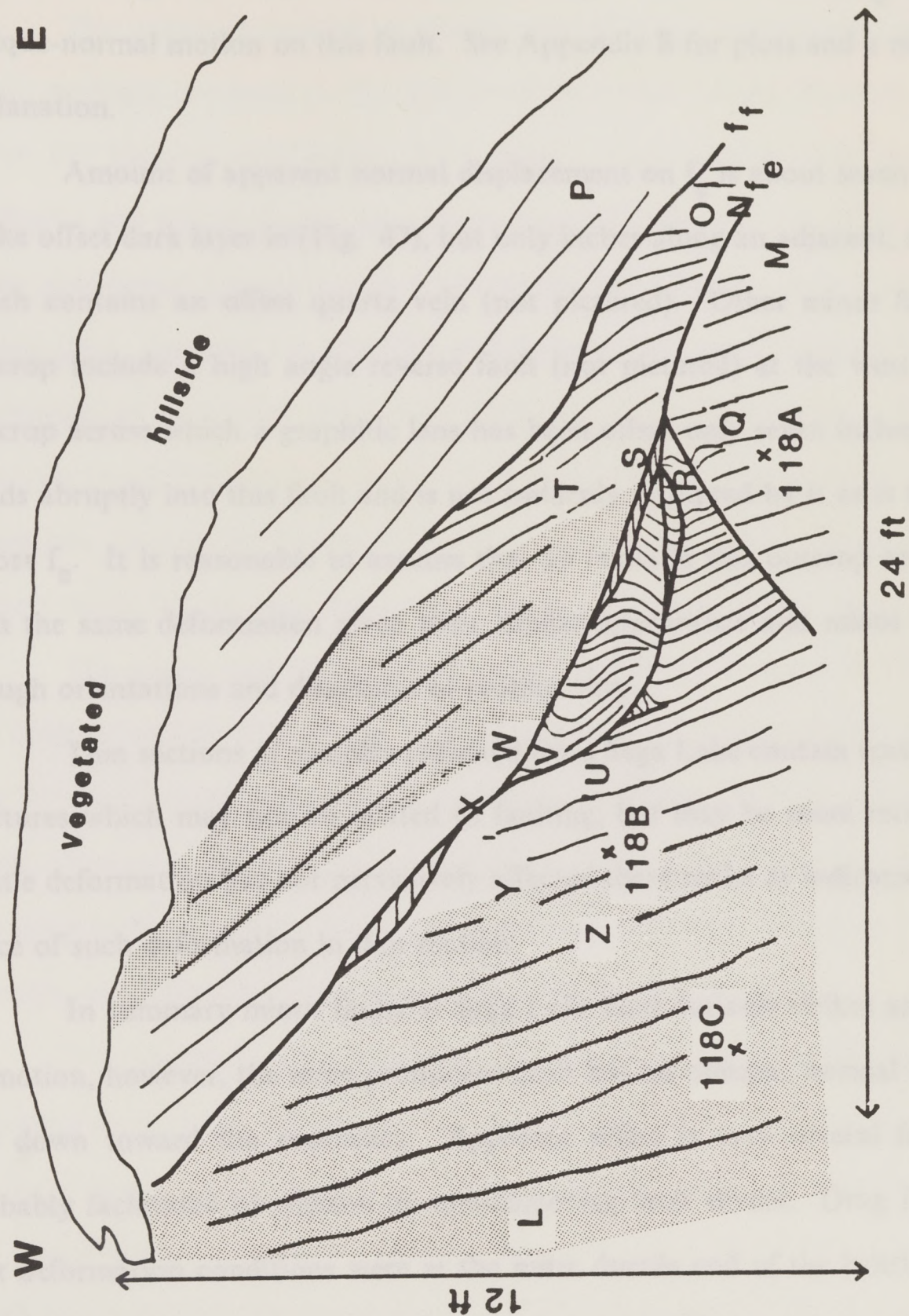


**Fig. 48.** Field sketch of Sega Lake roadcut, Rosman: Same view as Fig. 46. See text for explanation of symbols.



because fold motion (the kinematic  $\mathbf{a}$  direction of folds) is perpendicular to lineations. Changes in foliation orientation along 3 transects across  $f_e$  also support oblique-normal motion on this fault. See Appendix B for plots and a more detailed explanation.

Amount of apparent normal displacement on  $f_e$  is about seven feet as seen in the offset dark layer in (Fig. 47), but only inches along an adjacent, smaller fault which contains an offset quartz vein (not pictured). Other minor faults in this outcrop include a high angle reverse fault (not pictured) at the west end of the outcrop across which a graphitic lens has been offset only seven inches. Foliation bends abruptly into this fault and is not suddenly disrupted by it as is the foliation across  $f_e$ . It is reasonable to assume that all faults in this outcrop are associated with the same deformation given their similar appearance and minor offset, even though orientations and directions of motion vary.

Thin sections of samples collected from Sega Lake contain scattered, minor fractures which may not be related to faulting, but may be more recent features. Brittle deformation has not pervasively affected these rocks as indicated by the absence of such deformation in thin section.

In summary minor faults at Sega Lake have variable strikes and directions of motion, however, the most prominent fault has an oblique, normal motion with top down toward the southeast. Apparent offset is only several feet and was probably facilitated by motion on anastomosing fault slivers. Drag folds suggest that deformation conditions were at the more ductile end of the brittle field. Evidence of brecciation or cataclasis is not present in either outcrop or thin section. Brittle deformation appears concentrated along small faults and fault slivers within the Rosman fault.



## Quarry

The quarry is located at the contact of the Brevard Zone with the Blue Ridge geologic province in the southwestern corner of the Rosman quadrangle (Plate IV; Hatcher and Butler, 1979, p.96). The outcrop is in the brecciated phyllonite and ultramylonite, bpu, of the Rosman fault (Horton, 1982) and consists of an abandoned quarry face in a hillside and an adjacent, steep bank below the quarry road. Samples are graphitic and nongraphitic phyllite which both contain an abundance of quartz. Figure 49 shows the extent of the quarry face outcrop. The trees in the background are in the Blue Ridge geologic province which is exposed just behind the quarry along old U.S route 64. The Brevard/Blue Ridge contact which lies between the quarry face and background trees is not exposed.

The quarry appearance is described as a tectonic melange by Horton (1982) and Hatcher and Butler (1979). Unit descriptions by Horton (1982) describe bpu as a "broken formation derived by pervasive tectonic brecciation and mixing, at all scales. Numerous mesoscopic crosscutting faults (too small to show at map scale) and drag folds of various orientations produce a chaotic appearance at outcrop; however, southeast-dipping reverse faults are the most pervasive."

The extremely soft, weathered rock in this outcrop prohibited collecting structural data except for two fault planes and one set of dip-slip slickenside measurements (see Appendix B). Most faults are discrete, planar faults which are several feet long and die out or are covered at both ends. All folds appear to have behaved ductilely because of their graphite content and/or because of somewhat ductile deformation conditions (Fig. 50). No consistent sense of shear can be determined in outcrop because of variable drag fold orientations and poorly exposed material.



The vergence of what appear to be large folds in the quarry face suggests that a top to the west motion resulted in these folds (Fig. 49). Because of their association with brittle deformation features in outcrop, it is likely that these large folds are related to brittle deformation ( $F_5$  folds) rather than to earlier ductile  $F_2$ ,  $F_3$  or  $F_4$  folds. This fact, coupled with their poor exposure and unknown origin, makes these folds unreliable kinematic indicators. A 1 ft (0.3 m) thick pod of breccia was found, but no evidence exists to suggest whether: 1) it formed in response to an increase in strain rate during the brittle deformation responsible for faulting, or 2) it formed in a separate event after brittle deformation had ceased.

Thin sections from the quarry and an adjacent outcrop exhibit varying degrees of folding, faulting and brecciation. For example, Ros113B, 113D, 114E and



**Fig. 49.** Intense deformation along the Rosman fault: Exposure is at a quarry west of Rosman, NC. Apparent (group D?) structure is outlined.



114F contain open to isoclinally folded quartz ribbons that are beginning to be broken into large fragments (Fig. 51). Ribbons in these fragments and elsewhere in Rosman quadrangle most likely formed prior to group A features, but because of the chaotic nature of the structures, it is impossible to determine if folding of ribbons also belongs to group A. Other samples (Ros11C, 113A and 113C) show a more intensely brecciated, but previously ductilely deformed rock in which frag-



**Fig. 50. Folds in graphitic phyllite:** at the quarry outcrop. Relative timing of these folds is unknown.



ments of various sizes have rotated along anastomosing, iron-stained zones of graphite during cataclastic flow (Fig. 52). On the other hand, sample Ros114B, less than 150 ft (50 m) away from previous samples, is unaffected by nearby deformation. None of the microstructures found in quarry samples contain useful kinematic indicators.

Samples BR123A, BR123C and BR120 were collected from rocks of the Blue Ridge province just northwest of the quarry on old U.S. highway 64. BR123A and 123C were collected about 650 ft (216 m) from the quarry in a mylonite gneiss unit, while BR120 was collected 2400 ft (800 m) away in a biotite-muscovite gneiss unit (Horton, 1982). None of these samples contain any evidence of brittle deformation. BR123A contains quartz recrystallized by subgrain enhancement as indicated by the numerous subgrains present. Quartz ribbons with an excellent crystallographic preferred orientation and numerous muscovite buttons are present. BR123C and BR120 have undergone a slightly higher degree of recrystallization, by the same mechanism and they contain minor muscovite and very few, recognizable quartz ribbons. This evidence further indicates that late brittle deformation was localized along the northwestern edge of the Brevard Zone along the Rosman fault and that deformation did not affect the surrounding rocks.

In summary, folding and faulting at the quarry outcrop of the Rosman fault near Rosman, NC appear associated with a late, brittle deformation. Brecciation may possibly be a slightly later process resulting from an increase in strain rate during this event. There is no consistent sense of shear in the observed microstructures; however, apparent structure in outcrop suggests a generally west-directed motion which supports that of Horton (1982). Deformation is concentrated along the northwestern edge of the Brevard Zone.





**Fig. 51. Incipient brecciation of folded quartz ribbons:** in the Brevard Phyllite (Ros113D, plane light, bulk ss = indeterminate ld = 13.7 mm).

## SUMMARY

Group D features consist of brittle faults, breccia, and scattered drag folds and slickensides. These features are observed in widely scattered outcrops in each study area except the Tugaloo quadrangle in South Carolina. Evidence for brittle deformation is neither abundant nor pervasive, but where present such evidence is localized along the Brevard/Blue Ridge contact in each of the study areas. Amount of apparent displacement on faults at Sega Lake in Rosman is several feet at most, whereas at all other fault outcrops displacement is unknown.

Direction of motion is also unknown or highly variable on most faults in the northeastern study areas. At the quarry in Rosman, sense of motion on asym-



metric, mesoscopic folds appears to be generally west-directed. In the Ben Hill Granite, imbrication suggests northwest-directed thrusting, however, a bulk, oblique-slip thrusting motion can also account for these features. The overall bulk motion in the Brevard Zone during brittle deformation cannot be determined due to the lack of exposure and the variability in orientation and direction of motion on faults.

Group D features in the Ben Hill Granite are correlative with those in the northeast because of the following similarities: 1) brittle deformation in the Ben Hill Granite also postdates all preexisting ductile features; and 2) there is no evidence for retrograde metamorphism occurring after formation of group D microstructures.

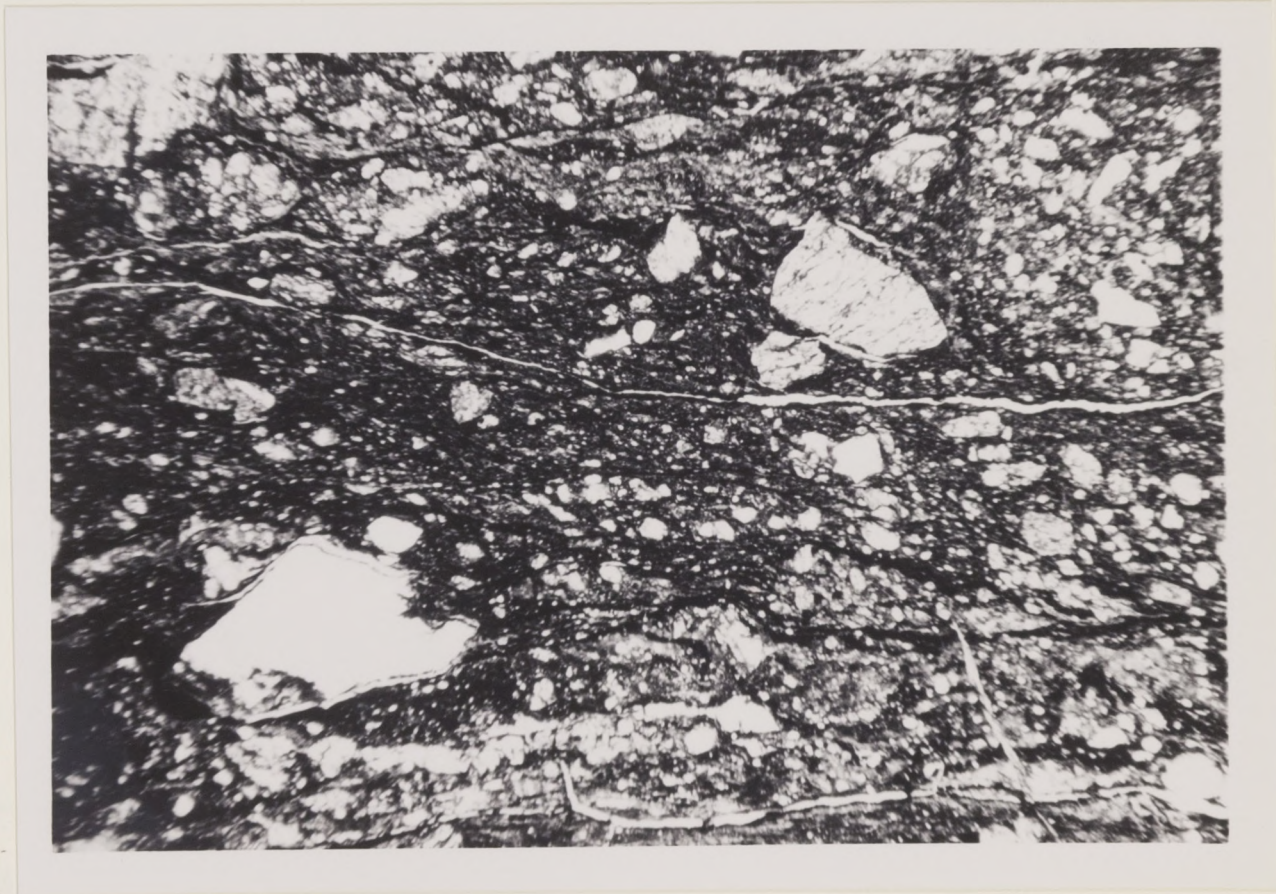


**Fig. 52. Intensely brecciated phyllite:** from the quarry, Rosman quadrangle (Ros112C, plane light, ss = indeterminate, ld = 13.2 mm).



Thus the presence of group D features indicates that a separate, more recent deformation occurred after that/those which formed microstructures in groups A, B and C. This brittle deformation was localized along the Brevard/Blue Ridge contact, but was apparently regionally extensive because evidence for such deformation is present in 4 out of 5 study areas. In the Rosman quadrangle brittle deformation was laterally continuous resulting in the Rosman fault, a narrow zone of faulting and brecciation parallel to the Brevard Zone/Blue Ridge contact. Bulk motion during this deformation is indeterminate in the study area.

ductile thrusting system. Group B microstructures are type II as defined, on surface F<sub>2</sub>, both and given present structures all of which are relatively younger than group A. The orientation of these features indicates that a period of bulk, dextral, strike-slip motion, possibly with a thrust component, was required for their formation. Group C consists only of microstructures, no structural orientation cleavage (ECC). ECC's postdate the microstructures in groups A and B, and they have a bulk sense of shear that is incompatible with either primary or secondary redeal shears in a dextral strike-slip shear zone. Thus ECC's represent a response to a change in the direction of bulk motion in the Brevard Zone. The most recent features are faults and associated breccia (group D) which do not reflect a consistent direction of bulk motion in the zone. Extrapolate evidence which indicated after formation of groups A, B and C, but prior to formation of group D.

Groups A, B and C formed under ductile conditions as seen in the deformation textures preserved and the types of microstructures formed. Associated textures are not present in any of the samples studied. The deformation conditions along strike in the northeastern study areas were different at some point in the deformation history of the Brevard Zone, prior to formation of group D features.



## SUMMARY

The results of this study indicate that there exists more than one direction of bulk motion within the Brevard Zone as indicated by the microstructures present. The relatively oldest recognizable microstructure is a pronounced foliation,  $S_1$ , for which the sense of shear is unknown. Extremely weathered garnets overprint  $S_1$ , reflecting their growth syn- to postkinematically with  $S_1$ . Group A microstructures are  $F_2$  and  $F_3$  folds which deform  $S_1$ , reflecting a west- to northwest-directed ductile thrusting motion. Group B microstructures are type II s-c mylonites, c-surfaces,  $F_4$  folds and garnet pressure shadows, all of which are relatively younger than group A. The orientation of these features indicates that a period of bulk, dextral, strike-slip motion, possibly with a thrust component, was required for their formation. Group C contains only one microstructure, an extensional crenulation cleavage (ECC). ECC's postdate the microstructures in groups A and B, and they have a bulk sense of shear that is incompatible with either primary or secondary riedel shears in a dextral strike-slip shear zone. Thus ECC's appear to represent a change in the direction of bulk motion in the Brevard Zone. The most recent features are faults and associated breccia (group D) which do not reflect a consistent direction of bulk motion in the zone. Retrograde metamorphism occurred after formation of groups A, B and C, but prior to formation of group D.

Groups A, B and C formed under ductile conditions as seen in the deformation textures preserved and the types of microstructures formed. Annealed textures are not present in any of the samples studied. The deformation conditions along strike in the northeastern study areas were different at some point in the deformation history of the Brevard Zone, prior to formation of group D features.



Group D features formed under relatively brittle deformation conditions and the presence of breccia suggests that a possible increase in strain rate occurred toward the end of this deformation.

The timing of formation of foliation ( $S_1$ ) in the Brevard Zone is unknown in the northeast. It is likely that these features were formed during the Taconic orogeny, preceding or synchronous with high grade metamorphism ca. 480-455 Ma (Glover et al, 1983), as this was the first and most intense, ductile deformation to affect the southern Appalachians. Gneiss in the northeast probably formed at this time because most overprint a foliation.

In both the Taconic and Alleghanian orogenies, tectonic models include west- to northwest-directed ductile thrusting which is compatible with group A microstructures from this study. If group A features are Taconic in age, then they formed during the presumed westward collision of the Inner Piedmont island arc with the North American continental margin (Fig. 5). This initial deformation would have formed the northwest-verging  $F_2$  microfolds and axial planar foliation,  $S_2$ , after the formation of  $S_1$  presumably earlier in the Taconic orogeny during initial deformation. Scattered refolded folds ( $F_3$ ) are coaxial with  $F_2$  and probably formed during the same event.

The Acadian orogeny is believed to have been less intense than the Taconic orogeny. Demonstrable evidence for the sense of shear during any Acadian deformation in the Brevard Zone is nonexistent, unless northwest-verging  $F_3$  folds are



## TIMING

The following is a discussion of the timing of formation of each of the above groups. This discussion is an attempt to associate these microstructures with the known deformational events in the southern Appalachians. Correlation is on the basis of known structural relationships and radiometric age determinations from the Brevard Zone.

The timing of formation of foliation ( $S_1$ ) in the Brevard Zone is unknown in the northeast. It is likely that these features were formed during the Taconic orogeny, preceding or synchronous with high grade metamorphism ca. 480-435 Ma (Glover et al, 1983), as this was the first and most intense, ductile deformation to affect the southern Appalachians. Garnet in the northeast probably formed at this time because most overprint a foliation.

In both the Taconic and Alleghanian orogenies, tectonic models include west- to northwest-directed ductile thrusting which is compatible with group A microstructures from this study. If group A features are Taconic in age, then they formed during the presumed westward collision of the Inner Piedmont island arc with the North American continental margin (Fig. 5). This intense deformation would have formed the northwest-verging  $F_2$  microfolds and axial planar foliation,  $S_2$ , after the formation of  $S_1$  presumably earlier in the Taconic orogeny during initial deformation. Scattered refolded folds ( $F_3$ ) are coaxial with  $F_2$  and probably formed during the same event.

The Acadian orogeny is believed to have been less intense than the Taconic orogeny. Demonstrable evidence for the sense of shear during any Acadian deformation in the Brevard Zone is nonexistent, unless northwest-verging  $F_3$  folds are



actually Acadian in age. Bond and Fullagar (1974) interpret a Rb-Sr whole rock age of  $387 \pm 14$  Ma (from the Henderson mylonite in the Rosman quadrangle), as a result of re-equilibration during Acadian metamorphism. Also, Odom and Fullagar (1973) postulated that their  $356 \pm 8$  Ma Rb-Sr whole rock age on the same rocks is a result of distributed shearing and recrystallization rather than major displacement during the Acadian orogeny. Both of these dates represent a resetting of the Henderson mylonite protolith. Sinha and Glover (1978) obtained a 596 Ma crystallization age (zircon discordia) and Odom and Fullagar (1973) obtained a  $535 \pm 27$  Ma crystallization and cooling age (Rb-Sr whole rock isochron) for the relatively undeformed protolith. Therefore, the Acadian orogeny is not a strong possibility for the time of formation of any of the microstructures in this study because 1) there is a lack of information concerning the nature and extent of deformation and 2) there is stronger evidence linking microstructures to either the Taconic or Alleghanian orogenies.

The Alleghanian orogeny is another possibility for the timing of formation of group A microstructures. In this case  $S_1$  and garnets would remain as the only evidence of Taconic deformation and metamorphism. West- to northwest-directed thrusting is compatible with at least part of an Alleghanian history for two reasons. One, the Blue Ridge province, Brevard rocks, and Inner Piedmont province were thrust westward as a unit along the Blue Ridge décollement during the Pennsylvanian and Permian. The timing of Blue Ridge and related thrusting is known because these thrusts deform Carboniferous rocks of the Valley and Ridge (e.g. Rodgers, 1967; Hatcher and Odom, 1980). The Brevard Fault Zone formed as a subsidiary thrust synchronous with, or just after, movement along the Blue Ridge décollement (Reed et al., 1970; Hatcher, 1978). Two, as the Brevard fault



zone formed, its movement brought to the surface an exotic slice of carbonate from the footwall underlying the decollement (Hatcher, 1971). Emplacement was accomplished by thrusting or oblique-slip motion and could have resulted in the formation of group A microstructures in the Alleghanian. Although the exotic slice present in Whetstone quadrangle appears to have been thrust into place under brittle conditions, it was probably emplaced under ductile conditions. Then, later brittle deformation (group D) overprinted previous ductile features, resulting in the final position of the slice close to the surface. Ductile Alleghanian microstructures (group B) have been documented in the Brevard Zone (see below), thus it seems likely that Alleghanian thrusting was also ductile.

In summary, structural relationships suggest that the  $S_1$  foliation is Taconic in age. Group A microstructures were formed in either the Taconic or Alleghanian orogenies. Recall that the Ben Hill Granite, an Alleghanian intrusive, does not contain any group A microstructures. This observation is the only evidence to suggest that group A microstructures in the northeastern areas are Taconic rather than Alleghanian in age.

The origin of group B and group C microstructures postdates that of group A and represents a period of ductile, dextral strike-slip motion in the Brevard Zone. Field data and thin section observations from this study attest to a striking similarity in the morphology, deformation conditions and direction of motion of microstructures in groups B and C in the northeastern study areas, with those from the sheared Ben Hill Granite in Atlanta. Sinha (pers. comm.) obtained a U-Pb zircon date of 280-290 Ma from the Ben Hill Granite which he interprets as a crystallization age. This intrusive was subsequently deformed by movement along the Brevard Zone, thus dating some of the most recent motion in the zone.



Therefore, microstructures in groups B, C and D preserved in the sheared Ben Hill Granite are no older than Alleghanian in age. By analogy, similar microstructures in Tugaloo, Whetstone, Tamassee and Rosman quadrangles must also be Alleghanian or younger in age.

Dextral strike-slip motion during the Alleghanian orogeny is supported by the research of Reed and Bryant (1964) and Bobyarchick (1983, 1984) who conducted field studies in the Brevard Zone in, and adjacent to, the Grandfather Mountain Window (GFMW) in North Carolina (Fig. 1). Reed and Bryant (1964) found that northwest-trending lineations in the GFMW gradually swing into parallelism with northeast-trending lineations in the Brevard Zone as the zone is approached. They interpreted this change in orientation as reflecting dextral strike-slip motion in the Brevard Zone. Bobyarchick (1983, 1984) working southwest of the GFMW interpreted the orientation of oblique crenulation cleavages in the Brevard Zone as also reflecting dextral offset. Dextral motion in the Brevard Zone is also compatible with the Alleghanian movement history of the Inner Piedmont (Bobyarchick, 1981; Gates et al., 1984).

Higgins (1966) suggested dextral motion along the Brevard in the Atlanta area, as did McConnell and Costello (1980, p. 253). The latter two researchers suggested a dextral displacement of 24 mi (35-40 km) on the basis of apparent offset in the Palmetto and Ben Hill Granites and in quartzites of the Sandy Springs group. Reed and Bryant (1964) estimate 135 mi (225 km) of late Paleozoic dextral offset. This estimate is calculated on the basis of exposed Henderson Gneiss stretching from Toccoa, GA to Lenoir, NC. However, Bryant and Reed (1970) suggest that the Brevard Zone experienced greater than 135 mi (225 km) of sinistral offset. The



microstructures in the present study are not quantitative strain markers and cannot be used to estimate displacement in the zone.

Ductile deformation conditions indicated by features in groups B and C are also consistent with an Alleghanian deformation. For example, the change in lineation orientations cited above (Reed and Bryant, 1964) and the oblique crenulation cleavages of Bobyarchick (1983) are also features which require ductile conditions for their formation.

The origin of group C features postdates that of group B. Group C microstructures, i.e. ECC's, crosscut preexisting features and are found both in the Ben Hill Granite and in the northeastern areas. Therefore, because the orientation of ECC's is not compatible with either thrusting or strike-slip motion, they must represent a change in the direction of bulk motion in the Brevard Zone. Group C features can be no older than Alleghanian because they are found in the Ben Hill Granite. However, it is possible that they are more recent than Alleghanian and related to Mesozoic rifting.

The timing of formation of group D features can be no older than Alleghanian in age because: 1) microstructures from group B are demonstrably Alleghanian in age; and 2) features in group D postdate those from groups A, B and C. The direction of bulk motion during this late brittle deformation is unknown because of poor exposure, localized extent and variable geometries and movement directions on faults. The presence of stages of microscopic faulting and brecciation, and drag folds and breccia in the same outcrop, both suggest that group D features formed under an increasing strain rate. I suggest that after formation of features in groups B and C earlier in the Alleghanian, that deformation conditions became more brittle toward the end of the Alleghanian, possibly as the strain rate increased



resulting in group D features. There are two alternatives to this theory. Rather than an increase in strain rate, cooling via unroofing of rocks in the Brevard Zone could have resulted in more brittle deformation conditions, if unroofing and deformation were synchronous. Alternatively, the extreme differences in deformation conditions and the apparently random nature of brittle features, suggests that this deformation could be a separate, more recent event, possibly related to the rifting events which led to the opening of the present-day Atlantic Ocean.

brittle deformation overprints all previous features and the rock motion at this time is unknown.

2. Observed microstructures can be separated into four groups on the basis of microstructure orientation, overprinting relationships and direction(s) of motion.

3. The oldest recognizable features are  $S_1$  and very weathered garnets.  $S_1$  is a prominent foliation defined by muscovite, chlorite and quartz ribbons.  $S_1$  and garnets probably formed during the Taconic orogeny.  $F_1$  folds are not observed but these are likely Taconic in age as well.

4. Group I features consist of tight to isoclinal  $F_2$  folds, an axial planar foliation,  $S_2$ , and scattered  $F_3$  folds.  $F_2$  and  $F_3$  folds deform  $S_1$ . Group A microstructures



## CONCLUSIONS

1. Microstructures from the Brevard Zone in the Northwest Atlanta, Georgia quadrangle, the Tugaloo, Whetstone and Tamasssee quadrangles in northwestern South Carolina and in the Rosman quadrangle in southwestern North Carolina indicate that there were at least two periods of ductile deformation in the Brevard Zone each representing a different direction of bulk motion. A late brittle deformation overprints all previous features and the bulk motion at this time is unknown.
2. Observed microstructures can be separated into four groups on the basis of microstructure orientation, overprinting relationships and direction(s) of motion.
3. The oldest recognizable features are  $S_1$  and very weathered garnets.  $S_1$  is a prominent foliation defined by muscovite, chlorite and quartz ribbons.  $S_1$  and garnets probably formed during the Taconic orogeny.  $F_1$  folds are not observed but these are likely Taconic in age as well.
4. Group 1 features consist of tight to isoclinal  $F_2$  folds, an axial planar foliation,  $S_2$ , and scattered  $F_3$  folds.  $F_2$  and  $F_3$  folds deform  $S_1$ . Group A microstruc-



- tures formed under a west- to northwest-directed ductile thrusting motion probably during the Taconic orogeny.
5. Group B microstructures include type II s-c mylonites, c-surfaces,  $F_4$  folds and garnet pressure shadows, all of which reflect a period of dextral strike-slip motion in the Brevard Zone. Group B features formed during the Alleghanian orogeny because the Ben Hill Granite in Atlanta, which contains these microstructures is dated at 280-290 Ma. The Ben Hill Granite is truncated by motion on the Brevard Zone which resulted in the formation of features in group B and possibly those in groups C and D as well.
6. Group C consists of extensional crenulation cleavages (ECC's) whose orientation suggests that they reflect a change in the direction of bulk motion in the Brevard Zone. These are either Alleghanian or Mesozoic in age.
7. A change in ductile deformation conditions occurred along strike in the northeastern study areas sometime prior to formation of group D features.
8. Retrograde metamorphism appears to postdate formation of groups A, B and C and predate formation of group D.



9. Group D contains microscopic and mesoscopic faults, breccias and drag folds which formed under brittle conditions and an unknown direction of bulk motion. Group D features probably formed toward the end of the Alleghanian orogeny, in response to an increase in strain rate after the formation of microstructures in groups B and C.
10. The results of this study confirm an episode of dextral, strike-slip motion in the Brevard Zone during the Alleghanian orogeny. This motion was regional in extent, having affected rocks from Atlanta, Georgia to the Grandfather Mountain Window in North Carolina. The amount of displacement during this deformation is unknown.



## APPENDIX A

### TABLES OF MICROSTRUCTURES

The following data tables were compiled for each quadrangle listing each thin section made, the general orientation (Cot) of the thin section with respect to lineation and foliation, the microstructures from groups A, B, C and D, if any, that are observed in each section, and any pertinent comments.

## APPENDICES



## APPENDIX A

### TABLES OF MICROSTRUCTURES

The following data tables were compiled for each quadrangle listing each thin section made, the general orientation (Cut) of the thin section with respect to lineation and foliation, the microstructures from groups A, B, C and D, if any, that are observed in each section, and any pertinent comments.

Section	Cut	A	B	C	D	Comments
Tu1	sp					
Tu2	sp					
Tu3	sp					
Tu4	sp					
Tu5	sp					
Tu6	sp					
Tu7	sp					
Tu8	sp					
Tu9	sp					
Tu10	sp					
Tu11	sp					
Tu12	sp					
Tu13	sp					
Tu14	sp					
Tu15	sp					
Tu16	sp					
Tu17	sp					
Tu18	sp					
Tu19	sp					
Tu20	sp					
Tu21	sp					
Tu22	sp					
Tu23	sp					
Tu24	sp					
Tu25	sp					
Tu26	sp					
Tu27	sp					
Tu28	sp					
Tu29	sp					
Tu30	sp					
Tu31	sp					
Tu32	sp					
Tu33	sp					
Tu34	sp					
Tu35	sp					
Tu36	sp					
Tu37	sp					
Tu38	sp					
Tu39	sp					
Tu40	sp					
Tu41	sp					
Tu42	sp					
Tu43	sp					
Tu44	sp					
Tu45	sp					
Tu46	sp					
Tu47	sp					
Tu48	sp					
Tu49	sp					
Tu50	sp					
Tu51	sp					
Tu52	sp					
Tu53	sp					
Tu54	sp					
Tu55	sp					
Tu56	sp					
Tu57	sp					
Tu58	sp					
Tu59	sp					
Tu60	sp					
Tu61	sp					
Tu62	sp					
Tu63	sp					
Tu64	sp					
Tu65	sp					
Tu66	sp					
Tu67	sp					
Tu68	sp					
Tu69	sp					
Tu70	sp					
Tu71	sp					
Tu72	sp					
Tu73	sp					
Tu74	sp					
Tu75	sp					
Tu76	sp					
Tu77	sp					
Tu78	sp					
Tu79	sp					
Tu80	sp					
Tu81	sp					
Tu82	sp					
Tu83	sp					
Tu84	sp					
Tu85	sp					
Tu86	sp					
Tu87	sp					
Tu88	sp					
Tu89	sp					
Tu90	sp					
Tu91	sp					
Tu92	sp					
Tu93	sp					
Tu94	sp					
Tu95	sp					
Tu96	sp					
Tu97	sp					
Tu98	sp					
Tu99	sp					
Tu100	sp					

Section number not parallel to lineation  
 Section number not perpendicular to lineation  
 Section number not visible to lineation  
 Microstructure within recrystallization texture  
 Recrystallization texture, a crystalline or amorphous  
 microstructure

Table A.1: Microstructure Table for Tugalo Quadrangle



Tugaloos data continued

Section Number	Cut	F <sub>2</sub> folds	S <sub>2</sub>	F <sub>3</sub> folds	Type II e-e microstructures	Recryst. qtz-fold tails on augen	C-surfaces	F <sub>4</sub> folds	Carnet pressure shadows	ECC	Recrystallization	Comments/other
Tu1	Pp											
Tu2	Pp	●										
Tu3	Pp	●	●									
Tu6	Pp											Sample from Chauga belt; Cren
Tu7	Pp		●									
Tu11	Pp	●	●									
Tu12	Pp		●									Seven parallel fractures marked by micas
Tu14A	P											Asphibolite from the Chauga belt
Tu15	Pp	●	●									Chauga belt sample
Tu16	Pp		●									Chauga belt sample; Highly recryst.
Tu17A	P											Chauga belt sample
Tu18	Pp	●										Oldest cren marked by recryst limbs in sheaves
Tu19	Pp	●										
Tu21	Pp	●								●		
Tu22	Pp	●	●									Oldest cren limbs visible in sheaves
Tu23	Pp	●										Perpendicular to Tu23A
Tu23A	P							●				F2/F4 fold interference pattern
Tu24	Pp		●									Blue Ridge sample; highly recryst; S2?
Tu26A	P											Blue Ridge sample; One vein
Tu27	P											Blue Ridge sample
Tu29	P											Chauga belt sample; cren
Tu30	Pp	●										Oldest cren limbs in sheave; vein
Tu31	P				●	●						
Tu32	OB	●	●									Cren

P=thin section cut parallel to lineation

Total number of thin sections= 73

Pp=thin section cut perpendicular to lineation

OB=thin section cut oblique to lineation

PRT=partial oblique recrystallization textures

Cren=S<sub>1</sub> is crenulated, a crenulation is present  
recryst=recrystallized

Table A.1: Microstructure Table for Tugaloos Quadrangle:







## Tugaloo data continued

Section Number	Cut	F <sub>2</sub> folds	S <sub>2</sub>	F <sub>3</sub> folds	Type II s-c microstructures	Recryst. qtz-feld tails on augen	C-surfaces	F <sub>4</sub> folds	Garnet pressure shadows	ECC	Brecciation	Comments/other
Tu73	Pp	●										
Tu75	Pp		●									Relic hinges in sheaves
Tu76A	Pp	●	●									
Tu76B	Pp											Not same sample as Tu76A
Tu78A	P				●	●		●				
Tu79	Pp	●										
Tu80	OB	●										
Tu81B	Pp											
Tu82	Pp	●	●									
Tu84	Pp					●						
Tu85	Pp											
Tu86	OB											
Tu87	Pp											Vein
Tu89	Pp	●		●								Veins
Tu92	Pp											PRT in qtz
Tu94	Pp											Alto Allocthon sample (Piedmont); PRT in qtz
Tu97	Pp	●	●									
Tu98	Pp											Cren
Tu99	OB											Veins
Tu100A	OB		●									Cren
Tu102	P											Chauga belt sample; veins; cren
Tu103A	Pp		●									
Tu137A	OB				●							Crystallographic pref. orientation of qtz
Tu137B	P				●							Tu137B cut 40° from Tu137BB
Tu137BB	P				●							Fold of unknown age; faint type II

Table A.2. Microstructure Table for Whitlow Quadrangle



Section Number	Cut	F <sub>2</sub> folds	S <sub>2</sub>	F <sub>3</sub> folds	Type II s-c microstructures	Recryst. qtz-feld tails on augen	C-surfaces	F <sub>4</sub> folds	Garnet pressure shadows	ECC	Brecciation	Comments/other
Wh52A	P							●				Axial planar foliation (S <sub>4</sub> ) Abundant chl, highly recryst. qtz
Wh127B1	Pp		●									Incipient shear band From sample Wh127B
Wh127B2	P		●									From sample Wh127B, qtz-filled fractures in porphs
Wh127C	P				●	●						Wh127B,C,D from HM near fault? contact w/ BP
Wh127D	P					●	●					Snowball garnets
Wh129	Pp											Three shear bands; obliquely recryst. qtz layers
Wh130	P							●	●			Grens
Wh131B	P							●			●	
Wh132F	OB										●	Float next to creek; numerous veins postdate brecciation
Wh133A	P										●	Fractured porphs; thin veins; one kink fold
Wh133B	OB										●	Thin veins
Wh135	P											Blue Ridge sample Recrystallized
Wh138	P				●	●						
Wh140A	P											Mylonite Gneiss of the Chauga belt; numerous augen
Wh140B	Pp											Ditto
Tg	OB											Blue Ridge sample Highly recryst.
CS2	OB										●	Carbonate-filled veins are broken; early ductile textures
CS3	OB										●	CS2 & CS3 from exotic slice; early ductile textures

P=thin section cut parallel to lineation  
 Pp=thin section cut perpendicular to lineation  
 OB=thin section cut oblique to lineation  
 chl=chlorite  
 porphs=porphyroblasts  
 Total number of thin sections= 18

**Table A.2: Microstructure Table for Whetstone Quadrangle:**



Section Number	Cut	F <sub>2</sub> folds	S <sub>2</sub>	F <sub>3</sub> folds	Type II s-c microstructures	Recryst. qtz-feld tails on augen	C-surfaces	F <sub>4</sub> folds	Garnet pressure shadows	ECC	Brecciation	Comments/other
Ta142	P				●	●						Type II is faint, late, qtz-filled vein
Ta143	OB	●					●		●			Tiny, recent qtz-filled fractures; staurolite present
Ta143A	OB									●		Cut perpendicular to Ta143 One staurolite grain seen
Ta149	P										●	Folds of unknown age
Ta150A1	OB								●	●		From sample Ta150A
Ta150A	P						●		●	●		Chlorite rims on garnets
Ta150B	P						●	●	●	●		Ditto
Ta150C	P						●	●	●			Ditto Folds are either F <sub>2</sub> or F <sub>4</sub>
Ta153	P							●				Weak axial planar foliation (S <sub>4</sub> ) to F <sub>4</sub>
Ta155	Pp					●						Three shear bands Fractured porphs
Ta158	Pp		●									PRT in a qtz vein

P=thin section cut parallel to lineation

Total number of thin sections= 11

Pp=thin section cut perpendicular to lineation

OB=thin section cut oblique to lineation

PRT=partial recrystallization textures

Table A.3: Microstructure Table for Tamasee Quadrangle:



Section Number	Cut	F <sub>2</sub> folds	S <sub>2</sub>	F <sub>3</sub> folds	Type II s-c mylonite	Recryst. qtz-feld tails on augen	C-surfaces	F <sub>4</sub> folds	Garnet pressure shadows	ECC	Bruciation	Comments/other
Ros112C	Pp										●	Qtz fragments contain PORT
Ros113A	OB										●	ditto
Ros113B	OB										●	Qtz ribbons contain PORT
Ros113C	OB										●	
Ros113D	OB										●	Folded qtz ribbons of unknown age w/ PORT
Ros114B	OB										●	
Ros114C	OB										●	Faint, thin veins
Ros114E	OB										●	Folds of unknown age PORT in qtz
Ros114F	OB										●	Folds of unknown age PRT in qtz
Ros118A	P									●		PRT in qtz ribbons
Ros118D	P											Open crens or ECC? PRT in qtz ribbons
Ros119	OB	●										Sheared veins of qtz w/ PRT
Ros120	P											From the Blue Ridge province
Ros123A	P											Blue Ridge province sample Open crens or ECC?
Ros123C	P											
Ros124	Pp											Faint, thin, recryst. veins
Ros126A	P				●	●						
Ros126B	P							●				
Ros162	OB											Folds of unknown age, sheared veins, PORT in qtz
SZA	OB											
SZB	OB							●				
SZC	Pp						●					
SZD	OB				●		●					From center of shear zone
SZE	P											

P=thin section cut parallel to lineation      Total number of thin sections= 24  
 Pp=thin section cut perpendicular to lineation  
 PORT=partial oblique recrystallization textures  
 PRT=partial recrystallization textures  
 OB=thin section cut oblique to S<sub>1</sub> and lineation

**Table A.4: Microstructure Table for Rosman Quadrangle:**



APPENDIX B

STRUCTURAL DATA

Features such as lineation, foliation, and lineation are measured and plotted on the map. The map shows the data is plotted by quadrangle. The map shows the data is plotted by quadrangle.

Section Number	Cut	F <sub>2</sub> folds	S <sub>2</sub>	F <sub>3</sub> folds	Type II s-c mylonites	Recryst. qtz-feld tails on augen	C-surfaces	Garnet pressure shadows	F <sub>4</sub> folds	ECC	Brecciation	Comments/other
At1	Pp											from the Long Island Gneiss
At2	P											ditto
At4	P				●				●			fractured, subhedral garnets
At5	P				●	●						ditto and fractured & rotated porphs
At6	P					●				●		fractured, anhedral garnets and ditto
At7	P				●	●						subhedral garnets
At12	P					●				●		fractured & rotated porphs

P=thin section cut parallel to lineation  
Pp=thin section cut perpendicular to lineation  
porphs=porphyroblasts

Total number of thin sections= 7

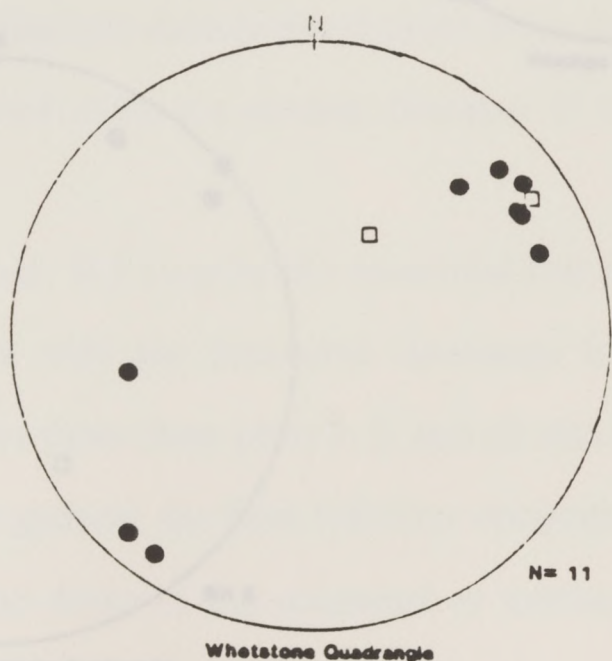
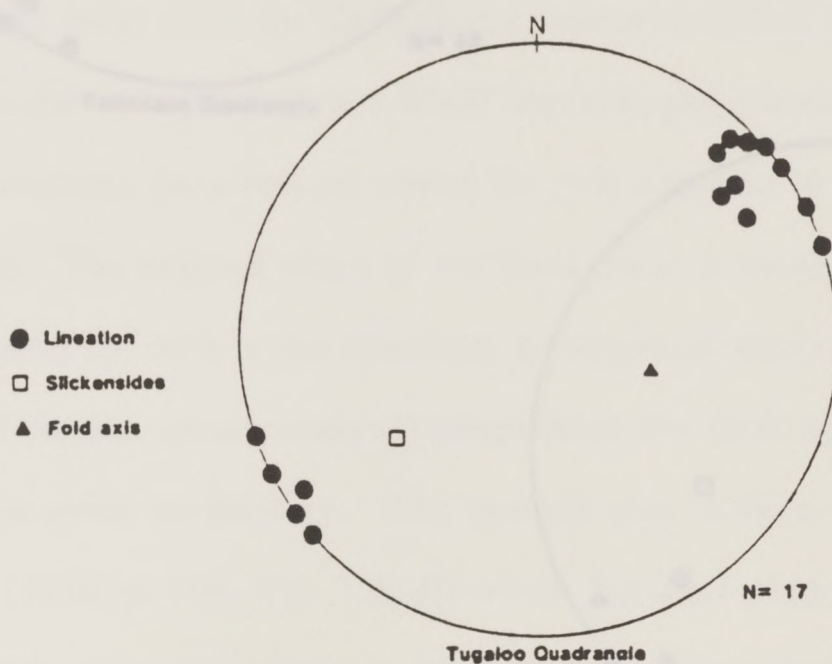
Table A.5: Microstructure Table for Northwest Atlanta Quadrangle:



## APPENDIX B

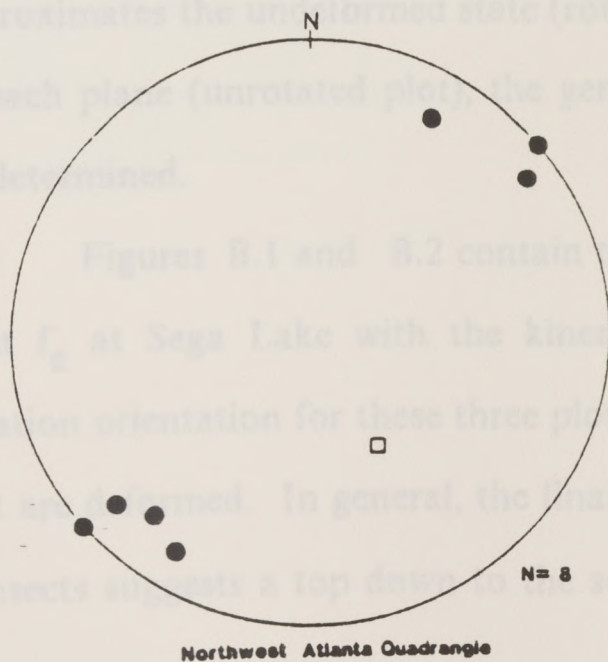
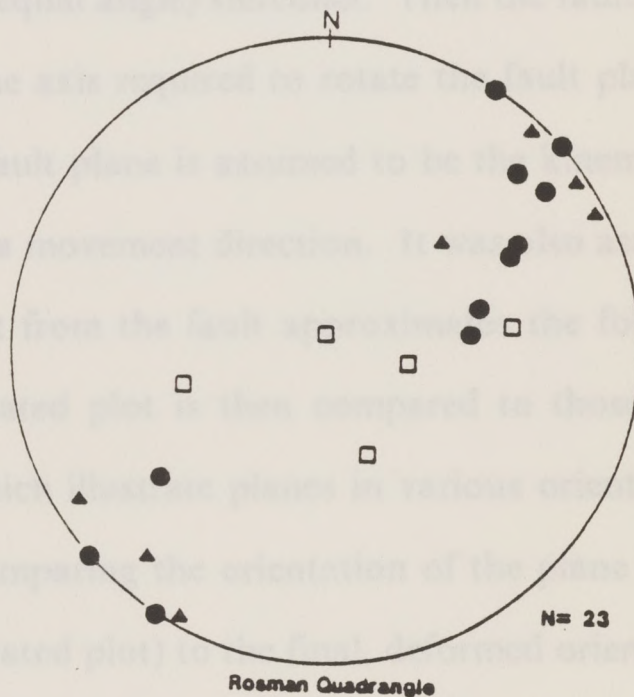
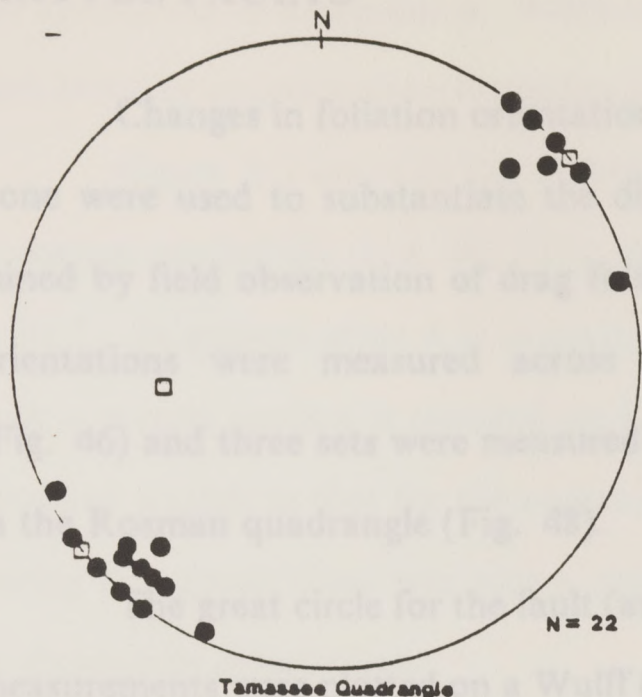
### STRUCTURAL DATA

Features such as lineations, slickensides and mesoscopic fold axes were measured and plotted on the Schmidt (equal angle) stereonet shown below. Data is plotted by quadrangle. "N" is the number of data points plotted.





## BRITTLE FAULTS





## BRITTLE FAULTS

Changes in foliation orientation across brittle faults exposed in the Brevard Zone were used to substantiate the direction of motion on these faults as determined by field observation of drag folds and offset beds where present. Foliation orientations were measured across two faults in the Tamassée quadrangle (Fig. 46) and three sets were measured across the main fault exposed at Segá Lake in the Rosman quadrangle (Fig. 48).

The great circle for the fault (as measured at that transect) and the foliation measurements were plotted on a Wulff (equal angle) stereonet. Then the fault plane and all foliations were rotated about the axis required to rotate the fault plane to horizontal. The original strike of the fault plane is assumed to be the kinematic **b** direction and  $90^{\circ}$  to **b** is the kinematic **a** movement direction. It was also assumed that the foliation measurement furthest from the fault approximates the foliation orientation prior to faulting. The rotated plot is then compared to those from Skjernaa (1980, p. 105, Fig. 7 (b-f)) which illustrate planes in various orientations during progressive deformation. By comparing the orientation of the plane which approximates the undeformed state (rotated plot) to the final, deformed orientation of each plane (unrotated plot), the general direction of motion on each fault can be determined.

Figures B.1 and B.2 contain the unrotated and rotated stereonet plots for fault  $f_e$  at Segá Lake with the kinematic directions labeled. The undeformed foliation orientation for these three plots is U and all other planes plotted are those that are deformed. In general, the final foliation orientation in each of these three transects suggests a top down to the southeast or northeast motion depending on



the orientation of kinematic **a**. When compared to the true fault plane orientation, each transect suggests normal motion on  $f_e$ .

Figure B.3 contains the unrotated and rotated plots for two small faults in Tamassee quadrangle (Fig. 46). The undeformed orientation is that of A for  $f_c$  and E for  $f_a$ . In general when A is compared to each deformed foliation adjacent to the fault a reverse motion is required on  $f_c$  to rotate A into that position. The same direction applies to that for the undeformed orientation of E on  $f_a$ . At some point during movement there was also a strike-slip component to motion on  $f_a$  as seen in slickenside orientations.

Station 1, 1000 ft. N. of fault

Station 2, 1000 ft. S. of fault

Station 3, 1000 ft. S. of fault

Station 4, 1000 ft. S. of fault

Station 5, 1000 ft. S. of fault

Station 6, 1000 ft. S. of fault

Station 7, 1000 ft. S. of fault

Station 8, 1000 ft. S. of fault

Station 9, 1000 ft. S. of fault

Station 10, 1000 ft. S. of fault

Station 11, 1000 ft. S. of fault

Station 12, 1000 ft. S. of fault

Station 13, 1000 ft. S. of fault

Station 14, 1000 ft. S. of fault

Station 15, 1000 ft. S. of fault

Station 16, 1000 ft. S. of fault

Station 17, 1000 ft. S. of fault

Station 18, 1000 ft. S. of fault

Station 19, 1000 ft. S. of fault

Station 20, 1000 ft. S. of fault

Station 21, 1000 ft. S. of fault

Station 22, 1000 ft. S. of fault

Station 23, 1000 ft. S. of fault

Station 24, 1000 ft. S. of fault

Station 25, 1000 ft. S. of fault

Station 26, 1000 ft. S. of fault

Station 27, 1000 ft. S. of fault

Station 28, 1000 ft. S. of fault

Station 29, 1000 ft. S. of fault

Station 30, 1000 ft. S. of fault

Station 31, 1000 ft. S. of fault

Station 32, 1000 ft. S. of fault

Station 33, 1000 ft. S. of fault

Station 34, 1000 ft. S. of fault

Station 35, 1000 ft. S. of fault

Station 36, 1000 ft. S. of fault

Station 37, 1000 ft. S. of fault

Station 38, 1000 ft. S. of fault

Station 39, 1000 ft. S. of fault

Station 40, 1000 ft. S. of fault

Station 41, 1000 ft. S. of fault

Station 42, 1000 ft. S. of fault

Station 43, 1000 ft. S. of fault

Station 44, 1000 ft. S. of fault

Station 45, 1000 ft. S. of fault

Station 46, 1000 ft. S. of fault

Station 47, 1000 ft. S. of fault

Station 48, 1000 ft. S. of fault

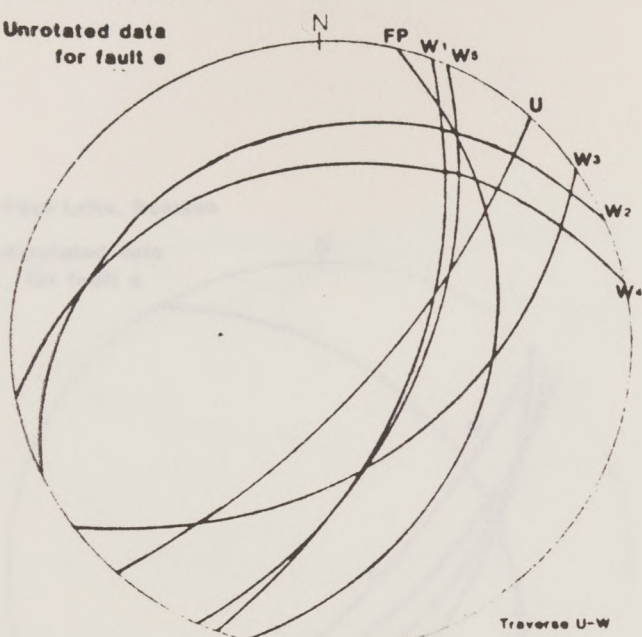
Station 49, 1000 ft. S. of fault

Station 50, 1000 ft. S. of fault

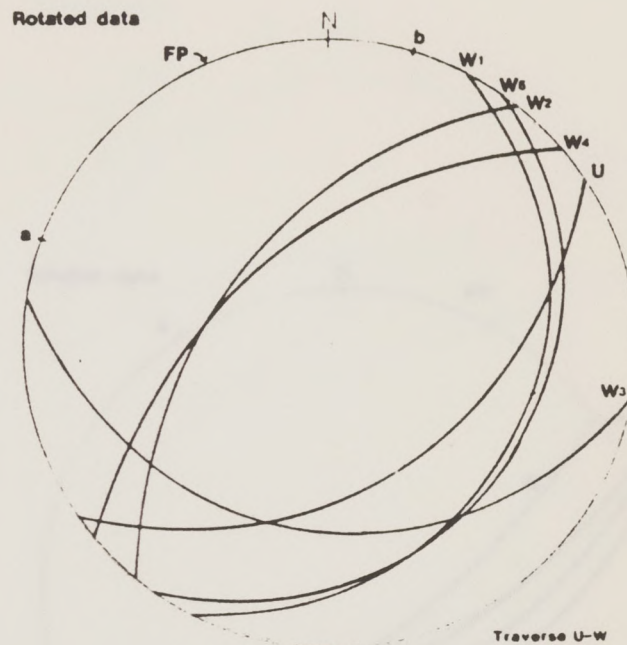
Fig. B.3. Stereonet plots of foliation planes across fault. Sept 1, 1960, Tamassee quadrangle.



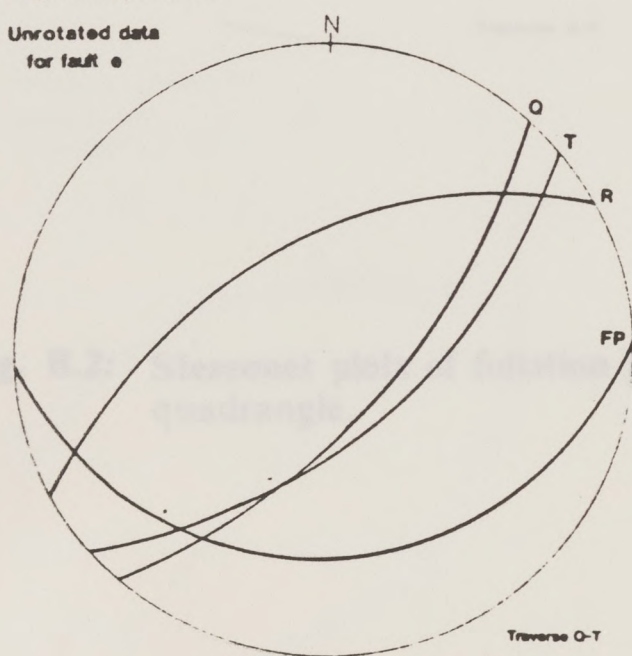
Sega Lake, Rosman

Unrotated data  
for fault e

Rotated data



Sega Lake, Rosman

Unrotated data  
for fault e

Rotated data

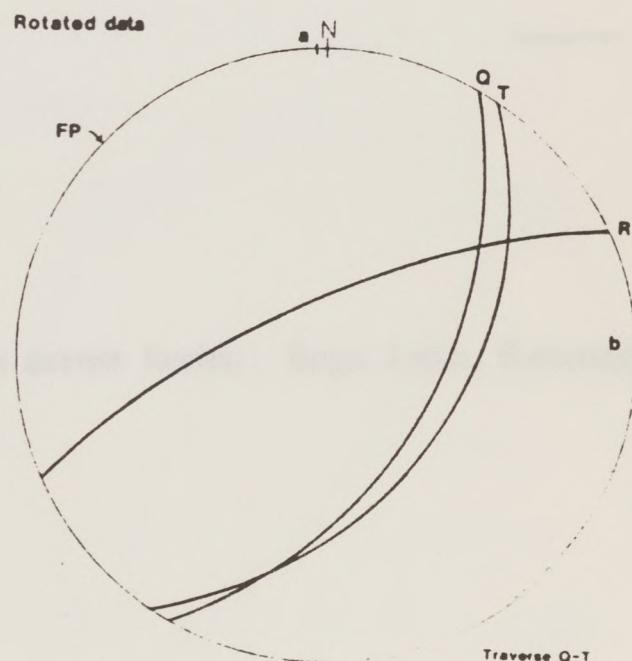
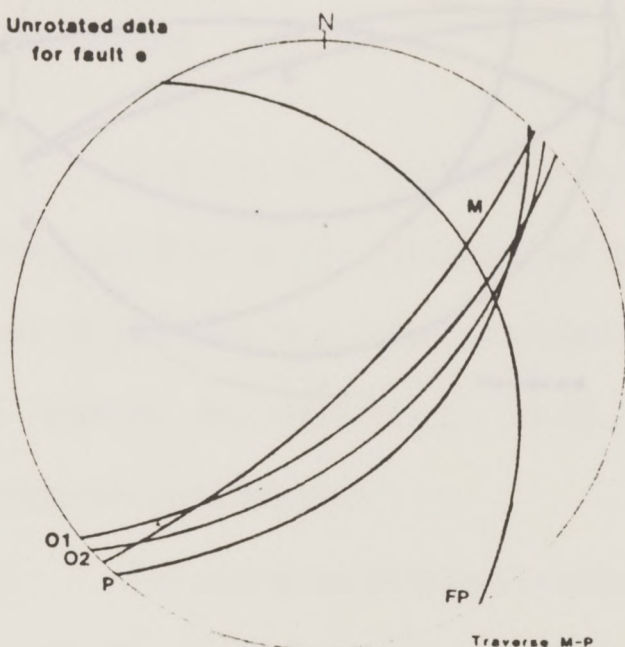


**Fig. B.1:** Stereonet plots of foliation planes across faults: Sega Lake, Rosman quadrangle.

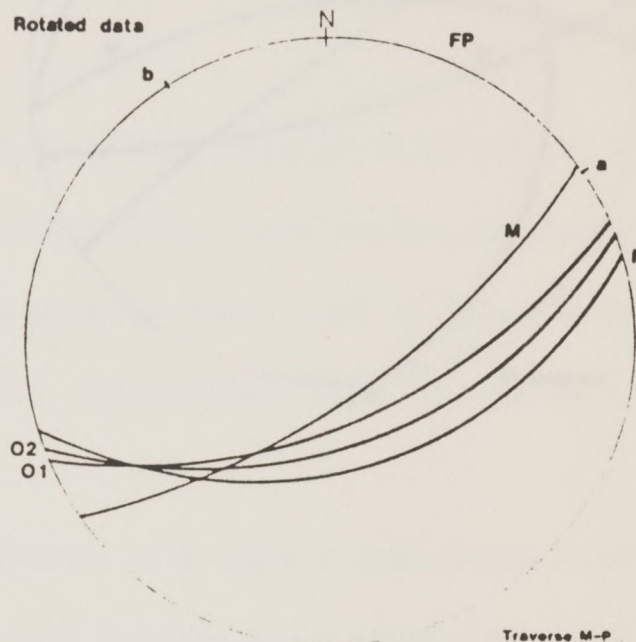


Sega Lake, Rosman

Unrotated data  
for fault e



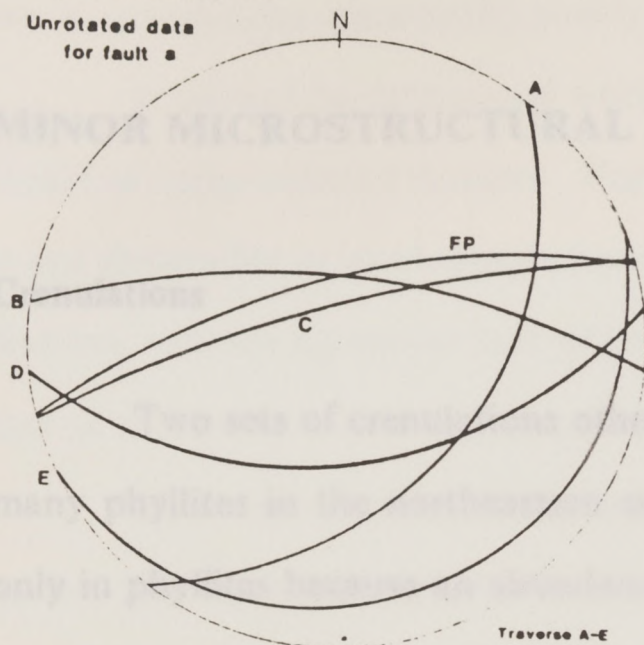
Rotated data



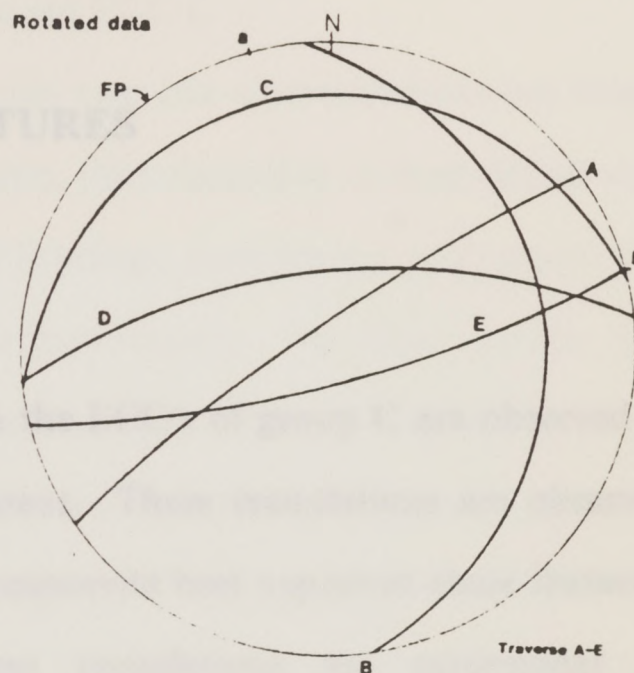
**Fig. B.2:** Stereonet plots of foliation planes across faults: Sega Lake, Rosman quadrangle.



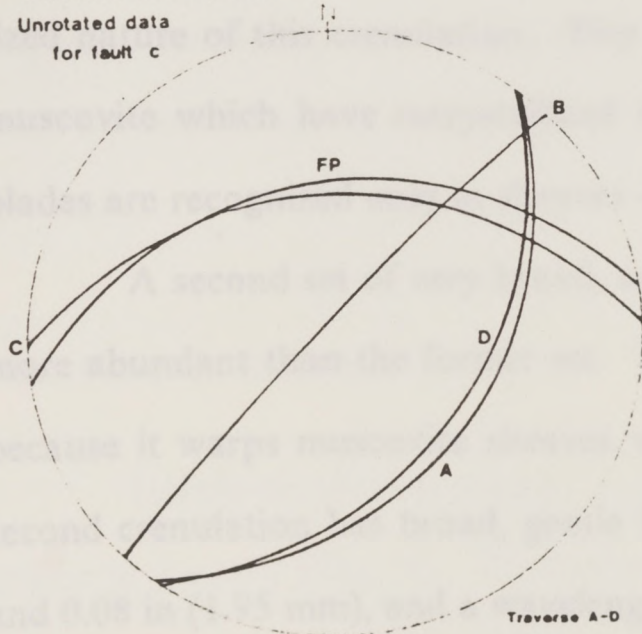
Tamassee Outcrop 150

Unrotated data  
for fault a

Rotated data



Tamassee Outcrop 150

Unrotated data  
for fault c

Rotated data

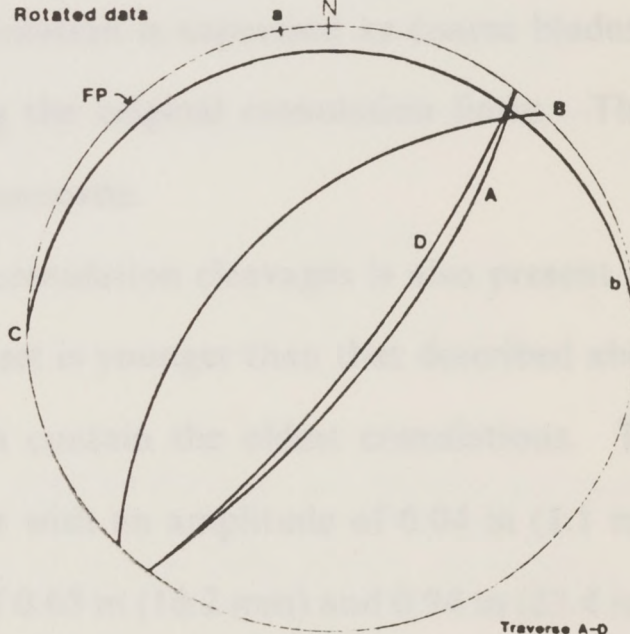


**Fig. B.3: Stereonet plots of foliation planes across faults: Tamassee quadrangle**



## APPENDIX C

### MINOR MICROSTRUCTURAL FEATURES

#### Crenulations

Two sets of crenulations other than the ECC's of group C are observed in many phyllites in the northeastern study areas. These crenulations are observed only in phyllites because an abundance of muscovite best expresses these features. It cannot be determined whether these crenulations are extensional or compressional features.

The oldest crenulation recognizable has a very small amplitude and wavelength, the original dimensions of which cannot be determined given the recrystallized nature of this crenulation. This crenulation is expressed as coarse blades of muscovite which have recrystallized along the original crenulation limbs. These blades are recognized only in sheaves of muscovite.

A second set of very broad, open crenulation cleavages is also present and more abundant than the former set. This set is younger than that described above because it warps muscovite sheaves which contain the oldest crenulations. This second crenulation has broad, gentle limbs with an amplitude of 0.04 in (1.1 mm) and 0.08 in (1.95 mm), and a wavelength of 0.65 in (16.2 mm) and 0.94 in (23.4 mm) in Tu32 and Tu89, respectively. The crenulations may have formed synchronous with or just after the formation of ECC's because the second set overprints both group A and group B microstructures. A lack of overprinting relationships and a



similar morphology in thin section are the only evidence to suggest that the second set of crenulations are actually poorly developed ECC's.

It cannot be determined whether these two sets of crenulations are extensional or compressional features. Furthermore, the orientation of crenulation axes is not discernible in hand sample because of lithology, interference with preexisting features, weathering and/or lack of extensive development. For these reasons, neither of the above two sets of crenulations were used as kinematic indicators.

In several sections a weak secondary foliation defined by rotated muscovite grains, has developed parallel to the apparent western limb of the second set of crenulations and thus it is probably related to the formation of these crenulations. In thin section, this foliation lies  $20^{\circ}$  clockwise from  $S_1$ , whereas  $S_2$ , the other foliation observed, lies in counterclockwise direction. This weak foliation is present in several sections in which crenulations are not observed, but it has a consistent angular relationship to  $S_1$  suggesting that it is the same weak foliation associated with the second set of crenulations. This foliation is also an unreliable kinematic indicator.

### **Rare Pressure Shadows**

Rarely-developed, rotated quartz pressure shadows are present on opaque grains in Ros119 (Fig. 4). These shadows or beards have grown on rectangular, opaque grains 0.02-0.04 in (0.5-1.0 mm) in length. Curvature on some shadows indicates clockwise rotation during growth, others counterclockwise rotation, and some have not undergone any rotation. These pressure shadows were not used as



sense of shear indicators because of their ambiguity, rarity and unknown timing of formation.

## Veins

Both deformed and undeformed veins are present in Brevard Zone rocks. Quartz is the predominant vein-filling although chlorite was observed in rare cases. The best example of sheared veins are three en echelon veins in Ros119 (one is shown in Fig. 5). These veins are filled with quartz which was sheared and partially recrystallized. Numerous other scattered veins are present (see comments in tables in Appendix A) varying from partially recrystallized (Ros162) to highly recrystallized quartz vein-fillings (Ros124) to calcite vein-fillings (CS2). Veins are generally less than 1.0 mm in width and are best seen in plane light. The timing of vein formation is unclear. For example, those veins that are sheared are no younger than group C microstructures. However, some undeformed veins are cut by brecciation (Wh133A) indicating that they formed prior to group D and that there was more than one episode of vein formation. The inconsistent orientation of veins and their unknown timing prohibited their use as kinematic indicators in this study.

## Kinks and Shear Bands

Rare, narrow kink bands are present at a high angle to  $S_1$ , some of which have developed a muscovite or chlorite foliation along their length (Tu12). The adjacent foliation bends into some kinks while it is abruptly truncated by others (Ros114C). These were observed only in the Brevard Phyllite.



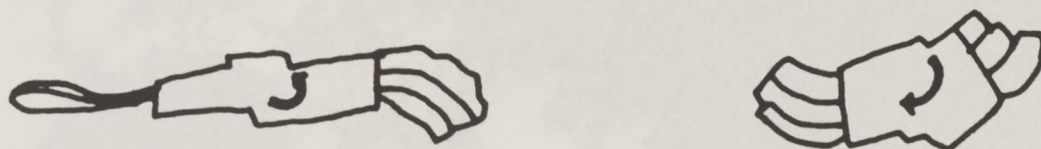


Fig. C.1 Rotated quartz pressure shadows on opaque grains: (Ros119).

Shear bands are used to describe very straight, thin (0.04-0.08 in, 1-2 mm) zones of ductile shearing that are also at a high angle to  $S_1$ . Intense recrystallization has occurred along some shear bands, and  $S_1$  is disrupted and/ or porphyroclasts are offset (Ta155). These shear bands are best developed in the Henderson Gneiss. Note that these are not the same as C-surfaces described under group B. Shear bands are not useful sense of shear criteria in this study because their direction of motion varies, their timing is unclear and their orientation in three dimensions cannot be well-constrained.





**Fig. C.2: Sheared veins.** Quartz filling has partially recrystallized. Timing of formation is unknown. (Ros119, xnicols,  $ld = 11.76$  mm).



## APPENDIX D

### QUARTZ C-AXIS DATA

Five samples (At12, Tu137A, Ros162, Tu3 and Ta142) were chosen from widely separated areas for quartz c-axis measurements. Sections At12 and Tu137A were chosen because they contain microstructures which reflect a dextral shear direction. Ros162 was chosen because it contains an extremely well-developed, partial, oblique recrystallization of quartz ribbons. Tu3 contains  $F_2$  folds of recrystallized quartz-feldspar layers and Ta142 exhibits a good crystallographic preferred orientation of quartz.

C-axis orientations were measured on the Universal stage relative to the fixed geographic coordinates (strike and dip) of each thin section. Plots were produced using the Cyber computer system and the Fortran plotting program written by Renee Dreier at the University of Texas at Austin. For each sample two quartz c-axis plots were produced on Schmidt (equal area) stereonets. Plot A is rotated so that  $S_1$  (as measured for that sample) is in a vertical orientation and L (a mineral elongation lineation, if present) is approximately horizontal. The data was then rotated again to produce plot B with  $S_1$  approximately vertical and L vertical. The number of c-axes measured and plotted is given as "N=".

In some cases (Tu3 and Ta142) c-axes plots did not yield recognizable patterns (Fig. D.1). On the other hand, the patterns in Tu137A, plot B and Ros162 (Fig. D.2) somewhat resembles a girdle maximum. At12, plot A (Fig. D.3) re-



sembles a weak single girdle such as that of Simpson and Schmid (1983, p. 1287, fig. 11) except that distinct maxima have not developed.

Simpson and Schmid (1983) used two criteria for inferring the sense of shear from quartz c-axis fabrics: 1) the asymmetry about the foliation (S) of maxima developed in a single girdle; and 2) the asymmetry of the "skeletal outline" in a crossed-girdle pattern. Neither of these patterns is recognizable in the plots from the present study and the sense of shear using these plots only is indeterminate. The scatter in these plots is probably a result of recrystallization at high temperature which involves both basal and prism slip in quartz. Several other reasons for this scatter are that: 1) more than one episode of recrystallization has probably occurred during the multiple deformation history of the zone; 2) the assumption of homogeneous strain (Simpson and Schmid, 1983) may be incorrect; 3) deformation(s) may have involved some flattening rather than only simple shear; and 4) samples are not quartzites but are rocks which contain a significant amount of muscovite and feldspar which can act as rigid bodies and influence quartz deformation. In summary, plots of quartz c-axes from a variety of samples within the Brevard Zone do not yield any useful sense of shear information.

Fig. 10.5 Quartz c-axis plots for T43 and T442. No pattern has developed.



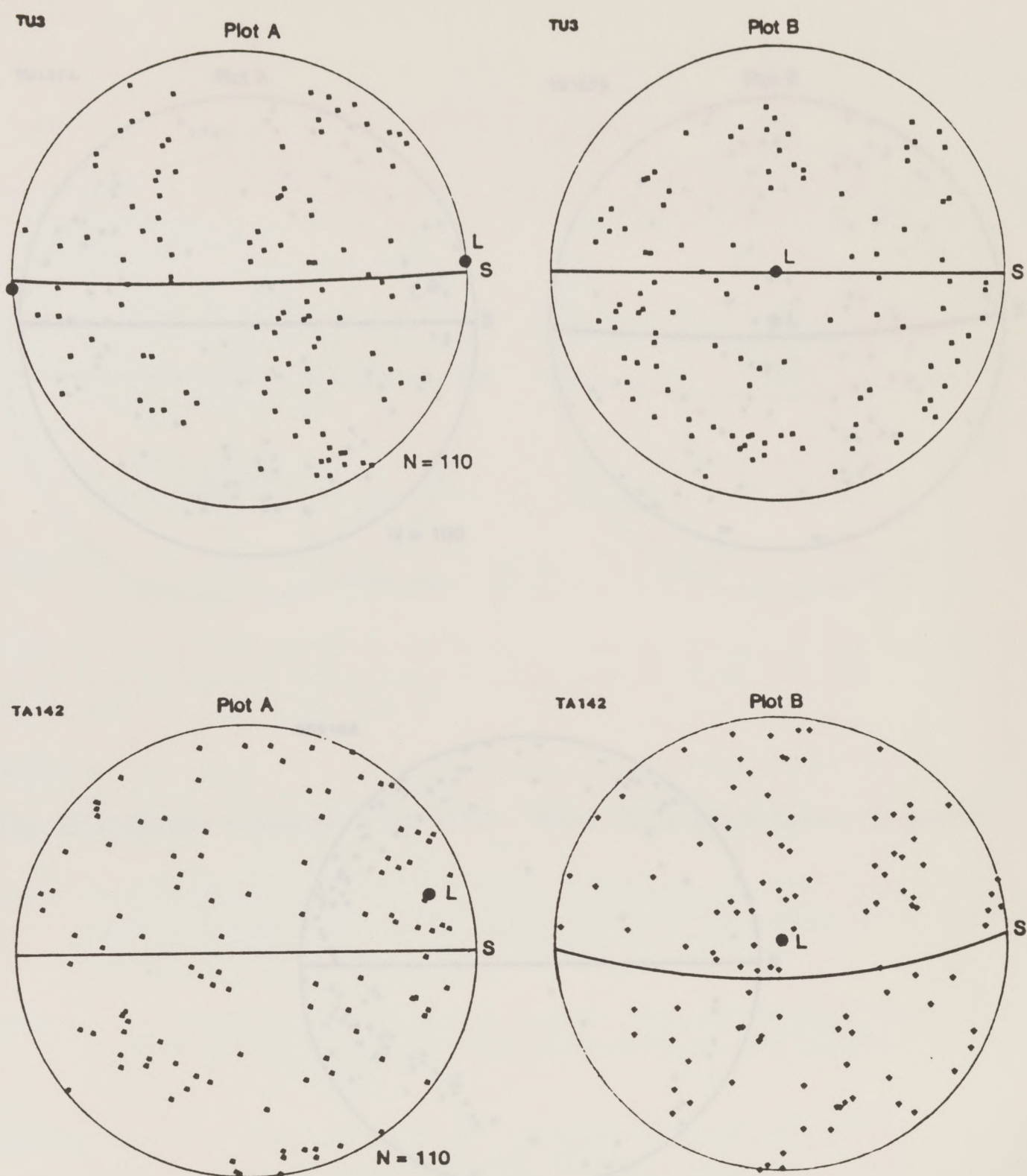
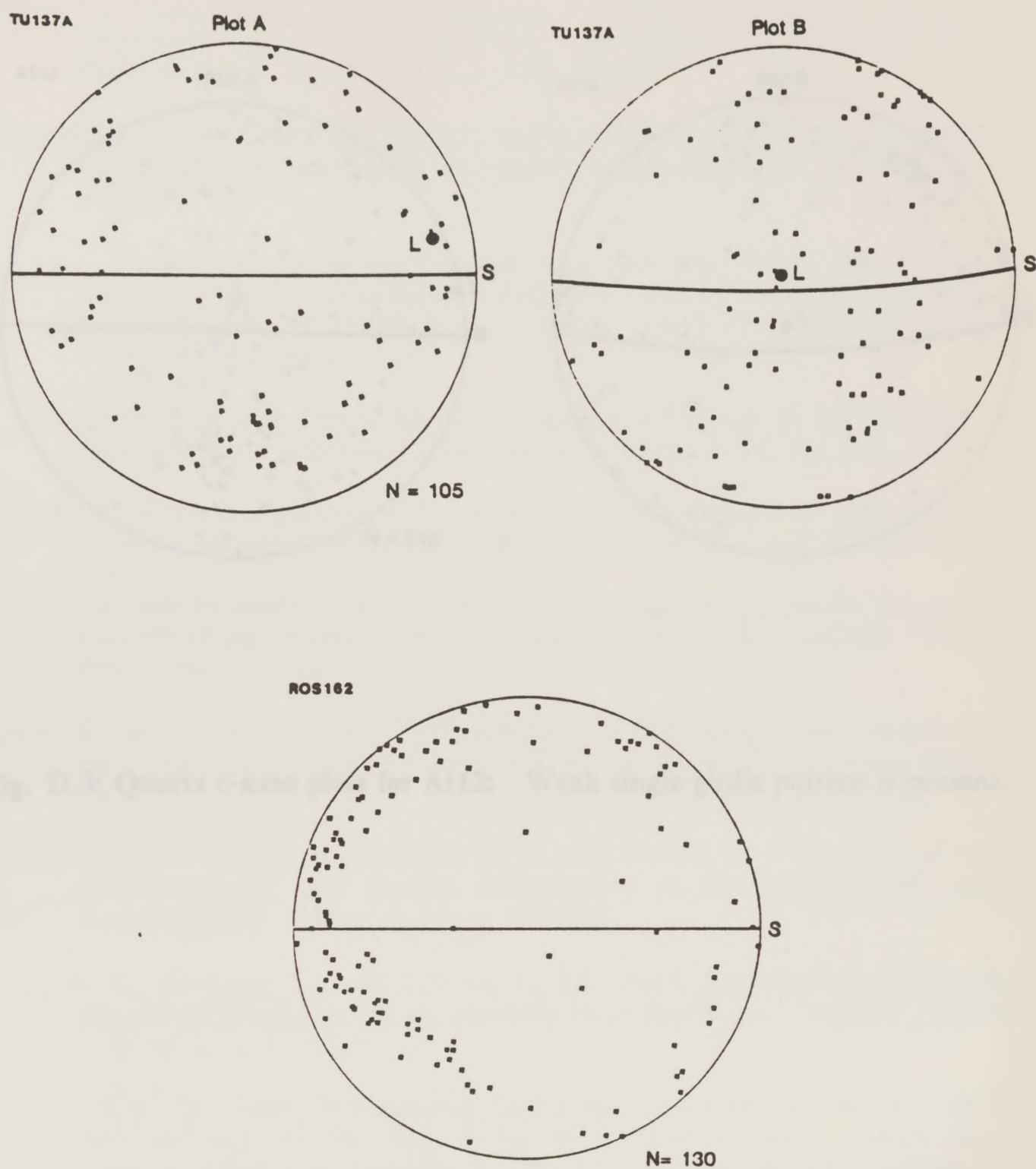


Fig. D.1: Quartz c-axes plots for Tu3 and Ta142: No pattern has developed.





**Fig. D.2: Quartz c-axes plots for Tu137A and Ros162: Possible weak girdle maximums have developed.**



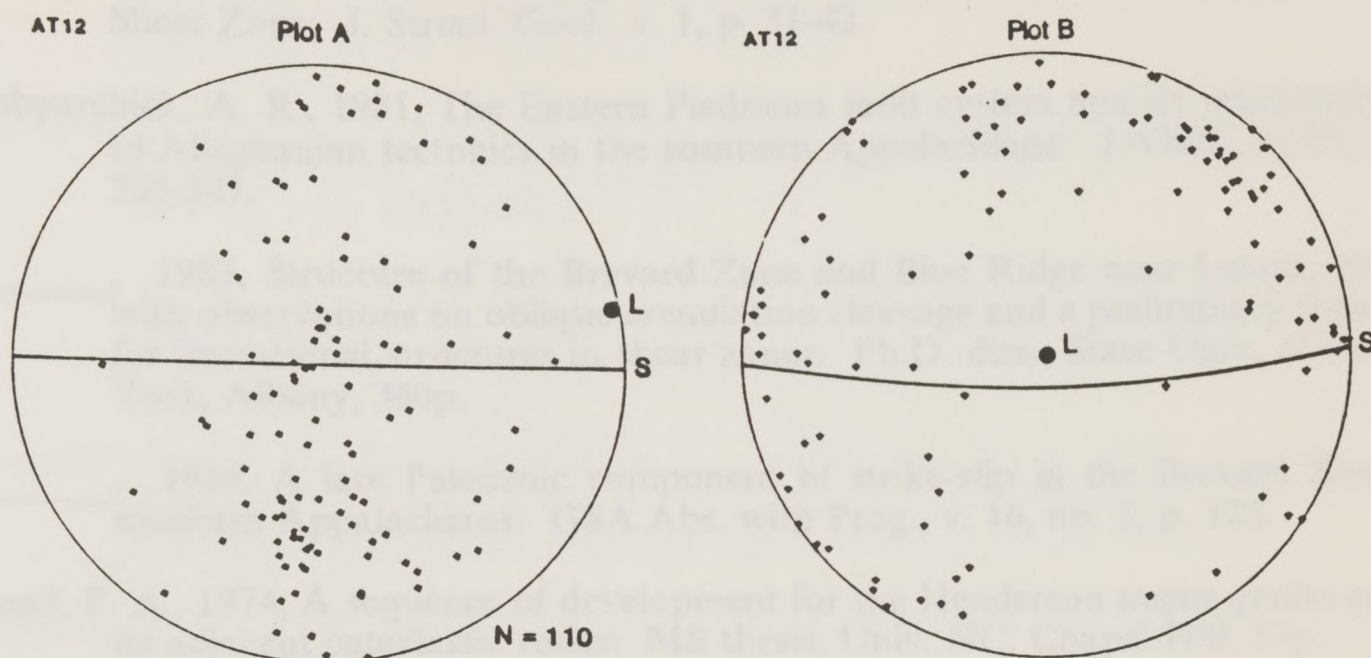


**Fig. D.3: Quartz c-axes plots for At12:** Weak single girdle pattern is present.



## REFERENCES

- Berthe, D., Choukroune, P., and Jegouzo, P., 1979, Orthogneiss, mylonite and noncoaxial deformation of granites: the example of the South American Shear Zone: *J. Struct. Geol.*, v. 1, p. 31-42.
- Bobyarchick, A. R., 1981, The Eastern Piedmont fault system and its relationship to Alleghanian tectonics in the southern Appalachians: *J. Geol.*, v. 89, p. 335-347.
- \_\_\_\_\_, 1983, Structure of the Brevard Zone and Blue Ridge near Lenoir, NC, with observations on oblique crenulation cleavage and a preliminary theory for irrotational structures in shear zones: Ph.D. diss., State Univ. of New York, Albany, 360p.
- \_\_\_\_\_, 1984, A late Paleozoic component of strike-slip in the Brevard Zone, southern Appalachians: *GSA Abs. with Prog.*, v. 16, no. 3, p. 126.
- Bond, P. A., 1974, A sequence of development for the Henderson augen gneiss and its adjacent cataclastic rocks: MS thesis, Univ. NC, Chapel Hill, 53p.
- Bond, P. A. and Fullagar, P. D., 1974, Origin and age of the Henderson gneiss and associated cataclastic rocks in southwestern North Carolina: *GSA Abs. with Prog.*, v. 6, no. 4, p. 336.
- Bryant, B. and Reed, J. C., Jr., 1970, Geology of the Grandfather Mountain Window and vicinity, North Carolina and Tennessee: *USGS Prof. Paper* 615, 190p.
- Glover, L., III, Speer, J. A., Russell, G. S., and Farrar, S., 1983, Ages of regional metamorphism and ductile deformation in the central and southern Appalachians: *Lithos*, v. 16, p. 223-245.
- Gates, A. E., Simpson, C., and Glover, L., III, 1984, Appalachian Carboniferous dextral strike-slip faults: an example from Brookneal, Virginia: *Tectonics*, v. 5, no. 1, p. 119-133.
- Hatcher, R.D., Jr., 1969, Stratigraphy, petrology, and structure in the Low Rank Belt and part of the Blue Ridge of northwesternmost South Carolina: *Carolina Geol. Soc. Guidebook*, Div. Geol., Devel. Board, Geologic Notes, v. 13, no. 14, p. 105-141.
- \_\_\_\_\_, 1971, Stratigraphic, structural and petrologic evidence favoring a thrust solution to the Brevard problem: *Am. J. Sci.*, v. 270, p. 177-202.
- \_\_\_\_\_, 1972, Developmental model for the southern Appalachians: *GSA Bull.*, v. 83, p. 2735-2760.



- \_\_\_\_\_, 1978, Tectonics of the Western Piedmont and Blue Ridge, southern Appalachians: *Am. J. Sci.*, v. 278, p. 276-304.
- Hatcher, R. D., Jr., and Butler, J. R., 1979, Guidebook for Southern Appalachian Field Trip in the Carolinas, Tennessee and northeastern Georgia. The Caledonides in the U.S.A., I.G.C.P., 117p.
- Hatcher, R. D., Jr. and Griffin, V. S., Jr., 1969, Preliminary detailed geologic map of northwestern South Carolina: South Carolina Dev. Board, Div. Geology, scale 1/125,000.
- Hatcher, R. D., Jr., and Odom, A. L., 1980, Timing of thrusting in the southern Appalachians., U.S.A.: Model for orogeny?: *J. Geol. Soc. London.* v. 137, p. 321-327.
- Hatcher, R. D., Jr., Price, Vaneation, Jr., and Snipes, D. S., 1973, Analysis of chemical and paleotemperature data from selected carbonate rocks of the southern Appalachians: *Southeastern Geology*, v. 15, p. 55-70.
- Higgins, M. W., 1966, The geology of the Brevard lineament near Atlanta, Georgia: *Georgia Geol. Survey Bull.*, v. 77, 49p.
- \_\_\_\_\_, 1968, Geologic map of the Brevard fault zone near Atlanta, Georgia: USGS Misc. Geol. Inv. Map I-511, scale 1:48,000.
- Horton, J. W., Jr., 1974, Geology of the Rosman area, Transylvania County, NC: MS thesis, Univ. of NC, Chapel Hill, 63p.
- \_\_\_\_\_, 1982, Geologic map and mineral resources summary of the Rosman quadrangle, NC, Map 185-NE, 4p.
- Jonas, A. I., 1932, Structure of the metamorphic belt of the southern Appalachians: *Am. J. Sci.*, v. 224, p. 228-243.
- Keith, A., 1905, Description of the Mount Mitchell quadrangle (NC-TN): USGS Geol. Atlas, Folio 124, 10p.
- Lister, G. S. and Snoke, A. W., 1984, S-C Mylonites: *J. Struct. Geol.*, v. 6, no. 6, p. 617-639.
- Livingston, J. L., 1966, Geology of the Brevard Zone and the Blue Ridge province in southeastern Transylvania County, North Carolina: Ph.D. diss., Rice Univ., 118p.
- McConnell, K. I. and Abrams, C. E., 1984, Geology of the Greater Atlanta Region: Georgia Geologic Survey, Dept. of Natural Resources, Bull. no. 96, 127p., 9pl.



- McConnell, K. I. and Costello, J. O., 1980, Guide to Geology along a traverse - through the Blue Ridge and Piedmont provinces of North Georgia: in *Excursions in Southeastern Geology*, pub. by Am. Geol. Inst., v. 1, p. 241-258.
- Mosher, S., Burks, R. J., Bristol, D. A., Carter, K. E., Evans, C. A., Gray, G. G., Kazmer, C. S., 1985, Differences in planar fabrics developed in shear zones: morphology, geometry and strain conditions: *GSA Abs. with Prog.*, v. 17., no. 7, p. 670.
- Odom, A. L. and Fullagar, P.D., 1970, Isotopic evidence for Late Devonian movement along the Brevard Zone: *GSA Abs. with Prog.*, v. 2, no. 7, p. 638-639.
- Odom, A. L. and Fullagar, P. D., 1973, Geochronologic and tectonic relationships between the Inner Piedmont, Brevard Zone and Blue Ridge belts, NC: *Am. J. Sci.*, v. 273-A, p. 133-149.
- Platt, J. P., 1979, Extensional crenulation cleavage: *J. Struct. Geol.* (abs.), v. 1, p. 95.
- Platt, J. P. and Vissers, R. L. M., 1980, Extensional structures in anisotropic rocks: *J. Struc, Geol.*, v. 2, p. 397-410.
- Reed, J. C., Jr. and Bryant, B., 1964, Evidence for strike-slip faulting along the Brevard Zone in North Carolina: *GSA Bull.*, v. 75, p. 1177-1196.
- Reed, J. C., Jr., Bryant, B. H. and Myers, W. B., 1970, The Brevard Zone: a reinterpretation, in Fisher, G. W., Pettijohn, F. J., Reed, J. C., Jr., and Weaver, K. N., eds. *Studies of Appalachian geology: central and southern*. Wiley-Interscience publishers, New York, p. 261-269.
- Rodgers, J., 1967, Chronology of tectonic movements in the Appalachian region of eastern North America: *Am. J. Sci.*, v. 265, p. 408-427.
- Roper, P. J., 1971, Petrographic analysis of the "button" or "fish-scale" phyllonitic schist of the Brevard Zone: *GSA Abs. with Prog.*, v. 3, no. 5, p. 346.
- , 1972, Structural significance of the "button" or "fish-scale" texture in the Phyllonitic Schist of the Brevard Zone: *GSA Bull.*, v. 83, p. 853-860.
- Roper, P. J. and Dunn, D. E., 1970, Geology of the Tamassees, Satolah and Cashiers quadrangles, Oconee County, SC: *South Carolina Dev. Board, Div. of Geology, Map Series (MS-16)*, 55p.
- , 1973, Superposed deformation and polymetamorphism, Brevard Zone, South Carolina: *GSA Bull.*, v. 84, p. 3373-3386.
- Roper, P. J. and Justus, P. S., 1973, Polytectonic evolution of the Brevard Zone: *Am. J. Sci.*, v. 273-A, p. 105-132.



- Simpson, C. and Schmid, S., 1983, An evaluation of criteria to deduce the sense of movement in sheared rocks: GSA Bull., v. 94, p. 1281-1288.
- Sinha, A. K. and Glover, L., 1978, U/Pb systematics of zircons during dynamic metamorphism - A study from the Brevard Fault Zone: Contr. to Min. and Petr., v. 66, p. 305-310.
- Sinha, A. K. and Zietz, I., 1982, Geophysical and geochemical evidence for a Hercynian magmatic arc, Maryland to Georgia: Geology, v. 10, no. 11, p. 593-596.
- Skjernaa, L., 1980, Rotation and deformation of randomly oriented planar and linear structures in progressive simple shear: J. Struct. Geol., v. 2, p. 101-109.
- White, W. A., 1950, Blue Ridge front - A fault scarp: GSA Bull., v. 71, p. 1309-1346.

Permanent address:

1100 Scott Avenue  
Rockville, Maryland 20851

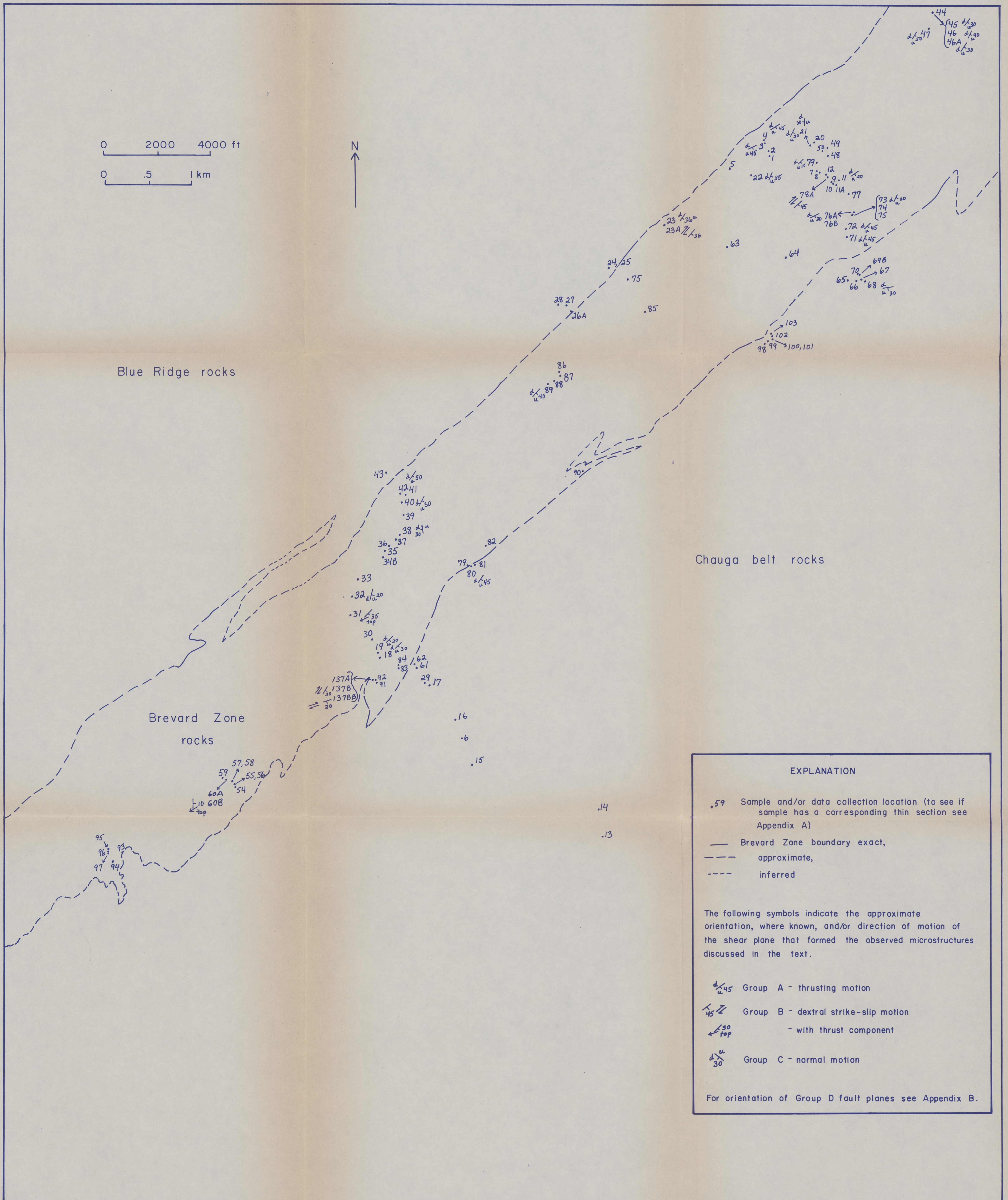
This thesis was typed by Carol Evans Avery



This document does not include the vita page from the original.



Tugaloo Quadrangle Sample Locations  
Overlay for Hatcher, unpub. map





Whetstone Quadrangle Sample Locations  
Overlay for Hatcher, unpub. map

For explanation of symbols see Plate I.

0                      2000                      4000 ft

0      .5      1 km

Blue Ridge rocks

Brevard Zone  
rocks

Chauga belt rocks

Geology by Carol A. Evans, 1985 - 86

Plate II



Tamassee Quadrangle Sample Locations  
Overlay for Roper and Dunn, 1970b

For explanation of symbols see Plate I.

0 2000 4000 ft

0 .5 1 km

N  
↑

Blue Ridge rocks

150  
• 155  
• 154

• 156

• 147

148

• 149

• 150A + A1 150 40 d  
150B 145 25 d  
150C 145

• 145

• 146

151

153

• 159

• 157

Brevard Zone rocks

Chauga belt rocks

• 144

• 143

• 141

130  
• 142



